

https://dspace.org/

Biological hydrogen production using an anaerobic fluidised bed bioreactor

Thompson, Liam Jed

2006-11-16T12:21:06Z
http://hdl.handle.net/10539/1812

Downloaded from a DSpace repository. https://dspace.org/

CHAPTER 1

LITERATURE REVIEW

CHAPTER 1A

ANAEROBIC FLUIDISED BED REACTORS – A REVIEW IN THE SOUTH AFRICAN CONTEXT

(submitted for publication in “South African Journal of Science”)

Abstract

Anaerobic fluidised beds (AFBR) represent an under-utilised bioreactor design with features placing it above more conventional reactors such as the fixed bed, upflow sludge blanket and tank reactors in terms of cost of operation, installation and performance. There has been considerable AFBR research at the bench and pilot scale, but full scale plants represent only 16% of the total anaerobic treatment plants. Benefits of AFBRs include high biomass retention, the separation of the solids retention time from the hydraulic retention time and stability to its microbial component in the form of biofilms (microorganisms attached to a solid surface). This allows the reactor to operate at the maximum microbial metabolic rate rather than maximum growth rate, allowing superior conversion rates of substrate to product. The biofilm component also permits operation under high organic load rates, toxin exposure and pH fluctuations. These reactors represent an exciting field of research for South Africa, not only in wastewater treatment where plant upgrades could include smaller, cheaper and more efficient fluidised bed units, but also in more advanced applications such as biochemical, antibiotics, therapeutics, bioenergy and biomass production. Research and development into this field could yield many economic benefits for South Africa and should be explored as an alternative to traditional bioreactors.

1a.1 Introduction

Anaerobic digestion processes are widely used in the treatment of wastewater from various sources. Anaerobic wastewater treatment started in the late 19th century in France and England. These early digesters had no mechanical stirring, were not heated and consequently were inefficient, unstable and slow (Gijzen 2001). Low rates of biodegradation under anaerobic conditions have until recently been the one major disadvantage of anaerobic wastewater treatment processes relative to aerobic processes. In the conventional anaerobic continued stirred tank reactor (CSTR) the maximum specific growth rates for anaerobic bacteria are reportedly greater than 0.014 h^{-1} (Denac and Dunn 1988). Therefore as a result hydraulic retention times (HRT – time which waste remains in the reactor being treated) ranging from 10 to 60 days for heated and 90 – 200 day for non-heated digesters have been necessary for wastewater treatment (Stronach, Rudd *et al.* 1986). Long HRTs are generally normal in conventional CSTR anaerobic wastewater treatment systems but can be decreased by increasing the bacterial biomass in the reactor. However, if the bacterial biomass in the bioreactor is not attached to a carrier substrate or flocculated, the rate of cell washout also increases with increasing HRT. During the 1970s it became clear that there were many benefits to increasing the rate, capacity and efficiency of anaerobic digestors for wastewater treatment. This stimulated research and development of high-rate, high-capacity anaerobic bioreactors, such as the AFBR and the upflow anaerobic sludge blanket bioreactors (UASB) (Gijzen 2001). Many operation limitations of anaerobic systems were overcome with these improved bioreactor designs. A key feature of design improvement that has been associated with the development of expanded bed, fluidised bed and sludge blanket bioreactor configurations has involved the immobilization of bacterial biomass, either as a flocculant in UASBs, or in biofilms in packed, expanded and AFBRs. Immobilization of microbial biomass allows for shorter HRT, higher volumetric bioreactor rates and lower cell wash-out. An increase in the capacity to digest high strength wastewater at high rates has been an important result in anaerobic bioreactor design improvement. Apart from increased efficiencies with regard to rate and capacity, improved anaerobic digestors have several advantages over more conventional aerobic treatment processes (Table 1a.1), for lower energy costs and lower sludge production.

With respect to energy requirements, solids production, treatment capacity, loading rate, hydraulic retention time and maintenance costs, AFBRs have been shown to be superior to other conventional wastewater treatment systems such as the CSTR, anaerobic filter, UASB, CASBER (carrier assisted sludge bed reactor), RBC (rotating biological contactor) and AEBR (anaerobic expanded bed reactor) that have been designed over the last 30 years. Since the 1970s the number of non lagoon anaerobic installations increased to approximately 2200 worldwide with the AFBR representing some 16% of those (Totzke 2004). Wider adoption of AFBRs has been prevented by false perceptions of high operational and maintenance costs and the complexity of AFBR operation. AFBR have shown to be best suited for high strength, low suspended solid wastes and are generally regarded as the highest rate reactor currently in use (Shieh and Keenan 1986; Sich and van Rijn 1997; Buffiére, Fonade *et al.* 1998; Alves, Melo *et al.* 2002; Sen and Demirer 2003).

1a.2 AFBR Operation

AFBRs retain microbial growth on granular support media [(e.g. silica sand or activated carbon granules (GAC)] which in turn is kept in suspension by drag forces exerted by flowing wastewater (either up or down) (Figure 1a.1). Wastewater is pumped through a bed of inert support media at sufficient velocities or flow rates to induce suspension, termed fluidisation (Table 1a.7). Once the bed is fluidised, each particle provides a large surface area for microbiological biofilm formation (Figure 1a.1). It is this factor that allows AFBRs to have such a large treatment capacity. The plug flow nature (little or no backward or forward mixing as wastewater moves from inlet to outlet) of AFBRs aids the even distribution of biofilm in the reactor (Gaudy and Gaudy 1981). The recycle and plug flow of AFBRs provides an advantage in the treatment of inhibitory wastes where the high flow rates and even distribution across the bed ensure the biomass is exposed evenly and for a short duration while the recycling mode ensures the breakdown of compounds. Other benefits of recycling include partial neutralisation of pH of the incoming wastewater, a reduction of the alkalinity (buffering carbonate / CO_3^{2-} ions) required, reduction of the effects of incoming wastewater shock loads and compensation for the fluctuations in the influent flow rate (Stronach, Rudd *et al.* 1986).

1a.3 Advantages of AFBRs

Regardless of the type of anaerobic process, there are general considerations that must be observed. These include the wastewater volume per unit of time, the possible requirement of wastewater pretreatment, operational temperature, macro and micro nutrient requirements, pH adjustments for optimum performance, odour and corrosion control, biogas utilisation, sludge disposal, degree of monitoring required for process control and importantly the level of staff training required to operate the plant effectively (Totzke 2004).

There are several important factors one must consider when comparing the AFBR with other reactor configurations. In the AFBR, maximal contact between the biofilm coated carrier substrate and the wastewater due to the fluidisation process reduce liquid film diffusion resistances (Figure 1a.1 - *L*) The nature of particle motion and liquid velocities in the AFBR also contribute to reducing diffusion resistances. Channeling, plugging and gas holdup problems are generally circumvented due to the lower hydraulic retention time (Table 1a.2) and the higher flowrates of the wastewater (Table 1a.6). Biofilm thickness can be controlled and optimised via the flow rate and shear force (Peyton 1996; Liu and Tay 2002). The high biologically active surface area reduces the reactor size and hence the land area necessary to build the treatment plant.

Packed bed reactors such as trickling filters and fixed bed reactors must have large support particles, giving large voidage or porosity as biofilm growth can quickly clog the reactor and cause increased pressure drops. The surface area of biofilm per unit reactor volume (Table 1a.3), and consequently the volumetric productivity of the reactor are reduced in these types of reactors (Table 1a.2) (Boening and Larsen 1982; Denac and Dunn 1988). In the AFBR, the smaller support particles expand during fluidisation to accommodate microbial growth, circumventing clogging problems without the associated reduction in volumetric productivity or increase in HRT (Andrews 1982). The problem of cell washout that handicaps operations such as continuously stirred tank reactors should not occur in an AFBR as long as

the superficial velocity (flow rate of wastewater in and out of the reactor) remains lower than the settling velocity of the support particles (Andrews 1982). Reactors such as the UASB developed in 1979 in Europe,(Lettinga, van Velsen *et al.* 1980) rely on the formation of granular sludge for operation. These reactors have a lower COD loading capacity and HRT than fluidised beds (Table 1a.2), but they are popular and there are over 1000 units currently in operation worldwide (Totzke 2004).

1a.4 Anaerobic Microbiology

In anaerobic wastewater treatment, 3 main groups of anaerobic bacteria (acidogens, acetogens and methanogens) (Figure 1a.2) work syntrophically or cooperatively to degrade complex organics such as carbohydrates, proteins and lipids to form CH_4 and CO_2 as final end products. The microbiology involved in an anaerobic process is more complex than the microbiology involved in an aerobic process mainly due to the lower amount of energy available for growth due to O_2 not being used (Table 1a.7) (Thauer 1990; Schink 1997). It is this low metabolic energy yield which forces microbes into syntrophic metabolic relationships (Garcia, Patel *et al.* 2000; Gavrilescu 2002).

1a.5 Biofilm Formation

As biofilms play such a critical role in the high volumetric conversion rate of AFBRs, it is important to understand the various processes and factors involved in the biofilm formation process. In addition the formation of biofilms is a major rate limiting step in generating a fluidised bed of biofilm coated particles. For the industrial application of AFBRs it is crucial that the biofilm formation process be optimised.

Bacterial colonization of a surface substrate in regular contact with water will eventually lead to biofilm formation. In general the process of surface colonization and biofilm formation proceeds through succession of several stages:(Davey and O'Toole 2000) The adsorption of organic molecules (e.g. sucrose) onto the surface of attachment is the primer. A number of transport processes (hydrodynamic, diffusion, gravity, thermodynamic (Brownian) forces and cell mobility) bring microorganisms into direct

contact with the primed substrate surface. Cells with flagella are able to overcome repulsive forces of the attachment surfaces and so adhere easier (Liu and Tay 2002). Primary colonisers are the first bacteria to attach to the surface making it easier for subsequent bacterial groups to attach. Attachment of the microorganisms to the surface occurs in 2 distinguishable steps. Firstly, reversible attachment where the rapid approach of the cell to the surface is influenced by repulsive, long range electrostatic and attractive van der Waals forces. Secondly, there is irreversible attachment of cells by polymer bridging to and steric interactions with the surface. Other interactions involved in this step include thermodynamic forces (free energy of surface and surface tension) and hydrophobic interactions. The production of exopolysaccharide (EPS) by the attached cells forms a protective buffering gelatinous matrix around the bacteria. The environment surrounding the biofilm induces metabolic changes and genetic competence within the bacteria, which further enhances and strengthens cell-cell interactions and so results in an increased density of cells within the biofilm. Detachment of the biofilms due to fluid shear forces or genetic control elements is the last step and characteristic of a mature biofilm. The biofilm that does not detach is shaped into certain physical structures by the surrounding fluid shear forces.

The nature and concentration of the wastewater has a large effect on bacterial EPS production. Wastewater may need to be supplemented with additional nutrients such as nitrogen, phosphorous or sulphur as deficiencies may result in lower generation of biomass on support particles. A deficiency in some nutrients (C, N or P) may encourage EPS production instead of cell growth, thereby causing problems with the density of the biofilm and so reducing the biomass holdup and reactor performance (Alves, Melo *et al.* 2002). Phosphorous concentrations are very important in the formation of biofilm, as a lack of P in the wastewater may prevent the biofilm from actually forming on the carrier substrate and so cause uncontrolled growth in the planktonic phase. For example in the Himmerfjärden wastewater treatment plant outside Stockholm city, Sweden, a lack of P in the wastewater caused the bacteria to detach from the carrier substrate. This problem was eventually remedied by increasing the P concentration by dosing with phosphoric acid (Bosander and Westlund 2000).

Due to biofilm growth under anaerobic conditions being slow, the generation of required critical biomass is the single most rate limiting process in the setting up of AFBRs (Table 1a.4). Reportedly, anaerobic biomass accumulation may be as short as 50 days (Stronach, Rudd *et al.* 1986; Stronach, Diaz-Baez *et al.* 1987) or as long as 6 months (Fox, Suidan *et al.* 1990).

1a.6 Biofilm Thickness and Density

Complete biodegradation of complex hydrocarbons is dependent on the syntrophic interactions between the bacterial species making up the biofilm consortium. Also, biofilm thickness and density is dependent on the species composition of the biofilm. Biofilm thickness is greatest for biofilm consisting of a mixed population of bacteria compared to monospecies biofilms (Christensen and Characklis 1990). There is also a difference between the type and quantity of biofilm produced by different bacteria. A common source of inoculum is sewage sludge and while this may include all the necessary organisms for a wide variety of wastewaters including obligate and facultative anaerobes, there may be unwanted, possibly antagonistic and/or pathogenic bacteria present that may present technical challenges. The total number of cells entering a wastewater treatment system in an AFBR may also have an effect on the formation of biofilm, not merely the residence time of the cells in the reactor or the cell concentration in reactor. Therefore when an AFBR is started up, a frequent and large concentration of cells as inoculum is recommended (Sreekrishnan, Ramachandran *et al.* 1991).

Total bioreactor biomass hold-up depends on biofilm thickness. Apart from fluid hyrodynamical factors, substrate supply rate, microbial biomass attrition and the physical characteristics of the carrier particle are the other factors controlling biofilm thickness and density. Biofilm thickness L_{bf} is related to the biofilm carrier particle as follows

$$L_{bf} = \left(r_{bp} - r_c\right)$$

where r_{bp} is the biofilm coated particle radius and r_c is the radius of the biofilm solid support particle. The mass of the biofilm coating the carrier particle depends of biofilm thickness and density

$$B_p = \rho_b \frac{4}{3}\pi\left(r_p^3 - r_s^3\right)$$

where, B_p is the dry mass contained in the biofilm covering the solid support particle, ρ_b is the biofilm dry mass per unit wet biofilm particle volume. biofilm biomass density (B_c) is dependent on the quantity of supporting material N_s per unit bioreactor volume V:

$$B_c = \frac{N_s\left[\rho_b \frac{4}{3}\pi\left(r_p^3 - r_s^3\right)\right]}{V}$$

Bioreactor volumetric reaction rate capacity is primarily determined by biofilm density and biofilm surface area rather than by biofilm volume. Thinner, denser biofilms obtained under higher shear stress forces and correct nutrient concentrations are more stable and have a higher biomass concentration, leading ultimately to a higher biofilm activity. This is a key factor in bioreactor operation (Alves, Melo *et al.* 2002). In addition the EPS allows biofilm microorganisms to grow for periods in dilute media due to its absorptive properties, and under high COD loads and large pH fluctuations due to its buffering capacity. Biofilm thicknesses may range from a few microns to more than 1000µm in thickness (Table 1a.6).

Generally, biofilm growth has no set pH and temperature optimum, as these conditions differ with the type of bacterial cultures used in the treatment process. Large fluctuations in pH and temperature can normally be tolerated in a steady state AFBR for a short period due to the biofilm's buffering effect on the bacteria within the biofilm. Most known AFBR treatment systems operate at mesophilic or submesophilic conditions, although there have been several encouraging results reported at psychrophilic and thermophilic temperatures (Vavilin, Lokshina *et al.* 1997; Marín, Alkalay *et al.* 1999).

1a.7 Biofilm Fluidisation

The term fluidisation is used to describe the vertical velocity of wastewater that expands the bed to a point beyond which the net downward gravitational force is equaled by the frictional drag of the support media (Stronach, Rudd *et al.* 1986). When the biofilm particle settles in a fluidised bed, it accelerates until the forces promoting settling or sedimentation, i.e., the particles effective weight, are balanced by the drag or frictional resistance of the liquid or fluid in which the particle is embedded. When equilibrium of forces is achieved the particle attains a constant settling velocity called the terminal settling velocity of the particle in the fluid. The relationship between the forces promoting settling and hydrostatic lift can be defined as follows:

$$F_s = V_p g\left(\rho_p - \rho_L\right)$$

where, F_s is the particles effective weight, V_p is the particles volume ($(4/3)\pi r^3$), ρ_s is the particle density, ρ_L is the liquid density, g is the gravitational acceleration. The drag force impeding sedimentation is

$$F_D = C_D A_p \frac{\left(\rho_L U_s^{\,2}\right)}{2}$$

where, F_D is the drag force, C_D is the drag coefficient, A_p is the projected area ($(1/4)\pi d^2$), and U_s is the superficial fluid velocity. The condition for the attainment of terminal velocity, U_t, is defined as follows:

$$gV_p\left(\rho_s - \rho_L\right) = C_D A_p\left(\frac{\rho_L U_s^{\,2}}{2}\right)$$

and under these conditions the terminal settling velocity of the bioparticle equals the superficial velocity of the fluid:

$$U_t = U_s$$

and solve for U_t by substituting

$$V_p = \frac{1}{6}\pi d_p^3$$

and

$$A_p = \frac{1}{4}\pi d_p^2$$

and rearranging to terminal velocity:

$$U_t = \left[\frac{4}{3}\left(\frac{g}{C_D}\right)\frac{(\rho_s - \rho_L)d_p}{\rho_L}\right]^{1/2}$$

Fluidisation of the bioparticles occurs when:

$$U_s > U_t$$

The Richardson-Zaki correlation relates the bed porosity ε_{BR} of the bioreactor with the superficial fluid velocity U_s as follows

$$\frac{U_s}{U_t} = \varepsilon_{BR}^{\ n}$$

where n is the bioreactor bed expansion index which in turn is a function of the bioparticles Reynolds number at terminal fluid velocity.

1a.8 Biofilm Abrasion and Shearing

As the fluid flow in the AFBR is normally laminar, the removal of biofilm from the carrier particles is more significantly affected by abrasion among carrier particles, than the flow of fluid past the biofilm surface (Peyton and Characklis 1993). Therefore adequate distribution of flow at the inlet is important to prevent channeling. Velocities greater than the optimal range can be inhibitory to the formation of biofilm on the carrier, due to shear. In addition to reducing HRTs, higher fluid velocities allow more wastewater solutes to be transported from the bulk liquid to the biofilm surface. Increased biofilm growth and higher rates of wastewater treatment rates occur at fluid velocities within a given range (Figure 1a.3). Outside this range attrition or stripping of biofilm increases as a result of the combined action of fluid shear forces and abrasive interactions between biofilm particles. Data shown in Figure 1a.3 shows the effects of shear stress on biofilm thickness and density (Chang, Rittman B.E. *et al.* 1991; Liu and Tay 2002).

In AFBRs the various properties of the carrier substrate will have an effect on biofilm generation by influencing the rate of microbial surface colonization. Biofilm density and thickness will also be affected by carrier properties. Within a fluidised bed, microbial colonization of carrier particle surfaces which have many shear faces, such as silica sand, may take longer compared to other biofilm carrier media such as granulated activated carbon (GAC). The startup period for biofilm formation in the reactor bed is shorter with a carrier medium such as GAC. This is because the irregular shape and high rugosity of GAC particles protects the colonising bacteria from excessive shear forces. The density of biofilm supporting particles is an important consideration, especially with regard to the superficial velocity required for fluidisation. In order to reduce the impact of shear forces on biofilm formation on the surface particles the superficial velocities necessary for fluidisation or bed expansion should allow 10-20% total expansion when seeding the reactor. In the case of particles with high densities such as silica sand a reduction in particle diameter would be necessary to ensure fluidisation at flow velocities that do not generate shear

forces that would inhibit biofilm formation or strip off attached biofilm (Table 1a.6) (Alves, Melo *et al.* 2002). Rate of biofilm shearing (B_s) is proportional to the specific power input ε ($W.m^{-3}$) and the kinematic viscosity < ($m^2.s^{-1}$) of the fluid

$$B_s = \exp\left(-\frac{\sigma_{bf}}{\tau_{bf}}\right)\left(\frac{\varepsilon}{\nu}\right)^{1/2}$$

where Φ_{bf} is the mechanical strength of the biofilm (Nm^{-2}) and ϑ_{bf} is the shear stress on the biofilm (Nm^{-2}). The specific power input of bioreactor depends on the reactor flow rate F ($m^3.s^{-1}$) necessary for biofilm particle fluidisation:

$$\varepsilon = \frac{FgL_{BR}}{V} = \frac{U_s A_{BR} L_{BR}}{V}$$

where g is gravitational acceleration ($m.s^{-2}$), L_{BR} is the bioreactor height (m), V is bioreactor volume (m^3), U_s is the fluidisation velocity ($m.s^{-1}$) and A_{BR} is cross-section area of bioreactor (m^2). Shear stress imposed on the biofilm depends on the biofilm particle's drag coefficient (C_d)

$$\tau_{bf} = C_d \rho_{rf}\left(\frac{F}{A_{BR}}\right)^2$$

where P_{rf} is the reactor fluid density ($kg.m^{-3}$) and A_{BR} is bioreactor cross-sectional area (m^2).

Particles with a lower density and a rougher surface such as GAC appear to be superior to silica sand as a fluidised bed biofilm carrier medium. Bed fluidisation power requirements would be proportional to particle density and diameter. An AFBR operational objective would be to operate at fluid velocities which facilitate bed fluidisation at the lowest possible specific power input. A high fluidisation velocity would not only limit the quantity of biofilm produced in the reactor bed but will also decrease the power efficiency of

the system (Ochieng, Odiyo *et al.* 2003). Given that the overall bulk density of the biofilm carrier particle decreases as the thickness of the biofilm increases, the power efficiency of the AFBR should increase with increasing biomass holdup.

1a.9 COD Loading and Reactor Kinetics

The performance efficiency of biofilms in a fluidised bed bioreactor depends on the following factors: number of support particles per unit bioreactor volume; average biomass hold-up per particle; average overall specific reaction rates of the immobilized biomass; average overall yield coefficients of the immobilized biomass. Under steady-state conditions the kinetics of the particle can be modelled by equating the diffusional transfer of the substrates through the boundary layer with consumption of the substrates by the bacteria in the biofilm. Thus the overall substrate consumption or reaction for an individual biofilm particle is

$$\mu_{max} = D_{bf} A_{bf} \left(S_c - S_{bf} \right) = \frac{A_{bf} S_{bf}}{\left(\frac{1}{D_{bf}} + \frac{1}{K_{bf}} \right)} = K_{bf}^{L} A_{bf} S_c$$

where D_{bf} is the mass-transfer coefficient, A_{bf} is the surface area of the particle, K_{bf} is the first- order reaction rate coefficient, K_{bf}^{L} is the overall or lumped first-order reaction rate coefficient, Sc is the bulk phase concentration the substrate, and S_{bf} is the substrate concentration at the biofilm-liquid interface.

The precipitation of a certain quantity of solids within an AFBR should not affect the conversion of wastewater substrate as the bed normally expands to cope with the extra solids. Extra solids within the bed promote the growth of granular sludge and serve as inorganic dampeners. Often they eventually dissolve or degrade, but if they have a negative effect on the operations of the bed, they should be removed.

1a.10 AFBR Design Considerations

Due to the large number of variables which affect the operation of an AFBR system, a rigorous characterisation of the design variables will not be covered. Instead, general considerations of AFBR design will be discussed.

Distribution of the Incoming Wastewater

There are 2 important design characteristics one needs to consider when building an AFBR. Firstly, the uniform distribution of influent wastewater over the cross-sectional area of reactor perpendicular to the flow should always be maintained to prevent channeling. This would decrease the collision frequency among bioparticles, thus preventing biofilm shear. Secondly, the kinetic energy of the influent needs to be dissipated at the reactor bottom to ensure that turbulence is minimised. Methods used to prevent these problems include the use of perforated plates and diffuser cones (Figure 1a.1) to ensure uniform wastewater distribution. Other devices include a downward flow distribution device consisting of a number of inverted conical shaped substructures.

Fluidisation Velocity

The carrier particles present in the bed are covered by a thin biofilm which at high fluid velocities may shear off due to abrasion. It is essential to ensure that during the start-up of the AFBR, the superficial upflow velocity is always maintained above the minimum fluidisation velocity of the media used. This will provide a lower shear environment for the carrier particles and thus enhance the development of biofilms on the fluidised carrier media. The incipient, or minimum fluidisation point represents the transitions between the fixed and fluidised state, and this velocity is sensitive to the carrier substrate shape, size and density (Couderc 1985). Several approaches to the prediction of the fluidisation point of media have been developed (Muslu 1987).

Control of Expanded Bed Height

Control of expanded bed height is important to prevent continuous washout of overgrown support particles and to ensure reactor performance is not affected as a result. The most practical way of controlling the expanded bed height is to allow the flow velocity to fluctuate over a range determined by the desirable bed height and the expansion rate of the fluidised bed (Shieh and Keenan 1986). However, there is conflicting evidence from a steady state AFBR setup, where it was shown that bed expansion ranging from 10-120% has little effect on biomass loss, and that it remains relatively constant over this range (Shieh and Hsu 1996). The effects of prolonged periods of expansion were however not evaluated and it is probable that extended periods of higher flow rates would cause biomass shearing even though the detachment of biomass from a smooth surface is reportedly be independent of fluid shear stress, loss would probably be caused by increased particle abrasion (Peyton 1996). In practice, it is uneconomical to maintain the biofilm thickness at a given level by continuous wasting of overgrown bioparticles, as this generates diluted sludge, requiring thickening before disposal. Other methods to control the amount of biomass present on the carrier substrate such as high speed mixers which shear off the biomass and return the carrier substrate back to the reactor. Additionally, vibrating sieves have also been used to remove excess biomass (Shieh and Keenan 1986). In this method, bioparticles are pumped out of the reactors and fed directly onto a vibrating sieve where the vibration forces remove excess biomass.

Carrier Type

Generally in most literature surveyed, silica sand is used as the carrier substrate, and high biomass concentrations have been achieved using this carrier media for reasons already mentioned. Other carriers have also been used e.g. Al_2O_3, GAC, diatomaceous earth, anthracite coal, gel beads and synthetic resins, with varying success (Gavrilescu 2002). GAC and various forms of it, is generally however seen as the best carrier substrate to use primarily because of its adsorptive qualities and irregular shape (Coelhoso, Boaventura *et al.* 1992). Clay and volcanic stone have also been used for these properties. When the density of the carrier media is high, e.g. sand and basalt, it is necessary to use smaller diameter

particles to achieve adequate fluidisation conditions (Alves, Melo *et al.* 2002). The surface characteristics of the supports (porosity/voidage, roughness and electrical charge) are very important in the early stages of biofilm formation (Alves, Melo *et al.* 2002). GAC is commonly used as a support as its irregular shape offers protection for microbes from shear forces. Its density is also lower than silica sand, and so it requires lower flow rates for fluidisation, so less shear force is exerted on the carrier particles. Biofilm growth on GAC is reportedly more evenly distributed compared with sand, where biofilm stratification occurs (Coelhoso, Boaventura *et al.* 1992).

Other considerations include cost of the material, especially when considering scale-up operations and physical and chemical properties. Physical properties to be considered are size, shape, particle density, hardness, rugosity and surface area (Marín, Alkalay *et al.* 1999).

1a.11 Alternative AFBR Configurations

1 and 2 stage configurations

The degradation of organic waste using an AFBR is more effective when run in a 2 stage configuration (Table 1a.5), effecting the separation of the acidogenic and methanogenesis phases of the reactor (Heijnen, Mulder *et al.* 1989). The two phases of anaerobic digestion differ widely in their physiological and nutritional requirements, thus if they are separated into 2 different reactors, they be able to operate under better controlled conditions leading to improvements in operational efficiency (Bull, Sterritt *et al.* 1984). There have been methods used to separate the acidogenic and methanogenic cultures including kinetic controls, chemical inhibition of methanogenesis, and dialysis, but non of these are practical in scaled-up operations or when using an AFBR (Bull, Sterritt *et al.* 1984).

Inverse / Downflow AFBR Configurations

The term fluidisation is normally applied to 2 or 3 phase systems, in which solid particles are fluidised by a liquid or gas stream in the opposite direction of gravity; here the particles would have a greater density than the fluid. In downflow (inverse) fluidisation, the liquid specific density is higher than the particle density and the bed is expanded downward by the fluid flow (García-Calderón, Buffiére *et al.* 1998).

Tapered AFBR Configurations

The tapered AFBR is differentiated from the conventional AFBR by a configuration resembling a truncated cone rather than a constant cross sectional column. Thus there is gradual expansion from a relatively small cross sectional area of entry to one several times larger at the top of the reactor. If the entry cross section is sufficiently small and the expansion is gradual (angle of a few degrees), the flow should be stable throughout the reactor (Scott and Hancher 1976).

This type of AFBR allows for a large range of flow rates without loss of bed material since the fluid velocity decreases with reactor height. Unlike conventional constant cross sectional area AFBRs (Figure 1a.1), at high flow rates the bed simply expands into a part of the reactor having a larger cross sectional area. In addition, the design reduces eddies and has no significant back mixing.

1a.12 Applications of the AFBR and South Africa

There are numerous types of wastewater that have been investigated on laboratory, pilot and full scale reactors, including carbon oxidation, nitrification, denitrification and organic treatment. The use of fluidised beds for wastewater treatment technology has been studied quite extensively in pilot and lab scale operations, however this has not translated into as many anaerobic or aerobic industrial scale plants being built (Marín, Alkalay *et al.* 1999). At the end of January 2004, the were 350 full scale AFBR operations

worldwide, treating a variety of wastewaters (Totzke 2004). During the period of 1986-1996 there were more than 20 anaerobic Anaflux® reactors installed in Europe for the treatment of food processing wastewater (food canning, jam/preserves, citric acid, chocolate, starch, milk/whey/soft drink, corn mill industries and rectified grape juice) (Holst, Truc *et al.* 1997). Other industrial application included perfume and pulp and paper processing (Holst, Truc *et al.* 1997). The Himmerfjärden wastewater treatment plant outside Stockholm city upgraded it's existing denitrification facilities with a fluidised bed reactor as opposed to an activated sludge which would have been a more expensive addition (Bosander and Westlund 2000).

AFBRs however may not find application only in water and wastewater treatment, especially when one considers commercial biomass conversion, ethanol and biochemical production and microbial culturing where high biomass hold-up and the ability to harvest very concentrated product is essential. Process intensification achieved in the AFBR makes this technology particularly useful for these applications.

There is certainly a place for AFBRs in South Africa and usage in particular would be municipal and industrial wastewater treatment plants. The only industrial scale fluidised bed reactor currently in operation in South Africa to our knowledge is a chemical fluidised bed at the Sasol, Mossref plant in Mossel Bay and therefore not relevant here (Totzke 2004). Many if not all wastewater treatment plants will need to be upgraded and expanded to cope with future increases in capacity demand as well as trying to adhere to increasingly stringent environmental standards. Cost effective, prefabricated AFBRs can be taken directly to the plant and installed in parallel with existing anaerobic digesters. Thus existing plant operations would not be seriously interrupted. For larger installations, a portion of the existing anaerobic tanks could be converted into AFBR modules, thereby reducing system downtime and capital expenditure. For systems requiring additional expansion due to increasing organic and hydraulic loads, the AFBR makes a suitable alternative as modules may simply be added on when required.

There is a market for treating high strength industrial wastewaters with a COD concentration of >1000 $mg.L^{-1}$, as the high cost of aeration can be avoided and useful fuels such as H_2 and CH_4 can be

harvested. This is especially relevant in South Africa where the generation of these fuels in areas outside the electricity grid could provide very important sources of electricity. Sludge transport and disposal costs are lower as the anaerobic process produces less sludge and doesn't require the associated O_2 pumping equipment. The low capital and operating costs for anaerobic fluidised bed treatment provides an economical alternative to sewer surcharges and industrial cost recovery charges.

The application of AFBRs need not be limited only to municipal or industrial wastewater treatment in South Africa. The biomass retention qualities of the AFBR make them an important consideration in biotechnological applications where efficient and competitive production of biochemicals (e.g. ethanol (Webb, Davison *et al.* 1995), xantham gum (Suh, Schumpe *et al.* 1992), and acetic acid (Sun and Furusaki 1990)) therapeutic agents (e.g. monoclonal antibodies (Shen, Greenfield *et al.* 1994), hormones (Terashima, Kamihira *et al.* 1994) and antibiotics (Ramsay, Wang *et al.* 1991)) and biomass (Fröhlich, Lotz *et al.* 1991b) is needed. We feel that this aspect of fluidised beds has not been thoroughly explored and presents an exciting opportunity for researchers and industry in South Africa to develop new and innovative fluidised bed bioreactor technologies that are both cheaper and more efficient than bioreactor technologies currently in use.

Table 1a.1: Comparison of anaerobic and aerobic systems (Stronach, Rudd *et al.* 1986; Global Water Engineering Ltd. 2001).

Aerobic Treatment	Anaerobic Treatment
Conditions	
Preferably used after preclarification	Can be used without presettling
Best for wastewater with low clarification and temperature	Best with medium to highly concentrated wastewater. Generally with temperatures >20°C, although there are exceptions (Sun and Furusaki 1990; Elmitwalli, Zeeman *et al.* 2001).
Toxic components often acceptable	Few toxic compounds allowed, except in biofilm systems
Neutralisation for alkaline wastewaters required	Neutralisation not required for alkaline wastewaters
Process	
Only continuous, no long shutdowns tolerated	Seasonal operation possible
Low effluent values can be attained through multi-stage or cascade design	Generally low effluent values obtained with a finishing aerobic treatment.
Simultaneous N and P removal possible	Significant N and P removal with correct cultures
High excess sludge production	Very little excess sludge production
Clogging danger when using carrier material	No clogging danger from sludge growth
Low volumetric loading rates	High volumetric loading rates possible
High maintenance (equipment)	Low maintenance costs
Possible odour problems and large volumes of waste air	No odour problems or waste air in case of closed tanks
Oxygen limitation	No oxygen needed by microorganisms
Byproducts	
Large quantities of excess sludge	Valuable biogas (CH_4 or H_2)
Costs	
Relatively low investment costs	Often higher investment costs
High operational costs for:	Low operational costs for:
Aeration (power)	*Power consumption*
Nutrients (N, P)	*Little extra nutrient addition needed*
Sludge disposal	*Little excess sludge to dispose*
Small plants also feasible	*Small plants less economical, unless using high biomass reactors such as AFBR.*

Table 1a.2: A comparison of the reactor loading rates in the mesophilic temperature range for several types of wastewater treatment reactors (kg.COD.m-3.d-1) (Stronach, Rudd *et al.* 1986; Gavrilescu 2002).

Reactor Type	Loading Rate ($kg.COD.m^{-3}.d^{-1}$)	HRT (d)	SRT (d)[a]	Suspended Solids
CSTR	0.25-3.00	10-60	10-60	High
Contact	0.25-4.00	12-15	20	Small but significant
UASB	4.00-20.00	0.5-7	20	Low
CASBER	4.00-5.00	0.2-3	20	Low
RBC	0.005-0.02	0.4-1	30	Low
Anaerobic Filter	1.00-40.00	0.5-12	20	Significant SS
AFFEB	1.00-50.00	0.2-5	30	Low
AFBR	1.00-100.00	0.2-5	30	Low

[a] Average Values

Table 1a.3: A comparison of the specific surface area and the biomass holdup of different reactor configurations (Stronach, Rudd *et al.* 1986).

Treatment Process	Specific Surface Area ($m^2.m^{-3}$)
Trickling filter	12.30
Rotating Biological Contactor	40-50
FBBR	800-1200
	Biomass Concentration ($mg.L^{-1}$)
Pure oxygen activated sludge	3000-5000
Conventional activated sludge	2000-3000
Nitrification activated sludge	1000-1500
FBBR (carbon oxidation)	12000-15000
FBBR (nitrification)	8000-12000
FBBR (denitrification)	30000-40000

FBBR – Fluidised Bed Bioreactor

Table 1a.4: Examples of startup times for various AFBR setups.

#	Time to Steady State	Reference
6	6 months	(Fox, Suidan *et al.* 1990)
2	46-128 days	(Sen and Demirer 2003)
1	50 days	(Stronach, Rudd *et al.* 1986), (Fox, Suidan *et al.* 1990)
3	68 days	(Shieh and Hsu 1996)
4	77 days	(Zhao, Hickey *et al.* 1999)
5	65 days	(Costa, Dijkema *et al.* 2000)
7	70 days	(Suidan, Flora *et al.* 1996)
	Average	**82 days**

Table 1a.5: Advantages of a 2-stage AFBR configuration over a 1 stage configuration AFBR for treatment of organic waste (Heijnen, Mulder *et al.* 1989).

1 Stage Configurations	2 Stage Configurations
- COD → $_{CH4}$	- COD → $H_2 + CO_2$ → VFA → CH_4
- Sludge activity 0.8 g COD/g day	- Sludge activity • 1st stage 0.8 g COD/g day • 2nd stage 2.0 g COD/g day
- Biolayer thickness variable	- Biolayer thickness more constant and easier to control.
- pH control difficult	- pH control unnecessary or straightforward[34]
- CH_4 sludge unstable at no feeding	- CH_4 sludge stable at no feeding - High process stability

Table 1a6: Data showing the different flow rates used to achieve fluidisation in different reactor setups of AFBRs.

#	Flowrate	Media	Diameter (mm)	Density ($g.cm^{-3}$)	Expansion (%)	Biofilm Thickness (μm)	Removal Efficiency(%)	Application	Reference
1	19 $m.h^{-1}$	Pumice	0.25-1.4	1.76	19-40	-	82	Textile	(Sen and Demirer 2003)
2	14.5 $m.h^{-1}$	R-633 beads	0.425-0.610	-	10-120	-	96	Acetic acid	(Shieh and Hsu 1996)
3	1.5 $L.d^{-1}$	GAC		0.5	50	-	97.2	Dechlorination	(Suidan, Flora *et al.* 1996)
4	4.6-7.6 $m.h^{-1}$ (9-15 $L.h^{-1}$)	Sand	0.22	1.22	20	-	75	Glucose	(Bull, Sterritt *et al.* 1984)
5	$3.26x10^{-5}$	Quartz	0.59-0.84	2.64	100			Saccharose	(Eramo, Gavasci *et al.* 1994)
	$4.45x10^{-5}$	Sand	0.51	2.90	100				
		Glass spheres							
6	0.047	Coal	0.17-0.20	1.17	100	-	90	Whey	(Boening and Larsen 1982)
	0.044	Sand	0.245	2.57	100				
7	45 $m.h^{-1}$	Sand	0.3-0.4	-	20-40	-	80	Sucrose	(Marín, Alkalay *et al.* 1999)
8	40 $L.h^{-1}$	Sand	0.3-0.5	-	100	-	75	Molasses	(Denac and Dunn 1988)
9	20 $m.h^{-1}$	Sand	0.3-0.5	-	100	-	84	Whey	(Denac and Dunn 1988)
10	10 $L.h^{-1}$	Basalt	0.839	2.99	100	50-400	-	Denitrification	(Alves, Melo *et al.* 2002)
11	0.85 $L.min^{-1}$	GAC	1.69	1.18	100	800	-	Denitrification	(Coelhoso, Boaventura *et al.* 1992)
12	39m/h	Sand	0.5	-	-	0-80	90	Denitrification	(Bosander and Westlund 2000)
13	9.96-24 $m.h^{-1}$	Sand	0.22	-	5-30	-	60-80	Synthetic	(Stronach, Diaz-Baez *et al.* 1987)
14	708 $ml.min^{-1}$	R-633 beads (diatomic clay)	0.43-0.61	-	35%	-	97	Acetic acid	(Hsu and Shieh 1993)
15	40 $m.h^{-1}$	Chalk	0.5-1.0	-	60%	30	-	Nitrification	(Green, Ruskol *et al.* 2001)
17	25.2 $m.h^{-1}$	Glass beads	0.68	2.42	-	40-1200	70-96	Denitrification	(Mulcahy and Shieh 1987)
18	-	Biolite	0.25-0.32	1.25	40-60%	344	-	Acetic acid	(Hidalgo and García-Encina 2002)
19	32.4 $m.h^{-1}$	Sand	0.7	2.5	-	1000	-	Denitrification	(Sich and van Rijn 1997)
20	12 $L.h^{-1}$	Sand	0.36	2.63	-	25-32	-	Glucose	(Rovatti, Nicolella *et al.* 1995)
21	-	GAC	-	-	30%	-	95-99	PCP	(Khodadoust, Wagner *et al.* 1997)
22		GAC	-	-	50%	-	95	Formaldehyde	(Moteleb, Suidan *et al.* 2002)

Table 1a.7: Reaction and standard changes in free energy[a] for methanogenesis (Garcia, Patel *et al.* 2000).

Reaction	$\Delta G^{\circ\prime}$ (Kj/mol CH_4)[a]
$4H_2 + CO_2 \rightarrow CH_4 + 2H_2O$	-135.6
$4Formate \rightarrow CH_4 + 3CO_2 + 2H_2O$	-130.1
$4Methanol \rightarrow 3CH_4 + CO_2 + 2H_2O$	-104.9
$4Methylamine + 2H_2O \rightarrow 3CH_4 + CO_2 + 4NH_4^+$	-75.0
$4Trimethylamine + 6H_2O \rightarrow 9CH_4 + 3CO_2 + 4NH_4^+$	-74.3
$4\ 2\text{-Propanol} + CO_2 \rightarrow CH_4 + 4Acetone + 2H_2O$	-36.5
$Acetate \rightarrow CH_4 + CO_2$	-31.0

a - calculated from the free energy of formation of the most abundant ionic species at neutral pH. Therefore CO_2 is $HCO_3^- + H^+$ and formate is $HCOO^- + H^+$.

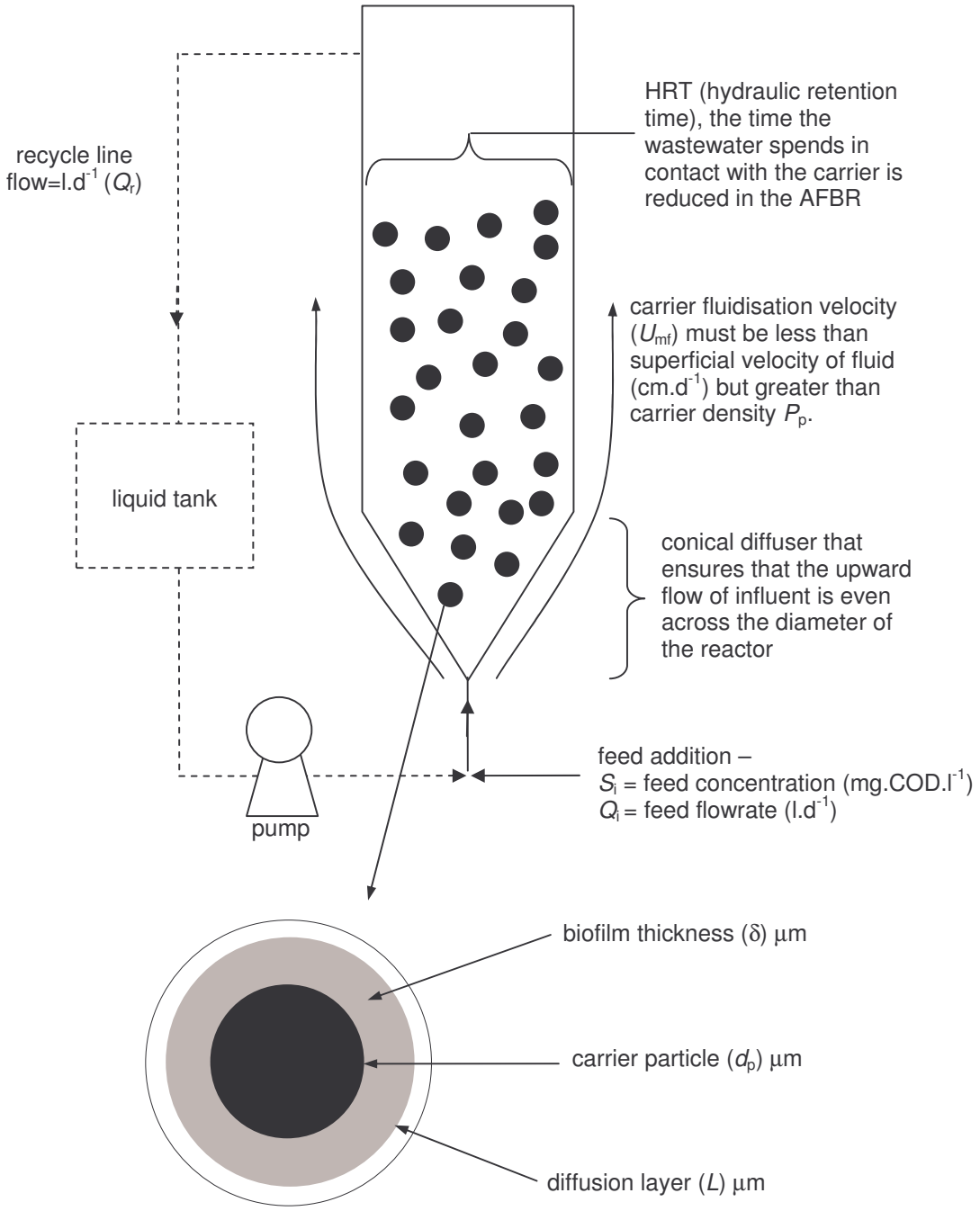


Figure 1a.1: A standard design for a fluidised bed bioreactor system showing the process of actual fluidisation through the distributor section showing the variables such as flow rate (U_{mf}) or minimum fluidisation velocity, feed addition concentration (S_i) and flowrate (Q_i), recycle flow (Q_r) as well as properties of the carrier particle such as biofilm thickness (δ), carrier particle diameter (d_p) and the diffusion layer (L) which would affect reactor performance.

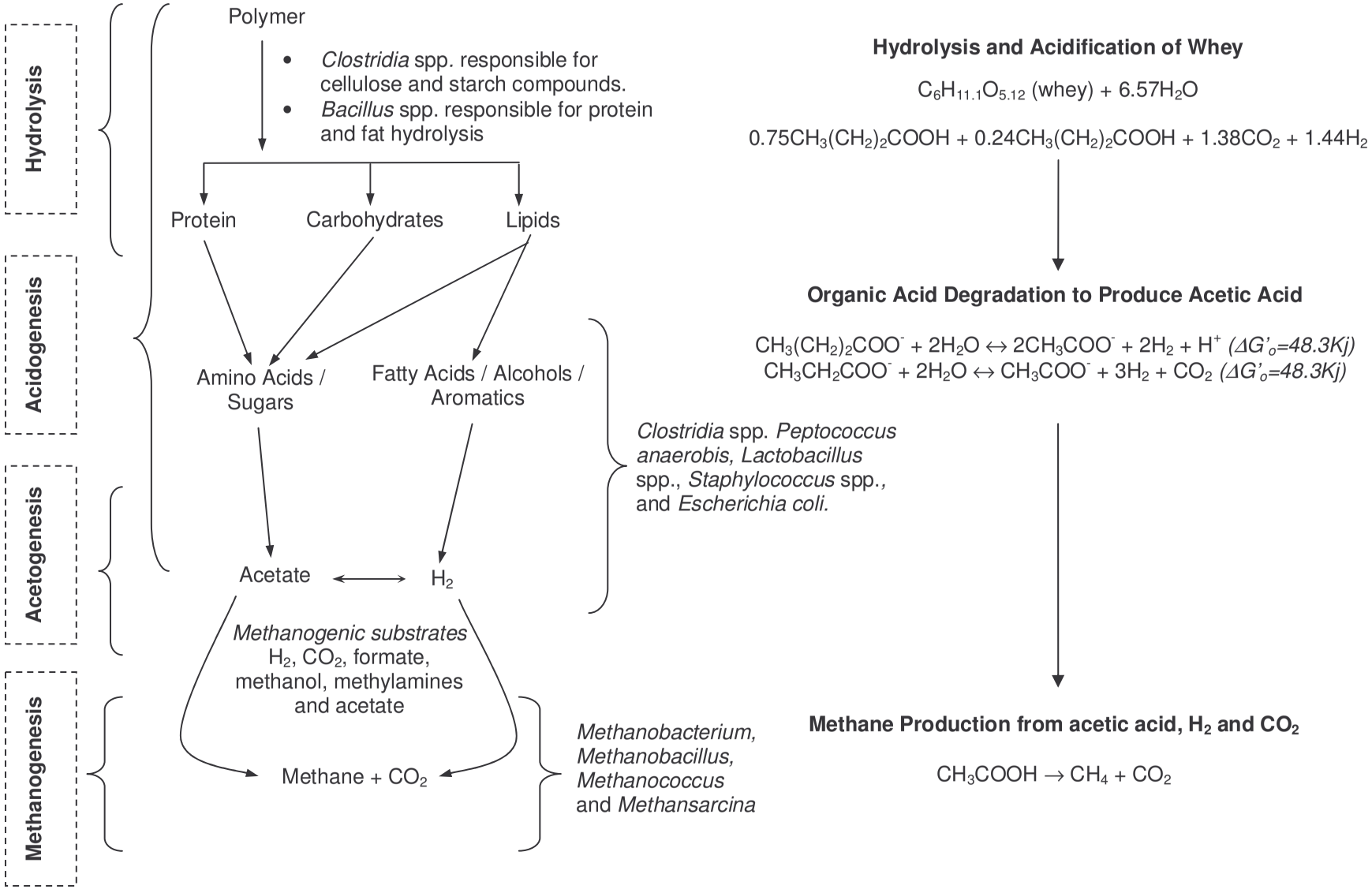


Figure 1a.2: This diagram shows the process of anaerobic degradation from the depolymerisation of polymers down into the subcomponents by certain groups of bacteria in different phases and the by-products that are produced as a result. An example of the breakdown of whey is given on the right (Stronach, Rudd *et al.* 1986).

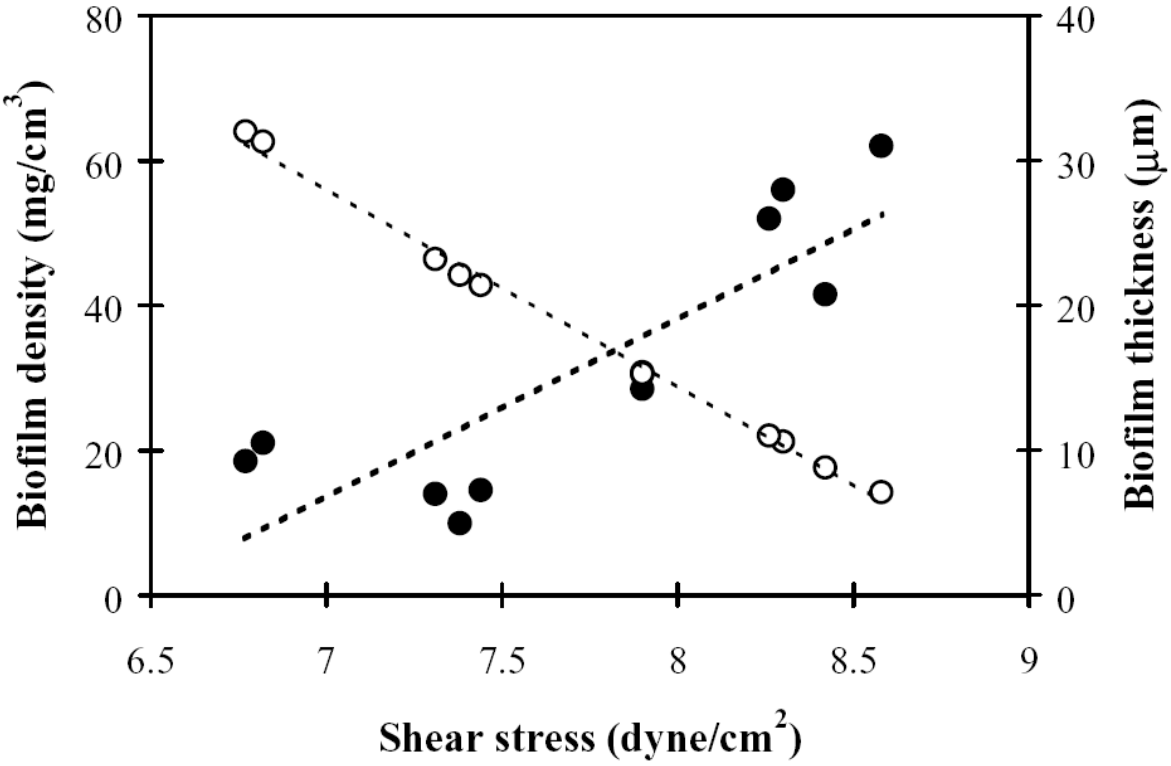


Figure 1a.3: Diagram showing the effect of shear stress on biofilm thickness and density (Liu and Tay 2002).

CHAPTER 1B

THE HYDROGEN ECONOMY AND FERMENTATIVE HYDROGEN PRODUCTION

1b.1 Introduction

Moving from Carbon Based Fuels

The case for moving away from carbon based fossil fuels will not be based on concerns arising from the possibility of their future depletion. Based on estimated sizes of the current conventional fossil fuel reserves and assuming no expansion of reserves by new discoveries, price increases, technological improvements or oil-friendly legislation it is predicted that fossil fuels will be depleted in 500 years (Scott 2005).

Therefore, there is no threat of short term depletion of global fossil fuel production. However, the danger comes from the damage caused by increased CO_2 in the atmosphere, which is thought will induce irreversible climate volatility. If all known reserves are utilised, then atmospheric CO_2 levels are estimated to rise to 250% of pre-industrial age levels, i.e. 700 ppm from the current 370ppm, and pre-industrial 310ppm. Should CO_2 rise to these levels, the climatic disturbances will be unlike anything experience by humans before (Scott 2004a; 2005).

The Cost of Moving to Hydrogen

The question often arises “What is the cost of a litre of H_2 compared to a litre of petrol?” There is however no simple answer. There is a misleading tendency to compare the cost of volume to the cost of energy. For example, 1L of liquefied H_2 or cryofuel contains about one third the amount of energy that 1L of petrol or diesel contains (Table 1b.2). However if one compares mass, H_2 contains approximately three times the amount of energy than the equivalent mass of fossil fuel. Therefore a kg of H_2 would cost more than a kg of petrol or diesel, as would be expected due to the large difference in energy content.

In a similar comparison, the energy density of diesel is slightly less than one litre of petrol (Table 1b.2). However, the lower energy density is countered by the fact that diesel engines convert the fuel more

efficiently in terms of forward motion or traction compared to their petrol based counterparts. One may suggest that vehicles running on H_2 fuel cells are roughly twice as efficient as their petrol counterparts. From this viewpoint, it is thus erroneous to compare the cost of 1L of petrol to 1L H_2.

There are several parameters not factored into fossil fuel usage which increases “costs” and are not internalised in the price. These include the economic and ecological damage due to acid rain, economic losses due to climate disruption, lost man hours due to respiratory ailments, increased medical costs, increased maintenance on buildings and interference with rainfall patterns (Dunn 2002). One factor rarely considered is that increased pollution from fossil fuel usage causes increased electricity consumption due to particulate matter blocking out natural light. This causes sunrises to occur later and sunsets to occur earlier. Therefore lights and heating equipment are switched on earlier and kept on later (Scott 2004b). Considering the usage of fossil fuels and the cost of damage that the use of these fossil fuels causes, one can see from Table 1b.1 that the annual worldwide environmental damage caused by fossil fuels in 1998 was $4 345 billion, or equal to 11% of the gross world product (Veziroglu 1998). Such vast sums of resources may be better spent on health care, education, disease research and control, poverty alleviation and nature conservation to name but a few..

There are no major technical obstacles to the H_2 energy pathway. However the political and institutional barriers are formidable as both government and industry have invested heavily in fossil fuel infrastructure. Hydrogen receives a fraction of the research funding allocated to coal, oil, nuclear, and other mature commercial energy sources (Dunn 2002).

1b.2 Industrial Uses of H_2

Petroleum Processing

In the petroleum industry, hydrogen is catalytically reacted with hydrocarbons by hydrocracking and hydroprocessing. Hydrocracking involves the cracking and hydrogenation of hydrocarbons to produce refined fuels with smaller molecules and higher H:C ratios. In hydroprocessing, hydrogen is used to hydrogenate sulphur and nitrogen compounds and to finally remove them as H_2S and NH_3 (Ramachandran and Menon 1998).

Petrochemical Production

Numerous petrochemicals are produced using hydrogen for example where hydrogen and carbon are reacted over a catalyst at high temperatures to produce methanol. Other petrochemicals that are produced include acetic acid from syngas and cyclohexane from benzene (Ramachandran and Menon 1998). Importantly, hydrogen is used in plastic recycling. In this process, plastic is melted at high temperatures and hydrogenated to crack the plastic polymers into shorter molecules which can then be repolymerised to produce new plastic products (Ramachandran and Menon 1998).

Oil and Fat Hydrogenation

Hydrogen is used extensively to increase the saturation of many fats and oils e.g. margarine (Ramachandran and Menon 1998). Some changes that take place in the final processed product include a change in melting temperature and enhanced resistance to oxidation.

Fertiliser Production

Ammonia, the main chemical in fertilisers, is produced by reacting nitrogen and hydrogen at high temperature. Reportedly this process consumes around 50% of the world's hydrogen production (Ramachandran and Menon 1998). With increasing use of farmland and the desire for greater crop yields, the demand for hydrogen to produce fertilisers is likely to increase further (Ramachandran and Menon 1998).

Metallurgical and Electronic Applications

Hydrogen is used to reduce nickel salt in the Sherrit Gordon process resulting in nickel powder. The process involves the conversion and precipitation of nickel sulphate to elemental nickel leaving ammonium sulphate (Ramachandran and Menon 1998). Hydrogen is also an important component of the silicon electronics industry as it removes native oxides from the silicon surface and so improves silicon chip purity (Ramachandran and Menon 1998). As H_2 becomes cheaper the production of steel could also be moved away from the use of carbon. Currently C removes O_2 from iron ore leaving iron and water (Scott 2004a).

$$2Fe_2O_3 + 3C \rightarrow 4Fe + 3CO_2$$

However if H_2 is used in the process then water becomes the effluent

$$Fe_2O_3 + 3H_2 \rightarrow 2Fe + 3H_2O$$

Hydrogen as an O_2 scavenger

Oxygen is a potent oxidising agent and can cause oxidative damage to industrial metal structures. In metallurgical processes, H_2 and N_2 are used for heating applications to remove O_2, such as in annealing and furnace brazing and powered metal sintering (Ramachandran and Menon 1998). Stainless steel wire annealing is done in artificial atmospheres of approximately 100% hydrogen. In float glass manufacturing, a mixture of 4% H_2 in N_2 is used to prevent oxidation of the molten tin bath the glass is made on by scavenging any oxygen present (Ramachandran and Menon 1998).

1b.3 Hydrogen as a Fuel

The primary application of hydrogen as a fuel is in the aerospace industry. The combination of liquid hydrogen and oxygen as rocket propellants has been used for a number of years and has been found to release the highest amount of energy per unit weight of propellant (Table 1b.2). This type of fuel, has not to date been applied generally, such as in transport vehicles, due to the cost of liquefying and keeping it safe while handling. Even though H_2 burns with a higher efficiency than petrol, safe storage remains a problem as current technologies are prohibitively expensive. For example, metal hydrides such as lanthanum pentanickel ($LaNi_5$) and titanium-iron (TiFe) adsorb hydrogen at room temperature and low pressures making H_2 safe to handle. However, the high cost of these alloys prevents their widespread use (Ramachandran and Menon 1998).

1b.4 Hydrogen Fuel Cells

Fuels cells are electrochemical power generation devices and are classified according to the electrolyte material used. These electrolytes include alkali, phosphoric acid, proton exchange membranes, molten carbonate and solid oxide composed of a zirconium oxide and calcium oxide mixture. H_2 as a fuel in the anode of a fuel cell releases electrons that are transferred through the external load to the cathode where

oxygen reacts with the protons to form water. The flow of electrons may be used for electricity generation. This type of electricity generation is currently under examination as the power source for the next generation of transport vehicles (Linssen, Grube *et al.* 2003).

1b.5 Production of H_2

H_2 may be produced from a variety of sources including steam reformation of CH_4 into H_2 and CO_2, the electrolytic decomposition of H_2S into H_2 and elemental S, thermal conversion of biomass, coal gasification, biological H_2 production via photosynthesis or fermentation and the non CO_2 emitting electrolysis of H_2O and photovoltaic H_2 production (Bockris 2002).

Fermentative Biological Hydrogen Production

Biological H_2 production is not a new discovery as H_2 has been known to be produced in anaerobic digestion (Fig 1a.2) however in conventional anaerobic digestion, the H_2 is consumed by hydrogenotrophic methanogens through a process known as metabolic syntrophy (Wu, Jani *et al.* 1992; Schink 1997; Schnürer, Zellner *et al.* 1999). Fermentative H_2 production is the most common of biological H_2 processes, and uses either biomass or the components from various waste streams for conversion to H_2. Importantly the process is not light limited like photosynthetic H_2 systems and so can operate 24 hours a day. Numerous studies have led to the elucidation of the biochemical pathways use in the process of H_2 formation (Nandi and Sengupta 1998).

The majority of biological H_2 fermentations are driven by the anaerobic metabolism of pyruvate, formed during the catabolism of various substrates. One of two enzymes is responsible for the conversion process. Most bacteria, whose growth is inhibited by molecular O_2, e.g. *Clostridia*, do not contain electron donors of the cytochrome type. Investigations have shown that the main factor which mediates electron flow from pyruvate to hydrogenase is an iron-containing complex designated ferredoxin. In facultative anaerobes, pyruvate is also produced as a key intermediate. Formate is then produced from pyruvate,

which is then converted to H_2 and CO_2 by an additional sequence of anaerobic reactions catalysed by the formate and particulate dehydrogenase enzyme complex (Gray and Gest 1965). Facultative anaerobes have also been shown to produce H_2 through the NADH pathway (Tanisho and Ishiwata 1995) and through end products such as butyric acid.

Generally, the conversion of organic substrates to H_2 is inefficient and results in only 10-20% stoichiometric conversions (Logan, Oh *et al.* 2002). Sustained economic viability of fermentative H_2 production can only occur once efficiencies reach 60-80% (Benemann 1996). It is theoretically possible to produce 12 mol H_2 from 1 mol glucose. However, from a thermodynamic perspective, the most favourable products from the breakdown of glucose are 2 mol acetate and 4 mol H_2 (Hallenbeck and Benemann 2002). A further 4 mol CO_2 per mol acetate could be gained from syntrophic acetic acid oxidation (Angenent, Karim *et al.* 2004). Thus the overall yield would approach 12mol H_2. However, in practice, no whole cell systems have been discovered or developed which are capable of performing stoichiometric conversions of glucose as such a system would not allow energy for cell growth. There are various studies on fermentative H_2 production being conducted worldwide which are focusing on different aspects of fermentative process optimisation (Table 1b.3) with pH, H_2 partial pressure, immobilisation of biomass, feed rates, acetic and butyric acid production being the main foci of study.

Fermentation Feedstock

For sustainable processes, the feedstock used in a fermentative H_2 process would need to be principally carbohydrate, be produced from sustainable resources and be of sufficient concentration that the conversion process is both economically and thermodynamically feasible. To date most investigations into fermentative H_2 production have focused on expensive substrates such as glucose and sucrose. Future feedstocks high in carbohydrates such as those released during the processing of food crops, such as sweet sorghum, sugar beet, corn, wheat or cassava.

The supplementation of an uncontrolled feedstock with mineral supplements would be necessary to ensure that all the nutrient requirements of the bacterial H_2 producing system are met. Numerous elemental deficiencies are known to cause reductions in H_2 production efficiency. For instance, a P limitation is know to cause redirection of the biochemical pathways towards ethanol, butanol and 1,3-propandediol (Dabrock, Bahl *et al.* 1992; Lin and Lay 2004b). Important elements needed within the feed are Fe, Ni, Se and Zn. Fe is a component of the hydrogenase complex, therefore Fe limitation results in lower hydrogenase activity (Lee, Miyahara *et al.* 2001; Lin and Lay 2005). For bacteria containing the formate-hydrogen lyase enzymes, the mineral elements Ni, Mo and Se are required as cofactors (Lengeler, Drews *et al.* 1999). The C:N:P ratio of the waste is also an important consideration that also determines the H_2 production rate (Lin and Lay 2004a).

Fermentation Process Control

The control of the fermentation process is important, especially if the inoculum is obtained from either heat or pH treated sewage sludge. The presence of H_2 consuming methanogens in untreated sewage sludge is problematic and two methods of limiting the growth of the bacteria include operating the reactor at a low pH and increasing the dilution rate to wash the methanogens out (Kim, Hwang *et al.* 2004). The suggested values for H_2 production vary widely however the general consensus is that a pH range between 5.0-5.7 gives the best results.

Numerous studies make use of heat treated sewage sludge to select for *Clostridia* which are known to give higher H_2 production rates than facultatively anaerobic bacteria such as *Enterobacter* spp. (Yokoi, Tokushige *et al.* 1998). However there remains a large number of unidentified bacteria within these inoculum sources which would not be eliminated by either thermal or pH treatment. These unidentified cultures could present process inefficiencies and H_2 sinks. The selection of numerous cultures known for their H_2 production capacity from genomic databases (Kalia, Lal *et al.* 2003) and literature sources would provide a better alternative than the proverbial black box currently in use. In addition, mixed or co-cultures

are known to possess a greater ability to withstand process fluxes than processes using pure cultures (Hashsham, Fernandez *et al.* 2000; Pynaert, Smets *et al.* 2003).

1b.6 Biochemistry and Biophysics of H_2 of Production

Effects of H_2 Partial Pressure

In conventional anaerobic digestors, the H_2 partial pressure is kept low by hydrogenotrophic methanogens. However, where the H_2 producing (acidogenesis and acetogenesis in Fig 1a.2) and H_2 consuming (methanogenesis) stages have been separated for H_2 capture, the H_2 partial pressure is a limiting factor on the thermodynamics of the hydrogenase enzymes. The reaction involves the enzyme-catalysed transfer of electrons from an intracellular electron carrier to protons (H^+). Unfortunately H^+ is a poor electron acceptor (E'_{H2} = -414mV). So the reducing agent must be a strong electron acceptor. Ferredoxin ($E^{o'}_{Fd}$ = -400mV depending on source) and NADH ($E^{o'}_{NADH}$ = -320mV) are two such strong electron acceptors used during H_2 production. The ability of reduced ferredoxin and NADH to reduce H^+ is determined by the redox potential under the experimental conditions. Assuming that the intracellular concentrations of the oxidized and reduced forms of ferredoxin and NADH are equal, H_2 production becomes thermodynamically unfavourable at H_2 partial pressures above:

$$P_{H2.\max} \leq \exp\left\{\frac{2F(E^{o'}_{H_2} - E^{o'}_{x})}{RT}\right\}$$

(Angenent, Karim *et al.* 2004)

where $E^{o'}_{x}$ is the redox potential of the electron donor, F is Faradays constant, R is the ideal gas constant and T is the absolute temperature. For ferredoxin, H_2 production can continue as long as the H_2 partial pressure is below ~0.3atm (3 x 10^4Pa), for NADH the partial pressure needs to be below ~6 x 10^{-4}atm (60 Pa) (Figure 1b.1). Microbes possessing the pyruvate:ferredoxin oxidoreductase can attribute most of the H_2 produced in the system to this reaction. If the H_2 partial pressure is low enough then NADH may also be used to produce H_2, but at best 2 moles of H_2 per mol of hexose. Most of the NADH will however be oxidized through other fermentation pathways such as the butyrate pathway (Figure 1b.1).

H_2 partial pressure has been thought to be responsible for the activation of the propionic acid pathway as H_2 is limiting to its production (Harper and Pohland 1986). However subsequent studies have found no connection between H_2 partial pressure and changes in the production of propionic acid (Inanc, Matsui *et al.* 1996; 1999). There are in addition other end products which present a reduction in H_2 production efficiency. The exact activation mechanisms are unknown; however every reactor will have its optimal range which would be controlled by feed rate, feed regime, feed type, pH range, H_2 partial pressure, redox potential and most importantly the types of cultures present within the reactor.

High Rate H_2 Production

The study of H_2 production has generally occurred in continuously stirred tank reactors, but their applicability for continuous H_2 production is reduced due to their inferior H_2 production potential and the low specific growth rates of the H_2 producers, necessitating low dilution rates (Chen, Lin *et al.* 2001). A higher H_2 production rate could be achieved using a higher dilution rate and consequently a lower hydraulic retention time (time waste spends inside reactor). Cell immobilization techniques have been used in previous studies to improve the cell retention time and showed considerable improvement in H_2 production rates (Kumar, Jain *et al.* 1995; Zhu, Ueda *et al.* 2002). Most H_2 fermentation studies associated with immobilised cell reactors have used packed or fixed bed reactors which often suffer from mass diffusion, clogging and gas holdup problems. To combat these problems the use of a 3 phase anaerobic fluidised bed reactor is (AFBR) advocated. AFBRs are becoming a preferred alternative to suspended planktonic based systems primarily because they are more efficient in solid/liquid separation and can be operated at high dilution rates without encountering washout of cells. Unfortunately, research conducted on H_2 producing fluidised beds is limited with only two previous studies being recorded (Guwy, Hawkes *et al.* 1997; Wu, Lin *et al.* 2003). The study by Wu, Lin *et al.* (2003) immobilised undefined acid treated sewage sludge using acrylic latex plus silicone supplemented with alginate and activated carbon. The study did not achieve high production rates, with ~23 mmol H_2 / (l x h) although the yield was high at 2.67 mol H_2 / mol sucrose. The HRT was as low as 2 hours, however the H_2 content of the biogas was never higher than 38%. The study by Guwv, Hawkes *et al.* (1997) using an undefined culture showed very low

concentrations of H_2 although the study was more focused on using H_2 and dissolved H_2 as indicators of process instability.

Motivation

The fermentative generation of H_2 presents an important part of the strategy aimed at reducing mans impact on the environment from the generation of air and water pollution caused by the use of fossil fuels for energy generation. Economic, monetary and environmental losses are incurred as a result of the continued use of fossil fuels and its associated air and water pollution. It is thus an important objective to increase the reliance on alternative and cleaner energy sources. Previous research in this field has not made major advances in terms of achieving theoretical yields.

No local studies have been reported on the production of H_2 using a high rate anaerobic fluidised bed reactor. However high rate, biofilm based reactors have provided some of the largest H_2 production rates. The source of inoculum for these studies has been mixed, undefined cultures from sewage sludge (Guwy, Hawkes *et al.* 1997; Wu, Lin *et al.* 2003). However the selection of mixed undefined cultures, and the lack of optimised nutrient conditions make comparisons between different H_2 production studies difficult. The majority of H_2 production studies still use mixed undefined cultures as sources of inoculum.

The unquestioned use of generally accepted culture conditions could prevent further progress in H_2 production optimisation efforts. A high rate, anaerobic fluidised bed bioreactor, containing 2 bacterial isolates and fed a modified medium, was investigated for the ability to produce H_2 at a high rate at different hydraulic retention times.

Table 1b.1: Figures of worldwide fossil consumption and environmental damage cost due to fossil fuel usage for 1998. Costing is in American Dollars due to its global applicability (Veziroglu 1998).

Fossil Fuel Consumption	10^{18} J per year
World coal consumption	112
World petroleum consumption-148--World natural gas consumption	105
World fossil fuel consumption	365
Environmental Damage Estimate	(1998 billion $)
Damage due to coal	1 625
Damage due to petroleum	1 853
Damage due to natural gas	867
Total Damage	4 345
Demographic and economic data	
World population (in billions)	5.96
Damage per capita	$ 730.00
World GWP (billion $)	$39 340.00
GWP per capita	$ 6 600.00
Damage/GWP	0.11

Table 1b.2: Comparison of the different energy densities of various fossil fuels compared to H_2 on both a mass (kg) and volumetric (m) basis (Veziroglu 1998).

Fuel	Chemical Formula	Energy per unit Mass Joules/kg	Energy per unit Volume Joules/m
Liquid fuels			
Fuel oil	$C_{\leq 20}\ H_{\leq 42}$	45.5	38.65
Petrol	$C_{5\text{-}10}\ H_{12\text{-}22}$	47.4	34.85
Jet fuel	$C_{10\text{-}15}H_{22\text{-}32}$	46.5	35.30
Liquid petroleum gas	$C_{3\text{-}4}H_{8\text{-}10}$	48.8	24.40
Liquid natural gas	$\sim CH_4$	50.0	23.00
Methanol	$CH_{3O}H_4$	22.3	18.10
Ethanol	CH_2H_5OH	29.9	23.60
Liquid H_2	H_2	141.9	10.10
Gaseous Fuels			
Natural gas	$\sim CH_4$	50.0	0.040
Gaseous H_2	H_2	141.9	0.013

Table 1b.3: Recent studies conducted on fermentative production if H_2, the different reactor types employed, the optimisation attempt, feed substrate used and maximum H_2 yield (Angenent, Karim *et al.* 2004).

Reactor Type	Optimisation	Substrate	Maximum H_2 Yield (mol H_2/mol hexose)	Reference
Batch	Initial pH & acetic/butyric acid	Sucrose / starch	1.8	(Khanal, Chen *et al.* 2004)
Fluidised Bed	Reactor configuration	Sucrose	1.3	(Wu, Lin *et al.* 2003)
CSTR	H_2 partial pressure	Wheat starch	1.9	(Hussy, Hawkes *et al.* 2003)
Batch-fed	Inhibition of acetic/butyric acid	Glucose	2.0	(Chin, Chen *et al.* 2003)
Upflow reactor	Reactor operation, temperature	Wastewater	2.1	(Yu, Zhu *et al.* 2002)
Batch	Immobilised biomass	Sucrose	2.0	(Wu, Lin *et al.* 2002)
Fermentor	Biomass granules	Sucrose	2.1	(Fang, Liu *et al.* 2002)
Fermentor	pH	Glucose	2.1	(Fang and Liu 2002)
Batch	H_2 partial pressure, substrate	Sucrose, lactate	0.5	(Logan, Oh *et al.* 2002)
CSTR	HRT	Glucose, sucrose	2.2	(Chen and Lin 2001)
Batch/Chemostat	Peptone addition	Cellulose	2.0	(Ueno, Haruta *et al.* 2001b)
Batch	Nitrogen source	Glucose	2.4	(Ueno, Haruta *et al.* 2001a)
Batch	pH and substrate levels	Sucrose	2.5	(van Ginkel, Sung *et al.* 2001)
CSTR	H_2 partial pressure	Glucose	1.4	(Mizuno, Dinsdale *et al.* 2000)

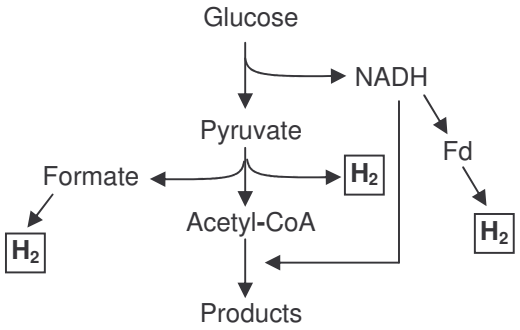


Figure 1b.1: The simple schematic representation of the breakdown pathway of glucose and the points at which H_2 is generated (Tanisho, Kuromoto *et al.* 1998).

CHAPTER 2

ISOLATION, CHARACTERISATION AND USE OF 2 BACTERIAL ISOLATES FOR INTENDED USE IN A FLUIDISED BED REACTOR

CHAPTER 2A

ISOLATION AND CHARACTERISATION OF BACTERIAL ISOLATES INTENDED FOR USE IN AN ANAEROBIC FLUIDISED BED REACTOR

Abstract

Anaerobic treatment research has recognised that biofilm reactors present distinct advantages due to increased conversion rates, capacity and efficiency. These advantages allow higher volumetric loading rates, shorter HRTs and lower biomass washout. Selection of suitable cultures for bioreactor research depends on equipment availability and biological demands of the culture. In H_2 production studies, the facultatively anaerobic *Enterobacteriacae* family is used due to their uncomplicated nutrient requirements and ease of isolation with selective media. Further determination of growth characteristics, such as growth rate and the effect of pH on growth of isolates, are important for bioreactor optimisation efforts. In this study, 2 strains from the *Enterobacteriacae* family, *Enterobacter cloacae* Ecl (*E. cloacae* Ecl) and *Citrobacter freundii* Cf1 (*C. freundii* Cf1), were isolated from partially treated sewage sludge and soil samples, respectively, using selective MacConkey agar, modified to include ferric citrate (1.5g/L) and sodium thiosulphate (5.0g/L), which increased the differentiating contrast between the two cultures based on colony colour. Isolates were further characterised by biochemical tests and identified using the Enteric/NonFermenter BBL™ Kit. Growth characteristics of these two isolates showed growth at a pH range of 5.5-8.5 after 24 hours in buffered nutrient broth. *In vitro* growth rates for *E. cloacae* Ecl and *C. freundii* in nutrient broth (NB) Cf1 were 33 and 35 minutes, respectively. The pH values showing growth and the growth rates of the isolates indicated that they would be able to grow under high dilution rates and over a wide pH range. In addition, the startup of a reactor utilising these bacteria could be accomplished relatively quickly due to these high growth rates. It was determined that these two isolates would perform adequately in bioreactor studies.

2a.1 Introduction

With regard to anaerobic treatment systems it was recognised in the 1970s that there were significant benefits in utilising biofilm reactors as this increased the rate, capacity and efficiency of the anaerobic digestion process. The immobilisation of biomass allows for shorter HRTs, higher volumetric loading rates and lower biomass washout. Often the culture compositions used within these reactors have not been given significant consideration, with largely undefined mixed cultures from sewage processes being the most popular inoculum source.

The use of smaller defined cultures in anaerobic treatment may not give the greatest system robustness, but using known cultures allows the development of a model system for baseline data. The choice of cultures for the production of H_2 depends on expertise and equipment available for culturing. Many of the best H_2 producing bacteria e.g. *Clostridia* spp. are also obligate anaerobes. Therefore basic Petri dish culture maintenance and inoculum preparation is complicated by the need to perform all operations with specialised anaerobic equipment. For relatively new and simple processes, the use of facultatively anaerobic bacteria has proved to be adequate. Most of the Family *Enterobacteriacae* are known to be H_2 producers with the two Genus's, *Enterobacter* (Rachman, Furutani *et al.* 1997; Rachman, Nakashimada *et al.* 1998; Yokoi, Tokushige *et al.* 1998; Kumar, Monga *et al.* 2000; Palazzi, Fabiano *et al.* 2000) and *Citrobacter* (Kanayama, Sode *et al.* 1987; Allan, Callow *et al.* 2002; Jung, Kim *et al.* 2002; Oh, Seol *et al.* 2003) being used in numerous H_2 production studies. Both are rod shaped, usually motile, gram negative bacteria that are found in a wide range of environments and are easy to work with and isolate (Krieg and Holt 1984).

The development of selective media for bacterial isolation is important when trying to quickly and reliably isolate strains from environmental samples. The use of selective differential media allows for the isolation of certain groups or species of bacteria based on metabolic or physiological characteristics. The inclusion of agents such as bile salts, crystal violet (MacConkey agar) or eosin (Eosin Methylene Blue agar) helps with the isolation of gram negative enteric bacteria. These media are still general selective media, as

numerous species from the *Enterobacteriacae* family can grow on them. Furthermore, in samples where two or more bacterial species are present, it is important to include additional differentiating mechanisms to a differential selective medium to increase the contrast between bacterial isolates that give similar colony morphologies.

Following isolation and identification, the determination of growth parameters for bacterial isolates is important for bioreactor optimisation. The generic growth conditions for a bacterial family or genus often need to be revisited for the isolates concerned to ensure more accurate growth conditions. Parameters such as the pH growth range and growth rates are two examples. Although microorganisms will often grow over wide pH ranges, there are limits to their pH tolerances. Drastic variations in pH will disrupt the plasma membrane or inhibit the activity of enzymes of membrane transport proteins (Prescott, Harley *et al.* 1999). The majority of bacteria maintain their cytoplasmic pH near neutrality, although they are able to grow in a much wider range of external pH values and will remain relatively unaffected. For example, *Escherichia coli* changes its internal pH by less than 0.1 pH unit per unit change in the external pH 4.5-7.9 range. This pH homeostasis is achieved by a combination of active and passive pH control mechanisms (Lengeler, Drews *et al.* 1999).

Population growth is traditionally analysed using a growth curve performed in batch culture. As no fresh medium is provided, nutrients decline and waste products increase as microbial cell numbers increase. There are typically four phases of growth that are observed during the growth curve. Lag phase is the first phase and is typically the period in which ATP, cofactors and ribosomes are replenished. Following this is the exponential phase at which the microbes grow at the maximum rate possible under the given conditions. The rate of growth in this phase is constant. The growth data from this phase is used for the calculation of generation times (*g*) and mean growth rate constants (*k*). Generation times are important as they allow an estimation of the dilution rate at which cell washout will occur if the biomass is not immobilised. The last two phases are the stationary phase and death phase which will occur when the cell concentration has reached approximately 10^9cells/ml, nutrients are limited and waste products have

increased. Increased levels of waste products and elongated periods of nutrient deprivation lead to the cell death phase.

The purpose of this study was to isolate strains of *Enterobacter* and *Citrobacter* using media developed specifically for their identification. Furthermore, the pH growth range and growth characteristics of the 2 selected isolates were determined for use as a baseline in future studies using an anaerobic fluidised bed bioreactor.

2a.2 Materials and Methods

Source of Inoculum

Partially treated sewage samples were obtained from Goudkoppies Wastewater Treatment Works (Johannesburg, South Africa), and garden soil samples were obtained locally. Five gram samples of garden soil and 10ml of sewage sludge was pre-incubated in 75ml distilled H_2O containing 5g/L lactose and 1g/L for 24 hour at 37^{o}C at 130rpm to boost numbers of *Enterobacter* and *Citrobacter* cells.

Isolation and Identification

A dilution series of the pre-incubated sewage sludge in 0.85% sterile saline was prepared and spread plated onto unmodified MacConkey agar (Merck, Midrand, South Africa). These plates served as presumptive isolation medium for *Citrobacter* spp. The highest plated dilutions showing growth were re-plated onto MacConkey agar modified with ferric citrate (1.5g/L) and sodium thiosulphate (5.0g/L). These additives permitted the differentiation of *Citrobacter* spp. from *Salmonella* spp. which normally form as 1-2mm, white, mucoid colonies. The additives allow the formation of a black H_2S precipitate to form at the centre of the *Citrobacter* spp. colonies, but not the *Salmonella* spp. colonies. Five presumptive *Citrobacter* strains were isolated in this manner. These isolates were then inoculated onto Kligler Iron agar slants. Subsequently, only two of these isolates were positive for *Citrobacter* spp. based on glucose and lactose

fermentation, gas and H_2S production. These two isolates were identified as *Citrobacter freundii* using Enteric/NonFermenter BBL™ Crystal identification kits (Becton Dickinson, New Jersey, USA) together with indole and oxidase tests.

For the isolation of *Enterobacter* spp., Eosin Methylene Blue agar (EMB) agar (Oxoid, Basingstoke, UK) was used with no modifications. A dilution series was also prepared in saline of the pre-incubated garden soil samples and spread plated onto EMB agar plates. Seven presumptive isolates were identified from the highest dilution based on the colony morphology characteristics of 4-6mm diameter, pink to purple colour, raised and mucoid, tending to become confluent and having grey-brown centres by transmitted light. Seven isolates were tested on Kligler Iron agar slants, of which only 6 were positive for *Enterobacter*, based on previously described criteria. Only 3 of the presumptive isolates were identified as *Enterobacter cloacae* strains using the Enteric/NonFermenter BBL™ Crystal identification kits (Becton Dickinson) together with indole and oxidase tests.

Citrobacter freundii Cit1 (South African Bureau of Standards, Pretoria, South Africa) was used as a positive control for *Citrobacter* spp. isolation, whereas *Klebsiella pneumoniae* Kle5 (South African Bureau of Standards) was used as a negative control for *Enterobacter* spp. isolation due to the similarity in growth characteristics. Isolates tested on selective media were transferred from fresh 24 hour NA plates to prevent interference between selective media. All incubations were carried out at 37^{o}C for 24 hours.

Growth Characteristics

The *in vitro* growth of both *Enterobacter cloacae* Ecl (*E. cloacae* Ecl) and *Citrobacter freundii* Cf1 (*C. cloacae* Cf1) was determined at 37^{o}C. Individual 100ml erhlenmeyer flasks containing 75ml each of nutrient broth (NB) (Merck) preheated to 37^{o}C were inoculated with approximately 3 log cfu/ml of either *E. cloacae* Ecl or *C. cloacae* Cf1, previously grown overnight. One millilitre aliquots were removed from the flasks at hourly intervals for 7 hours and the optical densities determined at 600nm. Uninoculated media was used as a negative control. In addition, growth of the isolates was also monitored by duplicate plating

of 1ml aliquots at the same time intervals using the droplet plate technique on NA (Lindsay and von Holy 1999). Plates showing colonies between 5 and 50 colonies were selected for counting. The experiment was repeated on 3 separate occasions with all plates incubated at 37°C.

Analysis of growth data was conducted using the following equations (Prescott, Harley *et al.* 1999):

$$n = \frac{\log N_t - \log N_0}{\log 2}$$

solving for *n* gives the number of generations in time *t*

$$k = \frac{\log N_t - \log N_0}{\log 2t}$$

k which is the mean growth rate constant is the number of generations per unit time

$$g = \frac{1}{k}$$

g is the mean generation or doubling time, and is expressed as hours or minutes per generation

Effect of pH on Growth

Thirteen 100ml ehrlenmeyer flasks each containing 75ml of buffered NB, adjusted to pHs ranging from pH4 to pH10 in increments of 0.5 pH units, were prepared. The following 0.01M buffers were used to stabilise pH during growth: Acetate (pH 5.0) for range 4.0-5.0, Pyridine (pH 6.0) 5.5-6.0, Phosphate (pH 7.5) for pH 6.5-7.5, Tris Buffer (pH 9.0) for pH 8.0-9.0, Tris Buffer (pH 10.0) for 9.5-10.0. All buffers were prepared at 20°C and used at 37°C (Beynon 1996). An uninoculated flask was used as a negative control. Broths were inoculated with 1ml of an overnight culture of either *E. cloacae* Ecl or *C. freundii* Cf1 serially diluted in sterile saline from 9.0 log cfu/ml to 3.0 log cfu/ml. Flasks were incubated in duplicate at 37°C for

24 hours (130rpm). One ml aliquots were removed from each flask after 1 hour and plated on NA using the droplet plate technique as described previously and incubated overnight at 37^{o}C (Lindsay and von Holy 1999). The experiment was repeated on 3 separate occasions.

2a.3 Results

Isolation of Presumptive Enterobacter *spp.*

Of the 7 presumptive *Enterobacter* spp. isolates that produced pink, mucoid and confluent colonies on EMB, 6 were positive for *Enterobacter* spp. status by the reactions presented on Kligler Iron agar slants. These results showed red slopes, yellow butts, gas production but no H_2S. Therefore only glucose was fermented by these isolates. Of the 6 isolates tested on BBL™ Crystal kits, 3 were identified as *Enterobacter cloacae.* One isolate, *E. cloacae* Ecl, was selected for use in further studies.

Isolation of Presumptive Citrobacter *spp.*

Samples of enriched sewage sludge were plated directly onto modified MacConkey agar. Only 5, 1-2mm, white colonies with brown-black centers were found in all isolation attempts. Only 2 of the 5 presumptive *Citrobacter* spp. isolates tested positive on Kligler Iron agar giving yellow slants, yellow butts, gas and H_2S production. This indicated that both glucose and lactose were fermented. Only one isolate was identified as *Citrobacter freundii* using a BBL™ Crystal kit. This isolate was labeled *Citrobacter freundii* Cf1 (*C. freundii* Cf1). Gram stains done on the isolates can be seen in Fig 2a.3.

Growth Characteristics of Enterobacter and Citrobacter Isolates

Both the *C. freundii* Cf1 (Fig 2a.1 A) and *E. cloacae* Ecl (Fig 2a.1 B) isolates demonstrated growth over a pH range of pH 5.5-8.5 with counts for *C. freundii* Cf1 averaging 9.4 log cfu/ml and *E. cloacae* Ecl averaging 9.4 log cfu/ml for the entire pH5.5-8.5 range (Fig 2a.1). Both isolates showed a small decrease

in counts to 9.0 log cfu/ml at pH 5.0 and pH 9.0. At both pH4.5 and pH9.5, both isolates showed limited growth with counts being reduced to near 4.0 log cfu/ml. Counts for both isolates decreased further to below the lower detection limit (1.0 log cfu/ml) when the cultures were grown at pH4.0 and pH10.0.

Both cultures displayed rapid growth in the growth curves performed in nutrient broth with the mean generation time (*g*) for both the *E. cloacae* Ecl and *C. freundii* Cf1 isolates being 33 and 35 minutes per generation, respectively (Table 2a.1).

2a.4 Discussion

The development of a more selective agar used in this experiment was successfully applied when isolation and identification of isolates of *Enterobacter* spp. and *Citrobacter* spp. were sought. When using two bacterial isolates which need to be enumerated from mixed samples, it is important to establish a selection method which allows for accurate and reliable identification. Ferric citrate (1.5g/L) and sodium thiosulphate (5g/L) in MacConkey were included as an additional differential agent, as the contrast between the *E. cloacae* Ecl and *C. freundii* Cf1 colonies was not always sharply defined as fermentation of lactose was the sole differentiating factor. The inclusion of ferric citrate and sodium thiosulphate aided in the identification of *C. freundii* Cf1 colonies. The ferric citrate resulted in white translucent colonies on unmodified MacConkey agar, growing as white colonies with black centres on modified agar due to the formation of $FeSO_3$ precipitates.

As the intention was to use the two isolates in this study for use in a fluidised bed bioreactor, it was important to establish the range of pH at which these isolates could grow. Both isolates are found in a wide range of environments, such as man and other mammals, and birds, reptiles, and amphibians. They are also found in soil, water sewage and food (Krieg and Holt 1984). Growth in a wide range of environments suggests a similar trend of versatile pH values. Results from this study on effects of pH on growth of these 2 isolates suggested that the optimum growth range was similar to that of other many members the *Enterobacteriacae* family (Atlas and Bartha 1998). The effect of pH on growth was an

important parameter to establish for the future use in the fluidised bed reactor, as pH fluctuations during fermentations are known to cause rapid pH drops due to the production of volatile fatty acids such as acetic, butyric and propionic acid. The effect of pH on the growth of the 2 isolates used in this study was carried out in NB. Although NB would not be utilised in an AFBR system, we propose that the bacterial cells would be affected similarly by pH independently of the type of growth medium used.

The growth curves performed in nutrient broth showed that *E. cloacae* Ecl and *C. freundii* Cf1 had generation times of 0.55 hours or 33 minutes per generation and 0.58 hours or 35 minutes per generation, respectively. This was comparable to the reported generation times of 21 minutes for *Escherichia coli* and 26 minutes for *Bacillus subtilis* (Prescott, Harley *et al.* 1999) in an unknown medium.

Bacteria present in matrix enclosures, termed biofilms, are different both in their genetic competence and their metabolic activity compared to their planktonic counterparts. Growth rates are often markedly different from the growth rates of the planktonic mode of growth. As such, growth rate data obtained from planktonic bacterial studies cannot be directly extrapolated to biofilm bacteria. However, the data may provide a baseline estimation which could provide information regarding the growth rates in future studies. Therefore the data gained from the planktonic growth rates shows that the time required for an AFBR to reach steady state will be shortened, as both *E. cloacae* Ecl and *C. freundii* Cf1 have high growth rates.

2a.5 Conclusion

1. The isolation of bacteria using modified media for use in a fluidised bed was successful as the isolates, *E. cloacae* Ecl and *C. freundii* Cf1, are part of the *Enterobacteriacae* Family. As such they are relatively simple to culture.

2. It was found that these two isolates are able to grow from pH5.0 to pH9.0 which will be useful when being used in a fluidised bed bioreactor as the pH values are likely to fluctuate widely during the initial

stages of bioreactor commissioning. Further they have growth rates of approximately 30 minutes, which may play a significant role in reducing the time required for the reactor to reach a steady state.

Table 2a.1: The following growth parameters were calculated using direct data, or log cfu/ml for both *E. cloacae* Ecl and *C. freundii* Cf1 isolates.

Parameter	Nutrient Broth	
	E. cloacae Ecl	*C. freundii* Cf1
n	0.91	0.86
k	1.82	1.72
g	0.55	0.58

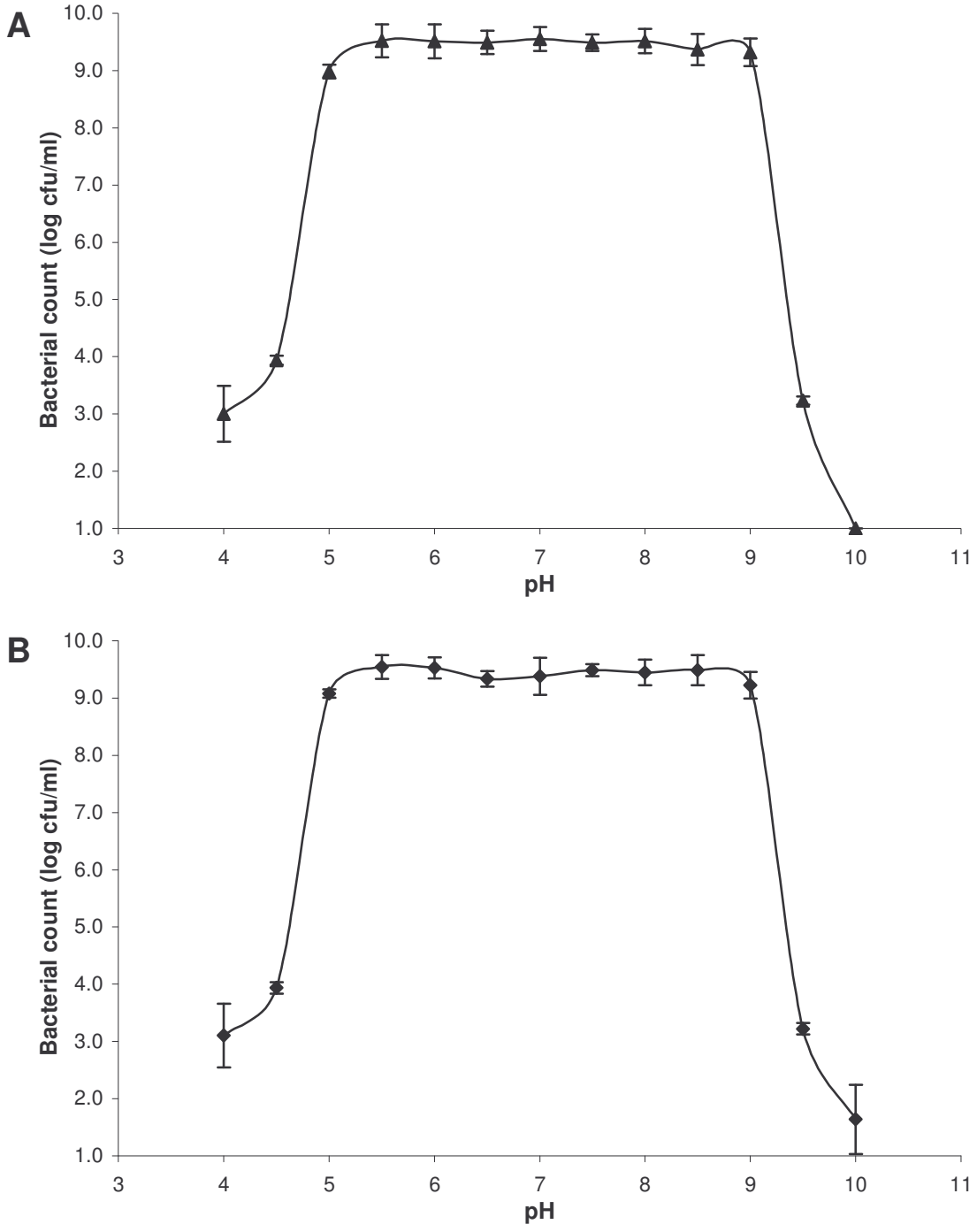


Figure 2a.1: pH growth range profile of the bacterial isolates (A) *C. freundii* Cf1 and (B) *E. cloacae* Ecl grown overnight at 37^{o}C in nutrient broth at pH values ranging from 4.0 to 10.0.

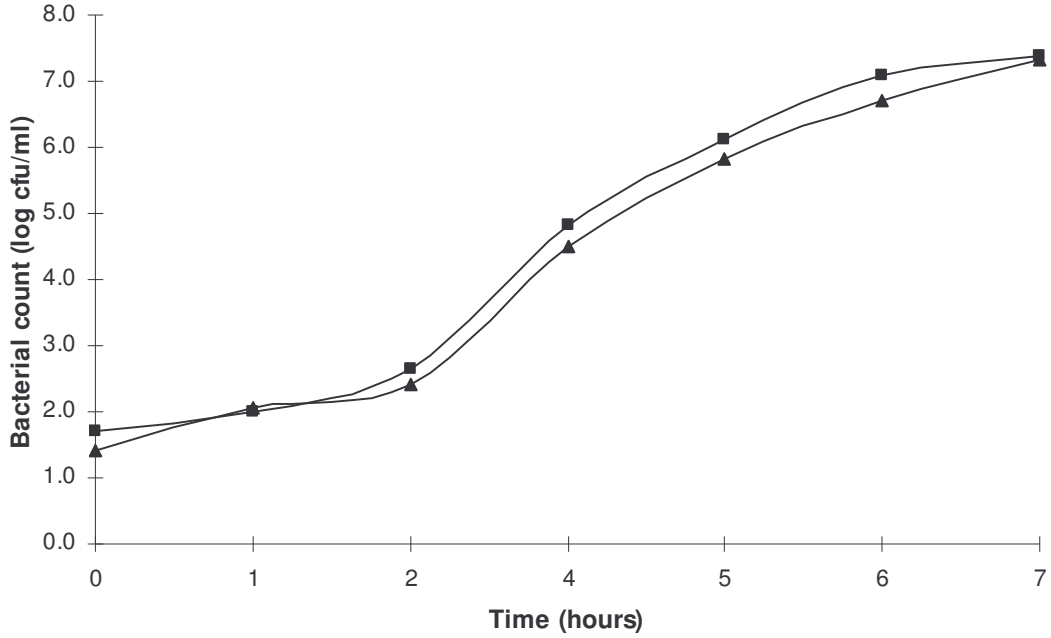


Figure 2a.2: Growth curve representing the increase in viability count (log cfu/ml) for bacterial isolates *E. cloacae* Ecl ▲ and *C. freundii* Cf1 ■ grown in nutrient broth over a period of 7 hours. Standards deviations not shown as it averaged at 0.14 log cfu/ml for *E. cloacae* Ecl and 0.11 log cfu/ml for *C. freundii* Cf1.

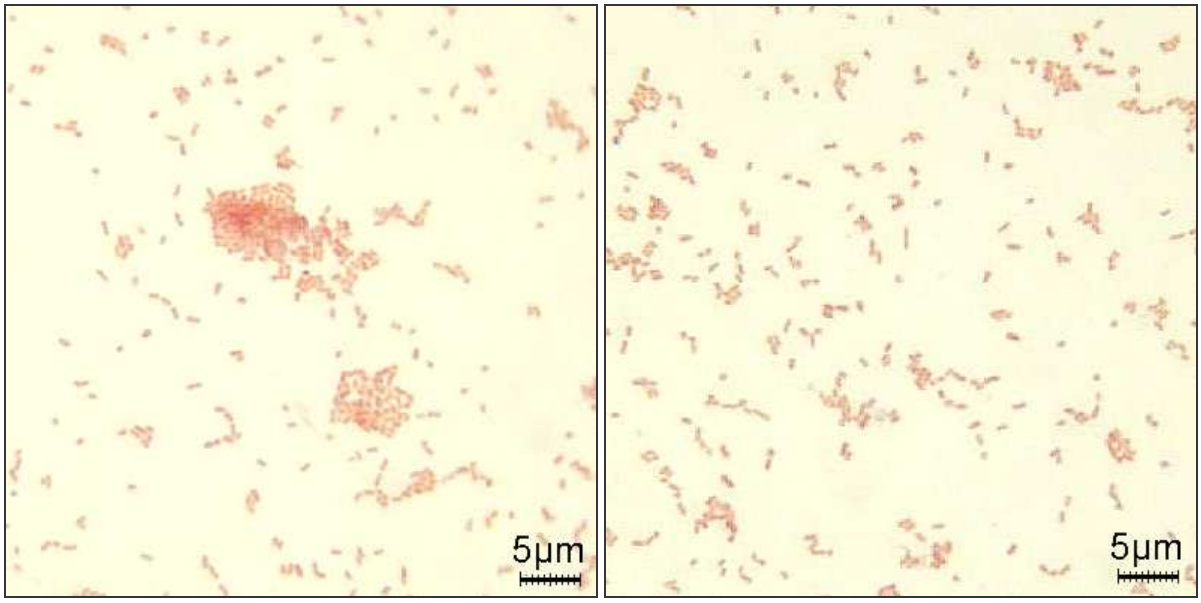


Figure 2a.3: Gram stain images of both *E. cloacae* Ecl (left) and *C. freundii* Cf1 (right) showing gram negative rods of size 2-3µm in length. (Magnification 1000x oil immersion)

CHAPTER 2B

CARBON : NITROGEN : PHOSPHOROUS RATIOS INFLUENCE BIOFILM FORMATION BY *ENTEROBACTER CLOACAE* AND *CITROBACTER FREUNDII*

(presented in part a poster at the 43rd Annual Conference of the Microscopy Society of Southern Africa titled “Scanning Electron Microscopy Study of Biofilm Formation using Different C:N:P Ratios”)

Abstract

Biofilms, defined as matrix enclosed bacterial populations, have been widely exploited in wastewater treatment, although determinants affecting bacterial attachment are not yet fully understood. In particular, the effect of different nutrients e.g. Carbon (C) to Nitrogen (N) to Phosphorous (P) ratios, on biofilm formation is poorly understood. Furthermore, in bioremediation processes, such as wastewater treatment, ratios of C:N:P are often based only on removal efficiencies and do not include biomass yields of the biofilm. In this study we utilised a well known nutrient medium formulation used in fermentative biohydrogen studies, the Endo formulation, to adjust the C:N:P ratios and hence test the biofilm forming response of *E. cloacae* Ecl and *C. freundii* Cf1. Two different C concentrations, one containing 17.65g/L and the other 8.84g/L sucrose, formed the basis for 4 different C:N:P ratios, 2 at higher C:N:P ratios (334:84:16.8 and 34:84:3) and 2 at lower C:N:P ratios (334:28:5.6 and 334:28:1). The ratios were calculated using relative proportions of C:N:P atoms between C:N:P chemical sources used in the medium. Each of the C concentrations, at all 4 C:N:P ratios, were tested on both single and binary biofilms of *E. cloacae* Ecl and *C. freundii* Cf1. Attached cells were enumerated after dislodging the biofilms which had formed on granular activated carbon (GAC). Bacteria in single species biofilms were plated on NA, whereas bacteria in binary species biofilms were plated on MacConkey agar modified with ferric citrate (1.5g/L) and sodium thiosulphate (5.0g/L). Scanning electron microscopy (SEM) was also used to observe the effect of the ratios on bacterial attachment and biofilm morphology. The modified medium containing 17.65g/L sucrose and having a C:N:P ratio of 334:28:5.6, resulted in significantly ($P < 0.05$) showed the greatest counts of attached cells for both single and binary species biofilms. At this ratio, for single species biofilms, counts of 7.73 log cfu/g GAC and 9.3 log cfu/g GAC were recorded for *E. cloacae* Ecl and *C. freundii* Cf1, respectively. Furthermore, in binary species biofilms, counts of 8.2 log cfu/g GAC and 6.34 log cfu/g GAC were recorded for *E. cloacae* Ecl and *C. freundii* Cf1, respectively. Scanning electron micrographs showed qualitative evidence that the 334:28:5.6 ratio encouraged more complex and extensive biofilm growth for both single and binary species biofilms. Further modification of this ratio is encouraged to establish boundary limits for biofilm formation *in vitro* as the information will be important for future biofilm bioreactor studies.

2b.1 Introduction

Biofilms, are defined as matrix-enclosed bacterial populations which adhere to each other and to surfaces (Costerton and Lewandowski 1995). Observations have conclusively shown that biofilm bacteria predominate, numerically and metabolically, in virtually all nutrient-sufficient ecosystems. Therefore as the biofilm mode of growth is especially predominant in aquatic systems, they have been exploited in wastewater treatment systems to great effect. There are numerous factors which affect the ability of bacteria to attach to and form biofilms on surfaces which are in regular contact with water. The substratum structure reportedly promotes the attachment of bacteria to the surface and there is greater evidence of attachment when the surface roughness or rugosity increases (Costerton and Lewandowski 1995). Other factors, such as the coating of the attachment substrate with biomolecules, e.g. proteins and polysaccharides, and the hydrodynamic flow velocity immediately adjacent to the attachment substrate, also influence biofilm formation. In addition, certain cellular properties of the attached bacteria, such as the presence of fimbriae and flagella, and the production of EPS, also play a role (Donlan 2002). The concentrations of nutrients in the aqueous medium surrounding the biofilm also affect biofilm development. Reportedly, increases in nutrient concentrations correlated with increased numbers of attached bacterial cells in a laboratory study (Cowan, Warren *et al.* 1991).

The attachment of bacteria to surface substrates in wastewater treatment readily occurs. However, the generation of suitable quantities of biofilm biomass is a critical factor, and is often affected to a large extent on the availability of nutrients, especially C, N and P. In other biological systems, the ratio of C:N:P has been shown to affect various organisms in that system e.g. plants and soil (Georg Joergensen and Scheu 1999; Misra and Gupta 2001; Baird and Middleton 2004; Saini, Bhandari *et al.* 2004). Within the context of microorganisms, N is required to form proteins, cell wall components and nucleic acids, with NH_4^+ being the preferred N source (Lengeler, Drews *et al.* 1999), P forms part of the ATP energy system and sugar phosphate backbones of nucleic acids, and C forms the major energy supply and comprises 50-80% of the exopolysaccharide matrix. Despite the importance of C:N:P ratios on microorganism growth, literature on the effect of C:N:P ratios on biofilm formation is limited. Literature is available for the

C:N:P ratios required for wastewater treatment, with a 100:5:1 ratio for aerobic treatment and 250:5:1 for anaerobic treatment (Ammary 2004). These theoretical ratios were formulated by simplifying organic matter to glucose, giving the formula $C_6H_{12}O_6$, with biomass given the formula $C_5H_7NO_2$. The derivation of these ratios and the subsequent ratios for various wastewaters in the past has not taken into account the different biomass yields that particular wastewaters achieve. Recently, it has been suggested that the following formula be used to select C:N:P ratios in wastewater treatment systems and is based on removal efficiency (E) and observed cell yield (Y_{obs}) (Ammary 2004). This formula to date has not been widely implemented.

$$C:N:P = \left[\frac{41}{(E)(Y_{obs})}:5:1\right]$$

The aim of this study was to establish the effect of four different C:N:P ratios and two different concentrations of a modified Endo formulation medium on the attachment and development of *E. cloacae* Ecl and *C. freundii* Cf1 single and binary species biofilms. The effect on both single and binary species biofilms was determined using scanning electron microscopy and plate counts.

2b.2 Materials and Methods

Bacterial Isolates

The bacterial isolates *E. cloacae* Ecl and *C. freundii* Cf1, used in this biofilm study have been previously isolated from garden soil and sewage sludge, respectively (Chapter 2a).

Nutrient Medium Formulation

The nutrient media used in this study were variations of the Endo formulation (Endo, Noike *et al.* 1982) (Tables 2b.1, 2b.2). C:N:P ratios were based on C, N and P, atom:atom, concentrations and not the COD equivalents. The first concentration of sucrose used in this study was 17.65g/L (Table 2b.1) and was

termed the Higher Endo Concentration. The second concentration of sucrose was 8.84g/L (Table 2b.2) and was termed the Lower Endo Concentration.

Four different ratios of C:N:P were used. Two of the ratios were termed High C:N:P and consisted of 334:84:16.8 and 334:84:3, while the other 2 ratios were termed Low C:N:P and consisted of 334:28:5.6 and 334:28:1 (Table 2b.1 and 2b.2)

Schott bottles containing 100ml of each medium formulation and 1g of 0.6-1.1mm washed granular activated carbon (GAC) (Associated Chemical Enterprises, Johannesburg, South Africa), were inoculated with 1ml of an overnight culture of either *E. cloacae* Ecl or *C. freundii* Cf1 for the single species biofilms or 1ml of an overnight culture from each isolate for the binary species biofilms. All samples were pre-warmed and incubated at 37^{o}C for 24 hours and 130rpm.

Biofilm detachment studies were conducted as described by Lindsay and von Holy (1997). Schott bottles were emptied of liquid contents and the GAC was rinsed 3 times in sterile saline to remove unattached cells. Twenty grams of 5mm diameter sterile glass beads and 9ml sterile saline were placed in the bottles containing the GAC. Samples were then shaken vigorously by hand for 10 minutes to remove the attached cells from the GAC surface, after which samples were allowed to recover for 20 minutes. Serial dilutions where then prepared in sterile saline before plating using the droplet plate technique as described previously (Lindsay and von Holy 1999). Dislodged bacteria from single species biofilm experiments were plated onto NA plates, whereas bacteria dislodged bacteria from binary species biofilm experiments were plated onto MacConkey agar modified with ferric citrate (1.5g/L) and sodium thiosulphate (5.0g/L).

Scanning Electron Microscopy

For binary species biofilms, 1g GAC samples were rinsed twice with sterile distilled water to remove unattached cells. A few granules of GAC were then fixed in 3% glutaraldehyde for 24 hours, processed

through an ethanol dehydration series of 20, 30 40 50 60 70 80 90, 95, 100% for 10 minutes each (Lindsay and von Holy 1997), mounted and coated with thin gold-palladium splutter. The samples were viewed using a JEOL JSM-840 SEM (Japan), at 20kV and a working distance of 15mm. The sizes of cells present on GAC were estimated using the scale bars on the SEM.

Statistical Analysis

Significant differences between counts obtained at different C:N:P ratios in both single and binary species biofilms were calculated. In addition, the significance of the effect the individual bacterial isolates had on the level of attachment in binary species biofilms was also determined using multi-factorial analysis of variance (ANOVA) at the 95% confidence interval with the STAGRAPHICS V. 7 (Manugistics Inc. and Statistical Graphics Corporation, 1993) program.

2b.3 Results

E. cloacae Ecl - *Higher Endo Concentration*

Fig 2b.1 presents attached counts of *E. cloacae* Ecl grown in the higher Endo formulation. The lower C:N:P ratio of 334:28:5.6 showed attachment in a single species biofilm at 7.73 log cfu/g GAC, whereas counts were similar (6.93 log cfu/g GAC) at the 334:28:1 C:N:P ratio. By contrast, counts at the higher C:N:P ratio of 334:84:16.8 and 334:84:3 were lower in single species biofilms (5.37 log cfu/g GAC and 5.24 log cfu/g GAC, respectively).

The binary species biofilms grown at the C:N:P ratio of 334:28:5.6, showed attachment at 8.2 log cfu/g GAC. These counts were similar to the 334:28:1 ratio in which counts of 8.23 log cfu/g GAC were observed. By contrast, counts of 4.61 log cfu/g GAC and 4.45 log cfu/g GAC were recorded for the ratios 334:84:16.8 and 334:84:3, respectively.

E. cloacae Ecl - *Lower Endo Concentration*

Both the 334:28:5.6 and 334:28:1 ratios showed high counts of attached cells in the single species biofilms (9.39 log cfu/g GAC and 8.41 log cfu/g GAC, respectively). However, the higher ratios of 334:84:16.8 and 334:84:3 had lower attached counts of 8.26 log cfu/g GAC and 6.43 log cfu/g GAC respectively (Fig 2b.1).

At the lower concentrations, the 334:28:5.6 and 334:28:1 ratios showed lower attachment for binary species biofilms than the single species biofilms (7.61 log cfu/g GAC and 7.55 log cfu/g GAC, respectively). Counts from attached binary biofilms at the 334:84:16.8 and 334:84:3 ratios showed lower attached counts (6.8 log cfu/g GAC and 6.94 log cfu/g GAC) (Fig 2b.2).

C. freundii Cf1 - *Higher Endo Concentration*

The lower C:N:P ratio of 334:28:5.6 showed counts for *C. freundii* Cf1 in a single species biofilm at 9.3 log cfu/g GAC. At the 334:28:1 C:N:P ratio the counts were similar at 9.45 log cfu/g GAC. In Fig 2b.1, the higher C:N:P ratio of 334:84:16.8 showed counts in single species biofilm at 6.62 log cfu/g GAC. At the 334:84:3 C:N:P ratio, the counts were similar at 4.96 log cfu/g GAC for *C. freundii* Cf1 (Figure 2b.1).

Binary biofilm counts for 334:28:5.6 were 6.34 log cfu/g GAC. These counts are similar to the 334:28:1 ratio which were 6.62 log cfu/g GAC. Counts for 334:84:16.8 ratio were 2.88 log cfu/g GAC. These counts were similar to the 334:84:3 ratio which were 3.04 log cfu/g GAC.

C. freundii Cf1 - *Lower Endo Concentration*

The lower concentration Endo formulation using the 334:28:5.6 C:N:P ratio showed counts in single species biofilms of 8.9 log cfu/g GAC (Fig 2b.2) compared to counts at the 334:28:1 ratio which were 8.52

log cfu/g GAC. Using the higher ratios, the 334:84:16.8 ratio showed 6.90 log cfu/g GAC while the 334:84:3 ratio showed counts of 5.76 log cfu/g GAC.

The binary biofilm counts at the 334:28:5.6 ratio showed counts of 7.42 log cfu/g GAC (Fig 2b.2) compared to the counts at the 334:28:1 ratio which were 7.56 log cfu/g GAC. The higher 334:84:16.8 ratio biofilm counts were 6.42 log cfu/g GAC, compared to the 334:84:3 ratio which showed biofilm counts of 6.43 log cfu/g GAC.

Statistical Analysis

Statistical analysis performed on counts obtained from the higher Endo concentration showed statistically significant differences ($P < 0.05$) between the 334:28 and 334:84 ratios. This was true for both single and binary species biofilms. Conversely, there were no statistically significant differences ($P > 0.05$) between counts obtained at C:N:P ratios 334:28:5.6 and 334:28:1, nor between counts obtained at 334:84:16.8 and 334:84:3 for both single and binary species biofilms. However, counts obtained from the 334:28:5.6 and 334:28:1 ratios were significantly greater ($P < 0.05$) than those obtained using the original 334:42:1 Endo formulation.

The differences in counts between *E. cloacae* Ecl and *C. freundii* Cf1 in binary species biofilms at ratios 334:28:5.6, 334:28:1, 334:84:3 and 334:42:1 also showed no statistically significant difference ($P > 0.05$). However, the 334:84:16.8 ratio showed that there was a significant difference ($P < 0.05$) between the attachment of the two isolates, with *E. cloacae* Ecl attaching at greater counts.

Scanning Electron Microscopy of C:N:P Ratio Biofilms

There is an observable difference in the attachment pattern between the 3 different C:N ratios of 334:28, 334:42 and 334:84. In the micrographs taken of the 334:84:16.8 (Fig 2b.3 A-B) and 334:84:3 (Fig 2b.4 A-

B) C:N:P ratios there was a lack of biofilm formation and bacterial attachment to the GAC surface. In addition, unusual cellular morphology of several attached cells showed rods up to 10µm in length.

Biofilm attachment showed an improvement in the GAC samples grown in the unmodified Endo formulation with C:N:P ratio of 334:42:1 (Fig 2b.3 C-D and Fig 2b.4 C-D). There was a qualitative increase in the number of attached cells on the GAC, but no unusual cellular morphology was observed in any of the rod shaped bacteria present. There was evidence of bacterial microcolony formation (Fig 2b.4 C-D). The GAC samples grown in the 334:28:5.6 (Fig 2b.3 E-F) and 334:28:1 (Fig 2b.4 E-F) showed the greatest visible biofilm coverage and attachment of cells out of all three samples.

2b.4 Discussion

The C:N:P ratios had a distinct effect on the number of cells present on the GAC surfaces. This was not an unexpected phenomenon as the Endo formulation has been used in numerous biofilm studies before. However it's poorer performance in aiding biofilm attachment was not expected as this medium has developed into a standard for H_2 production studies (Chang, Lee *et al.* 2002; Wu, Lin *et al.* 2003; Lin and Lay 2004a; Lin and Lay 2005). It is noted that many of the studies conducted using the Endo formulation utilised undefined mixed cultures in continuously stirred tank fermenters. The tradition of one size fits all in terms of nutrient formulation in fermentative H_2 production is problematic and there have been attempts to remedy this for wastewater treatment (Ammary 2004). The decision to alter the N and P values to higher ratios was made on the basis that no one nutrient formulation will provide optimal growth requirements for all the bacterial families involved in fermentative H_2 production.

The differences between the C:N ratios (334:28, 334:84, 334:42) were larger in terms of counts where there was a statistically significant difference ($P < 0.05$), than the differences between the different N:P ratios where no significant difference was found ($P > 0.05$). This was noted in both single and binary species biofilms (28:5.6 and 28:1, 84:16.8 and 84:3).

This study showed that attached counts at the C:N:P ratios of 334:28:5.6 and 334:28:1 were significantly higher ($P < 0.05$) than that obtained for the original Endo formulation. Furthermore, within the binary species biofilms, counts of *E. cloacae* Ecl and *C. freundii* Cf1 were not significantly different ($P > 0.05$) at the ratios of 334:28:5.6 and 334:28:1. This indicates that the differences in attached counts obtained between the different ratios was due to the effect of the C:N:P ratios on attachment and not due to the individual actions of the bacterial isolates on each other.

Fig 2b.1 and Fig 2b.2 showed an inverted change in attachment patterns between the single species and mixed species biofilms. In almost all cases, the *C. freundii* Cf1 isolate attached at higher counts compared to *E. cloacae* Ecl in single species biofilms at the same C:N:P ratio and concentration. These counts were confirmed to be statistically significant ($P < 0.05$). However, in binary species biofilms, *E. cloacae* Ecl showed no significant difference ($P > 0.05$) in attached counts compared to *C. freundii* Cf1. These findings suggested that in single species biofilms, *C. freundii* Cf1 attached at higher counts than *E. cloacae* Ecl, but in binary species biofilms, competition between the two bacteria ensured that their relative numbers remained similar.

Scanning electron micrographs also seemingly showed little difference in colony morphology, cell arrangement and attachment patterns between the N:P ratios (2b.3 A-B and 2b.4 A-B, 2b.3 C-D and 2b.4 C-D, 2b.3 E-F and 2b.4 E-F). There was also a smaller difference between the C:N ratio attachment consistency in the lower Endo concentration than in the higher concentration. These differences and the unusual cellular morphologies, point to inhibitory NH_4^+ concentrations. Previous studies conducted on *Listeria monocytogenes* have shown that environmental stresses caused an alteration of cell shape and surface roughness (Rowan and Anderson 1998; Rowan, Anderson *et al.* 2000; To, Favrin *et al.* 2002). It has previously been suggested that cell length may be linked to the level of adaptation towards an inhibitor, thus indicating damage. It has also been suggested that low C:N ratios indicate high ammonia concentrations and high C:N ratios indicate inadequate N supplies (Lin and Lay 2004a). The original Endo formulation C:N:P ratio of 334:42:1 also showed a visible increase in cellular attachment over the 334:84 C:N ratio, although still lower than the plate counts obtained from the 334:28 ratio. Therefore while the

higher NH_4^+ concentrations in the 334:84 and 334:42 ratios showed inhibitory effects due to NH_4^+ oversupply, it is unlikely that either of the N:P ratios used in any of the C:N ratios were limiting to biofilm formation due to inadequate P supply (Bosander and Westlund 2000).

The 334:28 ratio could have been modified further as suggested by Lin and Lay, (2004a). The study by Lin and Lay, (2004a) was focused on optimal C:N ratios for biohydrogen production, and did not take into account the C:N ratio needed for both optimal H_2 production and biomass growth. The optimal C:N ratio suggested was approximately 47:1, or 334:7 for an equivalent sucrose concentration used in this study. This ratio is four times less than that used in this study and could result in N and P growth limitation. The exact ratio is however difficult to compare due to the use of COD as opposed to atom:atom ratios. High C:N ratios are also know to produce reduced compounds, which will be important for bioreactor optimisation, as reduced compounds mean a lower H_2 yield (Yu and Fang 2001; Lin and Lay 2004a).

2b.5 Conclusion

1. The differences in attached counts of *E. cloacae* Ecl and *C. freundii* Cf1 in single and binary species biofilms between the different ratios was clearly due to the ratios themselves and not due to the individual actions of the bacterial isolates on each other. For this reason, 334:28:5.6 C:N:P ratio was selected for use in future bioreactor work. This was supported by observations made using SEM, where the 334:84 C:N ratios showed elongated, and therefore potentially damaged cells caused by high concentrations of NH_4^+ ions. The 334:84 ratio also showed low attached counts for *E. cloacae* Ecl and *C. freundii* Cf1 in single and binary species biofilms.

2. Although there was no significant difference ($P > 0.05$) between the N:P ratios in both attachment counts and scanning electron micrographs of the 334:28:5.6 and 334:28:1 ratios, the 28:1 ratio was not selected for future biofilm studies to prevent P becoming a limiting nutrient (Hendrickx, Meskus *et al.* 2002). The N:P concentrations used would be kept relative to the higher 17.65g/L sucrose

concentration as the bioreactor volume would have an additional dilutory effect on the concentration of the feed.

3. Additional modification of the C:N:P ratio is suggested by literature reports to between the 334:28 ratio used in this study and the 334:7 ratio suggested by (Lin and Lay 2004a).

Table 2b.1: Concentration of media used in the higher concentration Endo formulations. The higher concentration C:N:P ratios contained 17.65g/l sucrose.

Chemical Component (g/L)	334:28:1	334:28:5.6	334:84:3	334:84:16.8
Sucrose	17.65	17.65	17.65	17.65
NH_4HCO_3	3.490	3.490	10.48	10.48
K_2HPO_4	0.125	0.699	0.374	2.09
$NaHCO_3$	6.720	6.720	6.720	6.720
$MgCl_2{\cdot}6H_2O$	0.100	0.100	0.100	0.100
$MnSO_4{\cdot}4H_2O$	0.015	0.015	0.015	0.015
$FeSO_4{\cdot}7H_2O$	0.025	0.025	0.025	0.025
$CuSO_4{\cdot}5H_2O$	0.005	0.005	0.005	0.005
$CoCl_2{\cdot}H_2O$	1.24×10^{-4}	1.24×10^{-4}	1.24×10^{-4}	1.24×10^{-4}

Table 2b.2: Concentration of media used on the lower concentration Endo formulations. The lower concentration of sucrose was 8.84g/L. Ratios were worked out from this concentration.

Chemical Component (g/L)	334:28:1	334:28:5.6	334:84:3	334:84:16.8
Sucrose	8.84	8.84	8.84	8.84
NH_4HCO_3	1.75	1.75	5.25	5.25
K_2HPO_4	0.06	0.35	0.19	1.05
$NaHCO_3$	6.72	6.72	6.72	6.72
$MgCl_2{\cdot}6H_2O$	0.100	0.100	0.100	0.100
$MnSO_4{\cdot}4H_2O$	0.015	0.015	0.015	0.015
$FeSO_4{\cdot}7H_2O$	0.025	0.025	0.025	0.025
$CuSO_4{\cdot}5H_2O$	0.005	0.005	0.005	0.005
$CoCl_2{\cdot}H_2O$	1.24×10^{-4}	1.24×10^{-4}	1.24×10^{-4}	1.24×10^{-4}

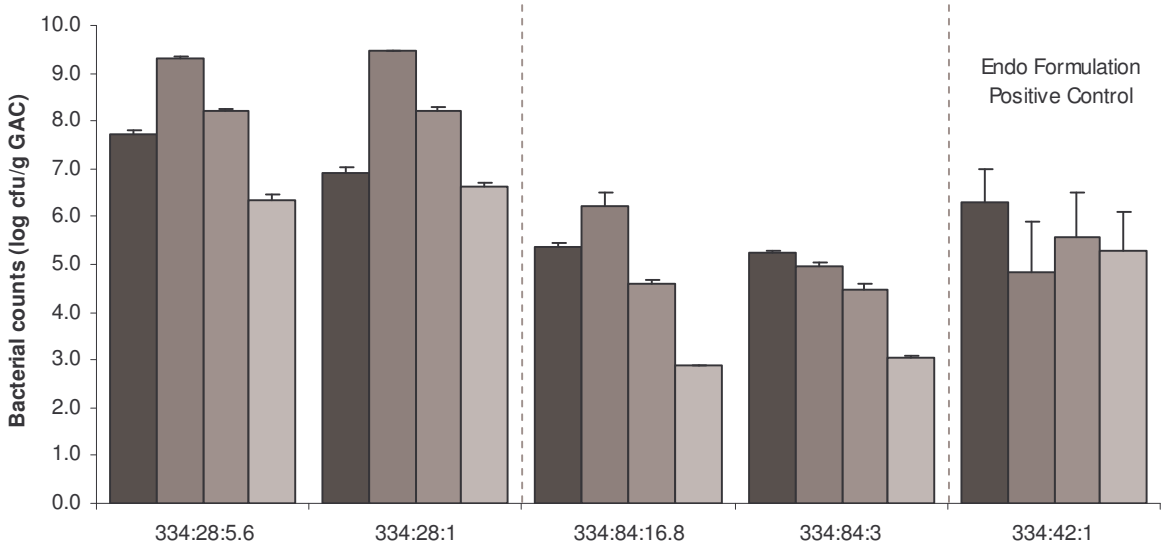


Figure 2b.1: Graph representing the attachment (log cfu/g) of *E. cloacae* Ecl ■ and *C. freundii* Cf1 ■ in single species and *E. cloacae* Ecl ■ and *C. freundii* Cf1 ■ in binary biofilms to 1g granular activated carbon in higher concentration Endo formulation (sucrose at 17.65g/L).

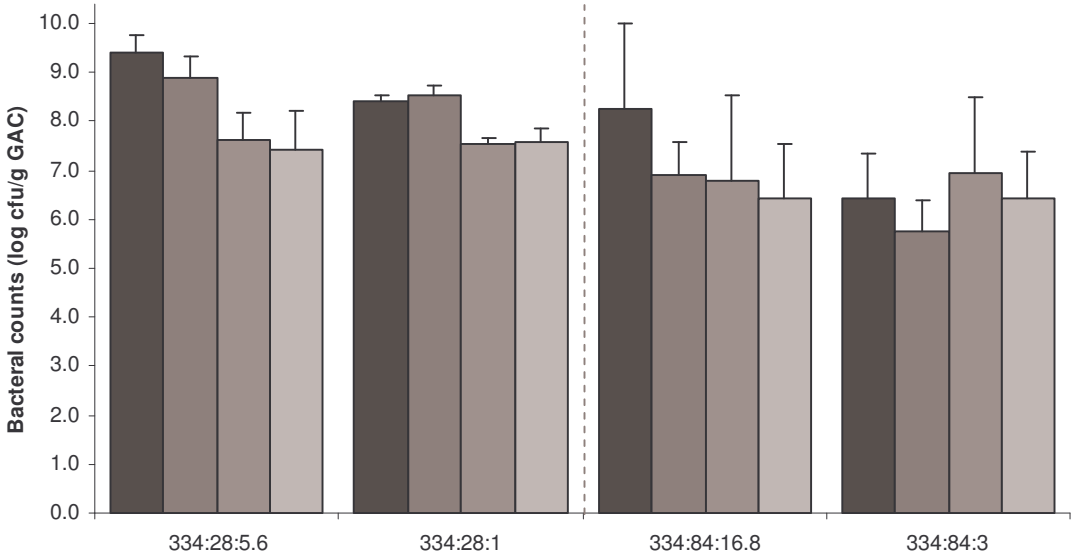


Figure 2b.2: Graph representing the attachment (log cfu/g) of *E. cloacae E. cloacae* Ecl ■ and *C. freundii* Cf1 ■ in single species *E. cloacae E. cloacae* Ecl ■ and *C. freundii* Cf1 ■ binary biofilms to 1g granular activated carbon in lower Endo formulation concentration (sucrose at 8.84g/L).

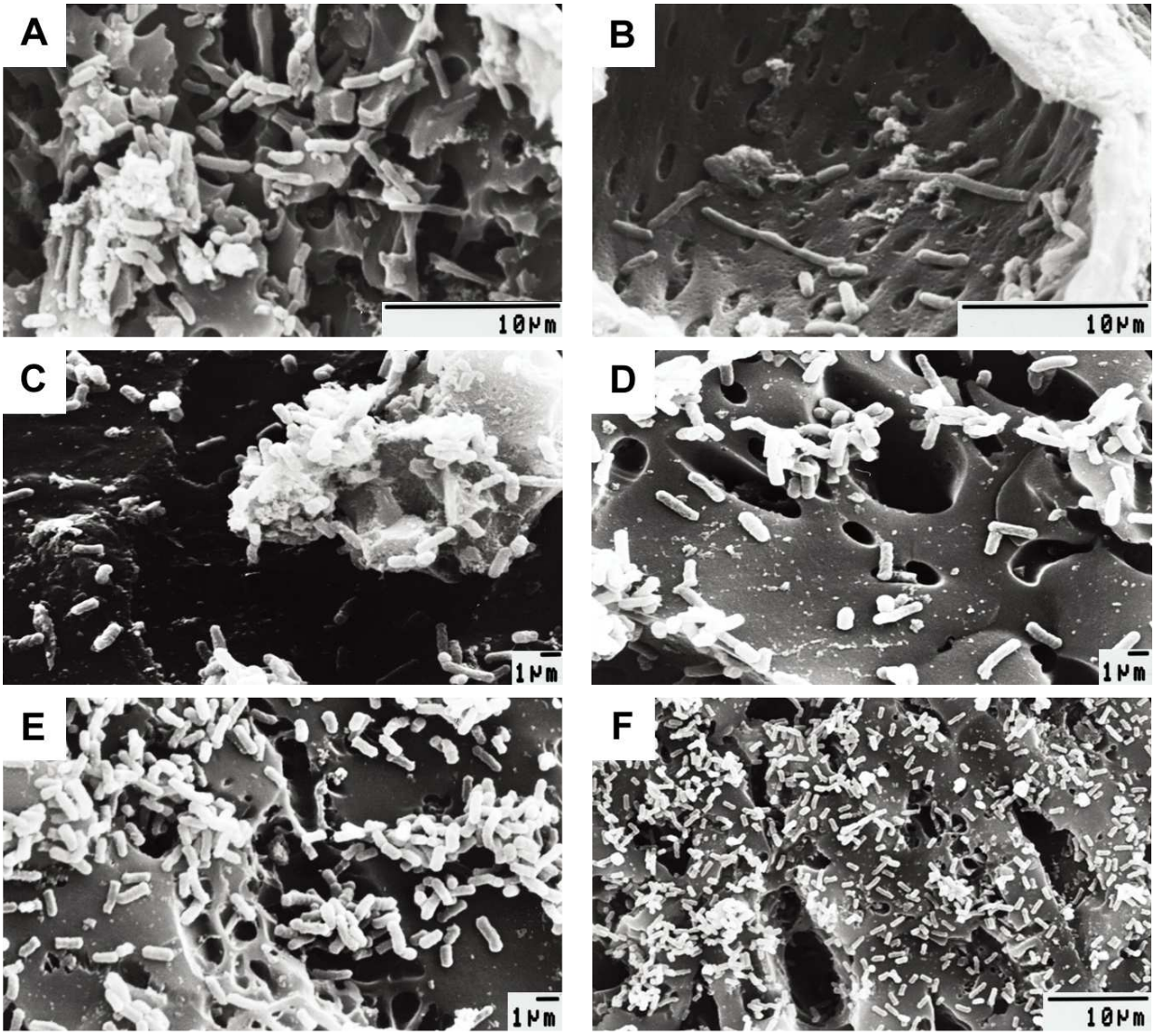


Figure 2b.3: Scanning electron micrographs of GAC grown in different C:N:P ratio Endo formulations (A-F). (A-B) shows biofilm grown in a 334:84:16.8 ratio, (C-D) shows biofilm grown in the unmodified Endo formulation (334:42:1), (E-F) showing biofilm grown in the 334:28:5.6 ratio. (A-B) shows little biofilm development, with uncharacteristic cell morphologies (B). (C-D) shows an increase in biofilm coverage, however cells are still present in small groups and show no large surface coverage. (E-F) shows large biofilm growth over the activated carbon surface. Cells are present not only in the protected crevices, but also on the more exposed flat surfaces.

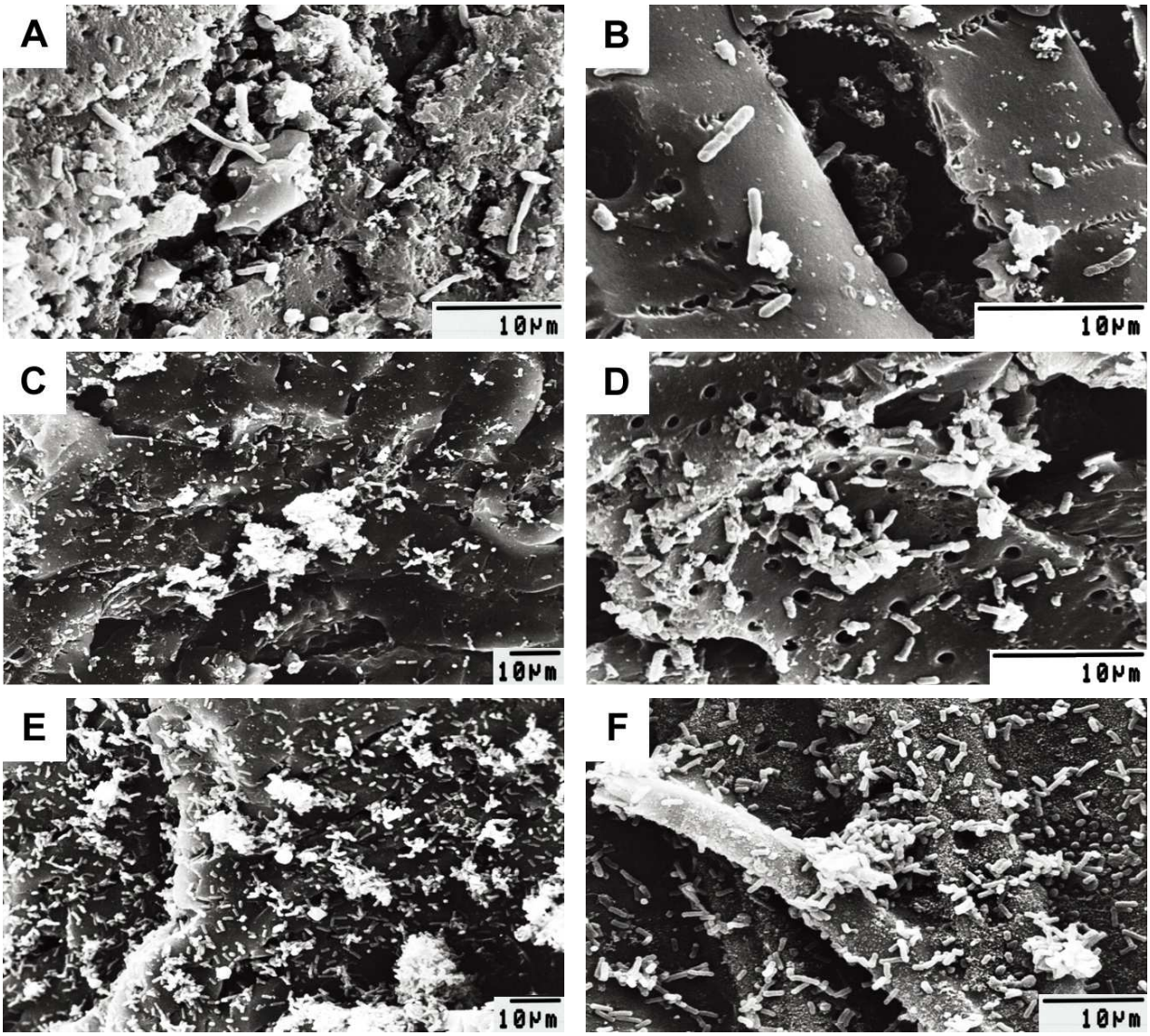


Figure 2b.4: Scanning electron micrographs of GAC grown in different C:N:P ratio Endo formulations (A-F). (A-B) shows biofilm grown in a 334:84:3 ratio, (C-D) shows biofilm grown in the unmodified Endo formulation (334:42:1), (E-F) showing biofilm grown in the 334:28:1 ratio. (A-B) shows little biofilm development, with the presence of elongated cells. (C-D) shows an increase in biofilm coverage, however cells are still present in small groups and are largely scattered. (E-F) shows large biofilm growth over the activated carbon surface. The presence of biofilm microcolonies is noted in E and F.

CHAPTER 2C

PILOT STUDY OF AN ANEROBIC FLUIDISED BED BIOREACTOR: INSTRUMENTATION, CALIBRATION AND MEASUREMENT PARAMETERS

Abstract

Anaerobic processes are still perceived as less reliable than aerobic processes due to their instability under certain operating conditions. It is therefore imperative to implement a suitable control system to prevent destabilising conditions occurring in the anaerobic process. Redox potential and pH are two such measurements used in the control of anaerobic bioreactors. This study was done to test the performance of the measurement and control instrumentation on a 23L fluidised bed reactor containing granular activated carbon and inoculated with *Citrobacter freundii* Cit1. Redox potential, pH, conductivity and both internal and environmental temperature were measured. The pH was corrected using peristaltic pumps attached to either acid or base reservoirs and temperature was controlled at 37^{o}C using a circulating waterbath. Results showed significant hysteresis effects due to pH over dosing which was corrected by reducing the number of points at which pH adjustments could occur. The redox potential revealed that the system operated anaerobically when no major system disturbances occurred. Redox potential showed an association with pH, especially when pH corrections occurred. Additionally, conductivity measurements showed clear influence from both internal and external temperature fluctuations. The internal reactor temperature showed similar cycles to the environmental temperature, thus indicating the need for heat insulation. Data points showed that reactor conditions changed at a slower rate than the rate they were being measured. This pilot study provided indispensable information regarding the functioning of a model reactor ensuring that the parameters of future studies utilising fluidised bed bioreactors could be better controlled.

2c.1 Introduction

An anaerobic digester constitutes a complex ecosystem of anaerobic bacterial species that degrade organic materials. At the industrial scale, non-lagoon anaerobic digesters have grown to an estimated 1300 units worldwide since the 1970s (Totzke 2004). These processes treat a variety of wastewaters including sugar; corn processing; beverage processing, such as beer; wine; canning and other industrial effluents, such as petrochemical and wood processing. The selection of a robust and reliable anaerobic treatment system is still complicated by the fact that under certain conditions the anaerobic process becomes unstable. Disturbances, such as sudden large increases in organic load, introduction of toxic chemicals and pH fluctuations, can destabilise the process and lead to accumulation of intermediate toxic compounds and result in the incomplete treatment of the wastewater. Subsequent damage to microbial biomass may take several weeks if not months to re-establish to full functionality (Steyer, Genovesi *et al.* 2001). It is a challenge for instrument and control sciences to generate more stable and reliable anaerobic digestion processes through the use of one-line sensors. The majority of anaerobic digesters to date have simple but insufficient management procedures with temperature, pH, liquid and gas flows being the main variables monitored.

During the last decade numerous studies have been conducted to improve instrumentation for anaerobic digestion processes with specific attention being paid to H_2 in the gas and dissolved phase (Archer, Hilton *et al.* 1986; Pauss and Guiot 1993; Strong and Cord-Ruwisch 1995), and volatile fatty acid and bicarbonate concentrations (Hawkes, Guwy *et al.* 1994; Guwy, Hawkes *et al.* 1997; Steyer, Bouvier *et al.* 2001) as well as redox potential.

Oxidation and reduction (redox) reactions mediate the behaviour of many chemical constituents in drinking and process wastewaters, as well as most aquatic components of natural water systems. The reactivity and mobility of important elements, in biological systems (e.g. Fe, S, N and C), as well as those of a number of other metallic elements, depend strongly on redox conditions. Reactions involving both electrons and protons are pH and Eh dependent, therefore chemical reactions in aqueous media may

often be characterized by pH and Eh together with the activity of dissolved chemical species. Like pH, Eh represents an intensity factor. It does not characterise the capacity of the system for oxidation or reduction (Franson, Clesceri *et al.* 1998). The redox potential gives information regarding the activity of the electrons within the biological medium (Kjaergaard 1977).

Many aerobic microbial processes take place at concentrations of dissolved O_2 that are impossible to measure using commercial probes for dissolved oxygen (Janssen, Meijer *et al.* 1998). However the supply of O_2 to the cultures is essential to aerobic microorganisms. Since the range of the oxygen-limited state is infinite i.e. completely anaerobic states to levels where the dissolved oxygen can be measured by commercial probes (<10µM). Many researchers consider the redox reading to be of little value as it comprises a variety of simultaneous, successive, and parallel chemical and biological reactions.

Most biological liquids are often not in equilibrium due to their complexity, therefore measured redox values are not correct from a chemical thermodynamic point of view. However, the measurement still yields information concerning the oxidative status of the liquid, thus elucidating biological significance (Kjaergaard 1977). There have been a number of investigations on the influence of redox potential on biological systems and the correlation between redox potential and extra- and intracellular processes (Plisson-Saune, Capdeville *et al.* 1996; Yu, Liaw *et al.* 1997; Li and Bishop 2002). Almost all have concluded that the measurement of redox is useful when the dissolved O_2 cannot be measured. For H_2 producing acidogenic systems, ORP has been connected to the specific production of certain fatty acids (Cohen, Zoetemeyer *et al.* 1979; Hawkes, Dinsdale *et al.* 2002).

Conductivity is a measure of the ability of an aqueous solution to carry electric current. This ability depends on the presence of ions, their total concentration, mobility and valence and on the temperature of the measurement (Franson, Clesceri *et al.* 1998). Conductivity readings are subject to signal drift due to microbial growth on electrodes. It has however been used nitrogen and phosphorous removal processes (Spagni, Buday *et al.* 2001), however, the presence of biogas within the wastewater can interfere with readings. This pilot study aimed to establish control of a laboratory scale AFBR functions, using online

instrumentation and measurements and for further development of online monitoring systems. pH, ORP, conductivity, and temperature were measured on a continuous basis in an electrode vessel attached to a datalogger and computer. Measurements from these electrodes were then used to implement control measures.

2c.2 Materials and Methods

Set-up and Operations of AFBR

A schematic description of the reactor fluidized bed reactor is shown in Fig 2a.1. Exact technical specifications are recorded in Appendix C. The reactor was constructed from Perspex and had the following dimensions: The inner diameter was 70mm, and the height to the solid liquid separator (Fig 2c.1.13) was 1m. The total reactor volume was approximately 7L. In addition the separate reservoir (Fig 2c.1.3) added a further 16L to the total system volume. A bypass (Fig 2c.1.11) and backwash line (Fig 2c.1.12) were connected to the outlet of the reactor to allow servicing of electrodes (Fig 2c.1.2) and to remove solids clogging the inlet sieve. Under normal flow conditions, all the flow was passed through to the electrodes which were in turn housed in a perspex cylinder. The feed (Fig 2c.1.9) and pH pumps (Fig 2c.1.8) were attached directly to the reservoir drum and feed, acid (Fig 2c.1.6) or base (Fig 2c.1.7) was all dosed at this point. The pH pumps were calibrated to ensure a flowrate of 20ml/minute.

The medium was passed through the column using a Boyser AMP-16 (Spain) (Fig 2c.1.10) peristaltic pump to allow attachment of bacterial cells to the carrier. Feed was introduced on an hourly basis for 6 minutes from a reservoir of 100x concentrated feed (Fig 2c.1.5) at a rate of 40ml per minute. The feed was not diluted before entering the reservoir system. Measurements of pH, redox, conductivity, reactor temperature and environmental temperature were taken every 20 minutes by the datalogger (Fig 2c.1.4). Operation temperature of the reactor was maintained near 37^{o}C using a water-jacket (Fig 2c.1.14) on the reactor and controlled using a Grant GD120 waterbath (Fig 2c.1.15). The pH was maintained near pH 5.7

(Chen, Lin *et al.* 2001) using 3M HCL and 6M NaOH for acid and base adjustments respectively. The reactor was operated for 27 days.

Support Matrix

Granular activated carbon (GAC) was selected as the carrier matrix for the fluidised bed reactor due to its higher rugosity and lower density as compared to silica sand. The GAC was purchased from Associated Chemical Enterprises, with an average diameter of 0.6 - 1.16mm. The GAC was washed to remove carbon fines and it was then autoclaved for 20 minutes. The reactor was filled with enough GAC to occupy 30% of the volume, or 300cm^3.

Reactor Inoculum

Citrobacter freundii Cit1 type strain (South African Bureau of Standards) was grown in two litres of nutrient broth (Merck) at 37^{o}C overnight to a cell count of approximately 8.9±0.08 log cfu/ml. The reactor reservoir was inoculated with this culture and allowed to acclimatise to the nutrient medium in the reactor described previously (Chang, Lee *et al.* 2002) for 48 hours. Chemicals used in the medium were all analytical grade.

Monitoring and Control

The reactor was monitored using 4-20mA GF-Signet (USA) pH (3-2714), ORP (3-2715) and Conductivity 10.0 cell (3-2822) electrodes with Amplifier (3-2720-2) and Transmitters for pH (3-8750-3) and ORP (3-8750-1) and conductivity (3-8850-XP). The electrode output was fed through a 120Ω resistor to reduce the measured voltage to below the specification limit of the datalogger of 5V. The datalogger received the output of the transmitters as a percentage of the 4-20mA electrode output range (Fig 2a.2). This reading was automatically converted into the correct SI units using spans defined in the datalogger program following. The datalogger controlled the Omron G2R-1-SN relays (USA) which allowed control of the peristaltic feed (Autoclude M045, Germany) and pH control (Autoclude M025, Germany) pumps.

CSCANS CALARMS CLEAR
'The above command clears all scans, clears all alarms and clears any stored data from the 'datalogger

S1=3.7000,10.000,0.0000,100.00"pH"	Span 1
S2=130.31,50620.0,0.0000,100.00"µS"	Span 2
S3=-968.00,1028.0,0.0000,100.00"mV"	Span 3

'The above spans are used to convert the current readings from the electrodes which are received as percentages of the 4-20mA from the transmitters. The percentages are then converted into either pH or S1, µS or S2 for conductivity and mV or S3 for redox.

BEGIN	Represents the beginning of the actual datalogger program
RA20M HA	Schedule A, measured every 20 minutes (20M)
1TK("Air Temperature",FF1)	Channel 1, Air temperature thermocouple, K type, 1 decimal place (FF1)
2PT385("Reactor Temp",100,FF2)	Channel 2, Reactor temperature, type PT385,100Ω, 2 decimal places (FF2)
RB20M HB	Schedule B, measured every 20 minutes (20M)
3L("Conductivity",S2,120,FF2)	
4L("ORP",S3,120,FF2)	
5L("pH",S1,120,FF2)	
RC1M HC	Schedule C monitored every minute
2ST("Feed Timer",60,R,FF0,1CV)	

Channel 3 used for Conductivity measurements is a current (mA) channel, uses Span 2, passes through a 120Ω resistor before entering the datalogger and returns a value of 2 decimal places (FF2). The same applies for Channel 4 and 5 which return redox and pH values respectively. The ORP or redox (Channel 4) utilises span 3, also passes through a 120Ω resistor and returns the reading to 2 decimal places. The same applies for Channel 5 which is used for pH readings.

RZ1M This is the start of the alarm definitions and is checked every minute (1M)

ALARMR1(1TK>35.000/5M)"Air Temperature Caution"
ALARMR2(2PT385<>35.000,38.500/5M)"Reactor Temperature Alert"
ALARMR3(1CV><0.0000,7.0000)1DSO"Feed On"
ALARMR4(5L>6.2000/21M)2DSO"Acid On. ?[RB1M]"
ALARMR5(5L<5.0000/21M)3DSO"Base On. ?[RB1M]"
ALARMR6(5L><5.0,6.0)2DSO 3DSO"Normal. ?[RB20M]"

The above Alarms are repeated (ALARMR) to ensure they are read each time the alarms are scanned. Alarm 1 is used to monitor air temperature and stipulates that if the air temperature is greater than 35°C then the system should wait 5 minutes (5M) before reporting "Air Temperature Caution" to screen. The same criteria are applied to Alarm 2 except that it is intended for the reactor temperature. If the temperature of the reactor fluid is less than 35°C or greater than 38°C then it should wait 5 minutes before reporting "Reactor Temperature Alert" to screen. Alarm 3 is utilised as a feed pump controller. Whenever the channel variable 1CV or minute count is greater than 0 and less than 7, Digital Output number 1 (1DSO) is activated and displays "Feed On" on screen. Alarm 4-7 are utilised for pH control with the IF alarm statement used to combine 2 different alarms. For pH control, if the minute count or CV1 is less than 1 and the pH is greater than 6.2 or less than 5.0, the system is instructed to wait 21 minutes before activating either Digital Output 2 (2DSO) or 3 (3DSO) which will activate either the acid or base peristaltic dosing pump. In addition, the system displays "Acid On" or "Base On" and changes the frequency of Schedule B from the default 20 minutes to 1 minute. Alarm 8 is utilised to return all digital output states to zero when the pH is in the correct range and also returns the frequency of Schedule B reading to every 20 minutes (RB20M).

END	This is the end of the program
P31=1	Sets date to dd/mm/yyyy format
P39=0	Set time to hh:mm:ss format
T=\T	Sets the logger time to the same as the computer
P22=44	The data delimiter set as a comma
LOGON	Switches logging on
G	Switches on all the Schedules and Alarms

Analytical Methods

The sucrose concentration in the reactor were measured periodically using the resorcinol method to determine the level of sucrose degradation in the reactor (Kerr, Huber *et al.* 1984). Standards for the sucrose concentration curve were 0.05, 0.1 and 0.15 g/L. Planktonic counts of *C. freundii* in the reactor were monitored periodically using the droplet plate technique (Lindsay and von Holy 1999) by plating 50µl on duplicate nutrient agar plates. Colonies between 5-50 colony forming units (cfu) were counted to calculate *Citrobacter freundii* Cit1 concentration per ml. Samples were incubated at 37^{o}C for 24 hours. Calibration and cleaning of the electrodes was performed weekly using appropriate standards for pH (pH 4.0 and 7.0) (Merck, Johannesburg, South Africa) redox (+80 and +475mV) (Action Instruments, Johannesburg, South Africa) and conductivity (Pratt, Koch *et al.* 2001). Conductivity standards were replaced regularly to ensure calculated conductivity values (µS/cm^{2}) in the standard did not drift due to evaporation or leakage (Shreiner 2002).

2c.3 Results

Temperature Profile

The stability of the temperature profile of the reactor (Fig 2a.3) showed distinct cycling during a normal day. There was a relationship between the temperature troughs and peaks of the environmental temperature and the reactor temperature. From Day 1 to the beginning of Day 5 the reactor operated at a temperature below the desired optimum of 37^{o}C (Point 3) at an average temperature of 33.6^{o}C. At the end of Day 5, a safety mechanism turned the waterbath off (Point 1) causing the temperature to drop to a low of 24.5^{o}C. The temperature of the reactor recovered to near the optimal 37^{o}C once the waterbath was switched back on (Point 2). A larger than normal decrease in the daily environmental temperature (Point 4) from the end of Day 14 to 19 showed a correlating decrease in temperature in the reactor. At points 5-7 there were additional periods of large temperature decreases caused by both stoppage of the heat exchange system and replacing the fluid in the waterbath with colder tap water.

Conductivity Profile

The conductivity profile (Fig 2a.4) showed the largest fluctuations in readings from all 3 measurements. Feeding started on Day 1 with a conductivity of approximately 1500µS.cm^{-2}. By Day 2 the conductivity had increased to approximately 13000µS.cm^{-2}. On Day 3, there was a very large fluctuation in conductivity resulting from a large addition of HCl and NaOH (Point 3). Following this over dose of acid and base the reactor did not manage to achieve a stable conductivity reading. Day 6 (Fig 2a.4) showed the clear effect of reactor temperature on the conductivity of the reactor wastewater. Point 2 was the period whereby there was no feed being added to the reactor and indicates the length of time needed for the conductivity in this system to approach a stable value. The only point at which there was relative stability in the conductivity was between days 19 and 21. At the end of Day 21 (Point 4), there was a large drop in the conductivity from 16000µS.cm^{-2} to approximately 180µS.cm^{-2} which correlated with the reactor volume being replaced with tap water. Following this there was a short increase in conductivity even though no feed or pH dosing occurred (Point 7). The reactor was flushed with tap water again and new culture was added on Day 26 (Point 6) after which feeding and pH dosing resumed. Excess gas in the system caused the anomalies seen from Day 26 to the end of Day 27 (Point 5-6) and the conductivity did not approach previous levels before the run was terminated.

Redox / ORP Profile

In Fig 2a.4, from Day 1 to Day 3 there was a large decrease in ORP by almost 540mV from +160mV to -376mV as the reactor was fed with nutrients and the pH was adjusted by the datalogger (Point 1). Following the stoppage of feeding and pH adjustment on Day 4, the ORP only assumes a level of stability on Day 10. From Day 10 to Day 21 there was a moderate decrease in ORP from -120mV to -140mV (Point 2). On Day 21, feeding of the reactor and pH adjustments resumed resulting in an immediate increase in ORP to +185mV (Point 3). The effects of both acid and base adjustments on the ORP readings were further demonstrated in Point 4-5 on Days 22 and 25 respectively. Point 6 on Day 26 showed the large decrease in ORP from +187mV to -360mV and correlates with the addition of bacterial

inoculum and acid to the reactor. The ORP readings decreased slightly further until Day 27 when the run was terminated.

pH Profile

Fig 2a.4, point 1 where a successful pH adjustment performed by the datalogger from above the calibrated measuring limit of the pH electrode of 7.3 down to a pH of 5.3 which was an overdose of approximately 0.4 pH units. The reactor was successfully fed for the next 2 days which resulted in the pH increasing to 5.79. From day 4 to day 21 the feeding of the reactor was suspended and the pH remained stable at pH 5.76 with minimal fluctuation in the pH reading between days. On day 21, feeding of the reactor was resumed and it was from this point that overdosing of acid and base occurred. From day 21 to 26 there were 3 separate pH over adjustments (Point 3-6). After point 5, the pH control system was switched off to prevent further over dosing of the reactor, but feeding was allowed to continue up to the end of day 27. The pH profile showed the expected relationship with the ORP profile (Fig 2a.4)

Reactor Analyses

The sucrose test was evaluated and was found to be reliable with the sucrose concentration within the reactor was 2.94±3.36 g/L at all times. The minimum and maximum sucrose concentrations within the reactor were measured to be 0.0 and 10.9 g/L respectively. Planktonic counts of *C. freundii* were 7.07±0.9 log cfu/ml throughout the study.

Reactor Structure Performance

The fluidisation of the GAC in the reactor was not influenced by channeling or eddies within the flow stream. The reactor was backwashed once a day to remove pieces of biomass blocking the influent sieve, which helped prevent permanent blockages from developing. To compensate for heat loss, the heat exchanger was operated at a much higher temperature than the internal temperature of the reactor. The

high temperature interfered with the sealant used to attach the outer water jacket and caused it to leak. We therefore suggest that similar, future studies run the heat exchanger at a lower temperature than was used in this study (50^{o}C).

Usage and servicing of the electrode vessel was problematic due to the manner in which the electrodes were fixed to the lid of the electrode vessel. Regular cleaning and removal of the electrodes from the rubber ring seals on top of the perspex lid reduced the glue seal integrity and on 2 occasions, measurements were not taken as repairs were performed on the glue seals. Even after repairs, it was noticed that the electrode box was not completely water tight as reactor contents were periodically expelled from the vessel.

2c.4 Discussion

General

Inspection of the smoothness of the data lines from Figures 2-4 showed a definite jagged trend along the line caused by on average 71 readings per 24 hour period. A glimpse of the raw data revealed that there were numerous successive data points of the same value. While this observation does not represent a problem, it showed that the program code controlling the datalogger and the memory space available for data storage was not being efficiently utilised. The datalogger should only store data that differs to a specified degree from the previous reading. This would eliminate unnecessary duplication of data permit more meaningful data to be stored for analysis. More detailed programming of the logger was not attempted, therefore the temperature, ORP, pH and conductivity would be changed to only measure once per hour in future runs. This is illustrated in the code below:

RA1H HA

1TK("Air Temperature",FF1)

2PT385("Reactor Temp",100,FF1)

The schedules for both the A and B schedule were changed to 1 hour RA1H and RB1H to help prevent the successive accumulation of duplicate datapoints.

RB1H HB

3L("Conductivity",S2,119,FF0)

4L("ORP",S3,119,FF0)

5L("pH",S1,119,FF1)

Schedule C could also be removed and merely included as an Alarm as the following

ALARMR3(2ST><0.0000,7.0000)1DSO"Feed On"

Temperature Profile

It was evident from the temperature profile in Fig 2a.3 that there was substantial heat loss from the reactor system as evidenced by the range of the daily temperature cycle (Point 3). The internal temperature of the reactor fluctuates over a range of 1.3° centigrade from 37.5° to 36.2° during a normal 24 hour period. This temperature range was not significant in terms of growth range of *C. freundii*, which is a mesophilic bacterium (Krieg and Holt 1984). However, fluctuations in the temperature range within the reactor should be kept to a minimum to ensure uniformity in growth conditions. Further, the influence of external temperature sources was evident in Point 4 where a drop in the external environmental temperature from a mean of 26.6℃ to 23.7℃ induced a similar drop in the reactor temperature from 36.9℃ to 34.6℃. This indicates the inability of the reactor heat exchange system and insulation to buffer external temperature influences.

Temperature fluctuations in the reactor highlight inefficient heat energy conservation as the heat exchange system continuously heats the reactor to stem heat loss. To maintain the temperature at the desired level of 37℃, the heat exchange system had to operate at an elevated temperature of 50℃ to compensate for heat loss. Due to the continuous operation of the thermostatic controller, a strain was placed on the heat exchange system and perspex reactor which could result in a shortened lifespan for the perspex reactor.

To prevent heat loss, fiberglass heating insulation could be installed on the reactor and the wastewater reservoir to minimise heat loss and maintain a more stable internal reactor temperature.

Conductivity Profile

The general trend of the conductivity graph (Fig 2a.4) during the first 2 days of operation showed a gradual increase in conductivity as the reactor was dosed with concentrated feed. From a basal conductivity of 1500µS.cm^{-2} which was approximately equal to a one times concentration feed, the conductivity increased almost exponentially as the bacterial cfu/ml and total dissolved solids increased. Dosing with acid also contributed to the change in conductivity. Upon reaching a conductivity of approximately 13 000µS.cm^{-2}, the system was dosed with acid and base by separate actions of the control system which resulted in a fluctuation in conductivity from a high of 17 400 to a low of 3500µS.cm^{-2} (Point 3). The effect of the interruption of feed following Point 3 on the conductivity profile was not as apparent as the stabilization of the pH profile due to zero feed input (Fig 2a.4). Following this, there was a definite cycling of conductivity that showed a connection with the temperature cycle as suggested in previous studies (Franson, Clesceri *et al.* 1998). This was especially evident at Point 8 where a drop in conductivity of 3 300 µS.cm^{-2} was seemingly related to the temperature drop. After Point 8 there were other momentary drops in conductivity that could be related to air pockets in the electrode measuring jar, preventing proper contact to the wastewater stream.

Point 4 showed that the effect of completely replacing the reactor contents with tap water, which as expected, brought a complete reduction in conductivity from 16600µS.cm^{-2} to 180µS.cm^{-2}. At Point 6 another dose of inoculum was added to the reactor, however automatic feeding of the reactor was not performed. There was subsequently only a small increase in the conductivity before the conductivity started tapering off due to a lack of feed. After 3 days the reactor contents were again replaced with tap water. Feed was resumed after this, and the conductivity showed a rapid increase until at Point 5, gas holdup in the electrode measuring jar again prevented proper electrode wastewater contact.

The conductivity electrode was intended to indirectly monitor nutrient depletion within the reactor. Fig 2a.4 showed that the practicality of using this measurement to introduce new feed was distorted due to interference by temperature fluctuations, pH changes with acid and base and biogas holdup within the electrode vessel and within the conductivity electrode housing. For this type of reactor, it does not seem that a conductivity measurement will add value to process analysis and should rather be used to monitor the conductivity of the feed being introduced into the reactor as a control.

ORP Profile

As this was an anaerobic system, the dissolved oxygen concentration would be below measurable limits. In addition, biological substances such as enzymes, vitamins and metabolic processes correlate strongly with ORP values (Li and Bishop 2002). ORP was measured primarily to gain insight into the stability and usefulness of the reading in estimating what ORP ranges the process would produce the biggest quantity of biogas. Biogas was not measured in this pilot study, but the ORP readings showed a correlation with pH changes due to the effect of H^+, OH^- and buffering species on both the pH and redox potential (Fig 2a.4). From Day 1, where the medium within in the reactor still contained a fairly high oxygen concentration, the system rapidly descended by 220mV to -380mV from +160mV. It is well known that the concentration of dissolved oxygen within a system is correlated to the ORP (Kjaergaard 1977). Following the stopping of feed on Day 4, there was a slow but steady increase in ORP, most likely due to a decrease in available nutrients in solution from bacterial metabolism, but also because the metabolic activity of the biological system has mostly shut down due to this lack of nutrients. On Day 21, the contents of the reactor were replaced with tap water, and as expected there was an almost immediate increase in ORP due to its higher O_2 concentration. Following this, additional inoculum was added to the system, invoking a short lived rise in ORP before dropping drastically again on Day 26 when feeding and pH control resumed. Biogas was not measured in this pilot study, but ORP will be used to determine any correlation between ORP, hydrogen and butyrate production as suggested in previous studies (Cohen 1982). It is important that the ORP and subsequently the O_2 concentration remain low as oxygen is known to interfere with the H_2 producing enzymatic system (Lengeler, Drews *et al.* 1999).

pH Profile

The pH profile (Fig 2a.4) provided an informative display of the ability of the data controller code to maintain a stable pH within the reactor system. It was evident from points 3-6 highlighted in Fig 2a.4, that there was a significant hysteresis effect when the reactor was dosed with either acid or base to correct the pH. The cause of this was that the dosing point and the pH electrode were situated at opposite ends of the reactor setup. The result was when the system required a pH adjustment, the dosing pumps would continue to dose until the effect of the acid or base was noted by the pH electrode. Accordingly, due to the low flow rate, the amount of acid or base required to adjust the system pH to the required value was significantly smaller than was actually dispensed. As neither the recycle flow rate nor the position of the electrodes could be easily altered, it would be better to adjust the coding of the data controller so that pH corrections could only occur within a specific time frame, i.e. for one minute per hour. This would allow the acid or base to fully circulate before another pH reading. This would result in a slower rate of pH correction, but would help significantly in preventing hysteresis. This is highlighted in the coding below.

IFR27(2ST><0.0,1.0)AND
ALARMR28(4CV>7.0)2DSO"Acid Dose. ?"
IFR29(2ST><0.0,2.0)AND
ALARMR30(4CV<6.5)3DSO"Base Dose. ?"

2ST is the variable for minutes therefore if the minutes are between 1 and 0 and the pH is incorrect then the acid pump is switched on for 1 minute. The same occurs for the base pump and basic adjustment.

It was noted that when pH dosing occurred there was significant gas generation which resulted in large bubbles erupting through the GAC bed which interfered with fluidisation and occasionally caused GAC loss. This could be prevented by placing the pH dosing points at a different location in the reactor setup.

Bacterial Planktonic & Sucrose Analysis

The bacterial planktonic component of the reactor remained high at 7.47 log cfu/ml throughout most of the monitoring period of 27 days (Table 1). This indicated bacterial growth and viability during the study. From

the analyses that were performed, the resorcinol method (Kerr, Huber *et al.* 1984) of quantifying the sucrose levels within the reactor was reliable. The feeding regime was not optimal and would require the feeding arrangement to be appropriately diluted to prevent metabolic waste product buildup and reactor poisoning.

2c.5 Conclusion

1. This pilot study demonstrated the effect of a lack of heat insulation had on the reactor temperature profile. To minimise energy loss and strain on the heat exchanger, insulation would need to be placed on the reservoir and other major areas of heat loss.

2. In addition, results showed that as pH corrections were too drastic, we suggest that acids and bases of lower molarity be used, as well as to reduce the number of times per hour which the data controller could perform a pH correction. The effect of the presence of a fully colonised reactor on the pH profile was not established and it was unclear how well the control system would maintain the pH with the generation of butyric, propionic and acetic acids by the bacteria.

3. To allow biomass within the reactor to develop in an optimal environment, the method of dosing concentrated feed into the reactor would need to be altered by including the required diluting volume of water with the feed. The same relay could be used to power both feed and diluent peristaltic pumps to ensure operational uniformity. This would prevent the reactor from becoming poisoned with waste products produced by the bacterial biomass.

4. Furthermore, we suggest that the cylinder housing the electrodes be re-designed or re-configured to include the replacement of rubber seals with caps seal which would screw around the electrodes and ensure an air and water tight electrode box.

5. The prevention of unnecessary duplication of data points could also be achieved by reducing the frequency of recordings from the various electrodes.

6. Overall, this pilot run provided insight into the functioning of the reactor and ensured that the datalogger has consistent control over the system. The results gained from this study would confidently lead to a successful control and monitoring strategy for further fluidized bed reactor operations.

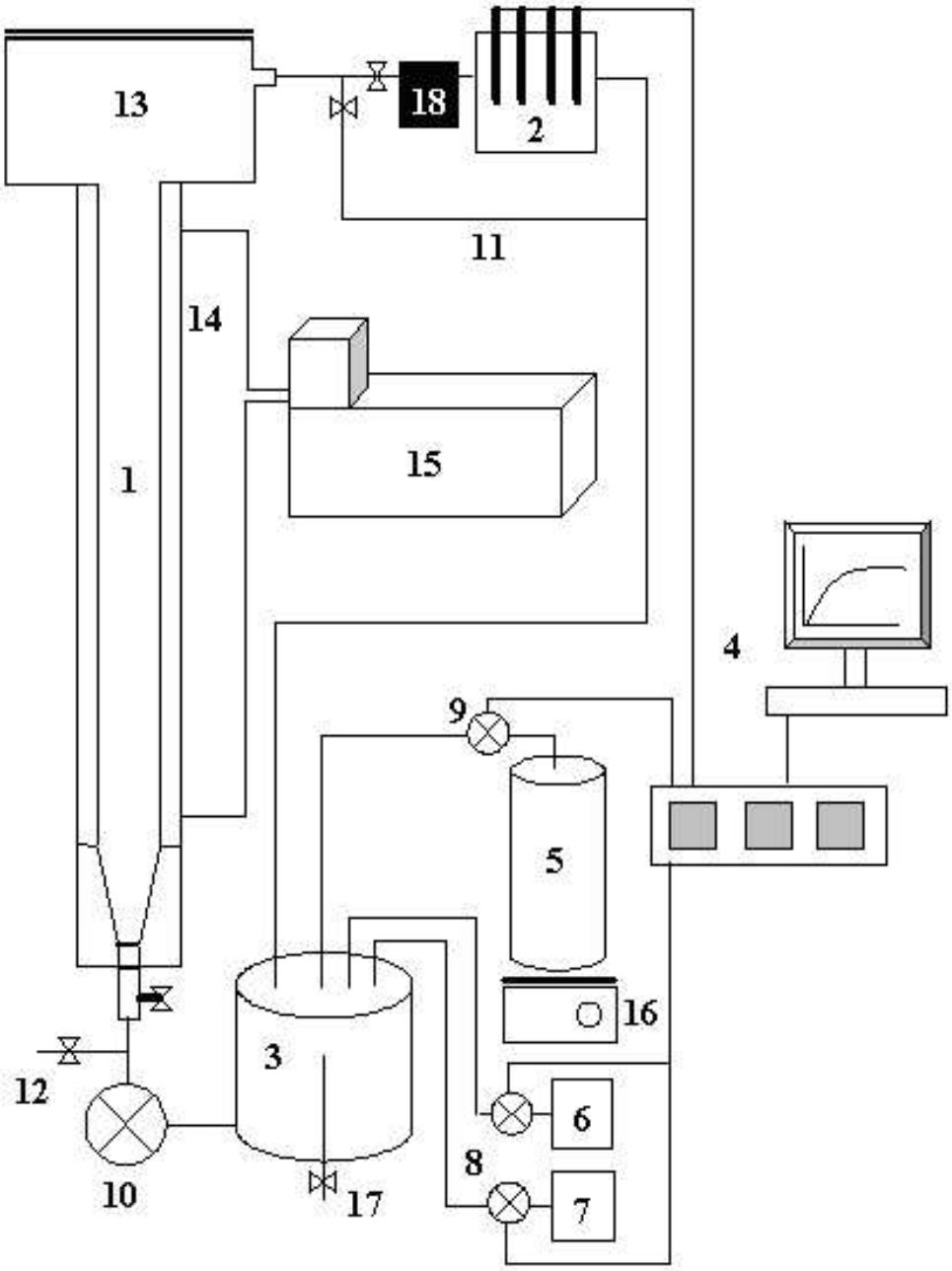
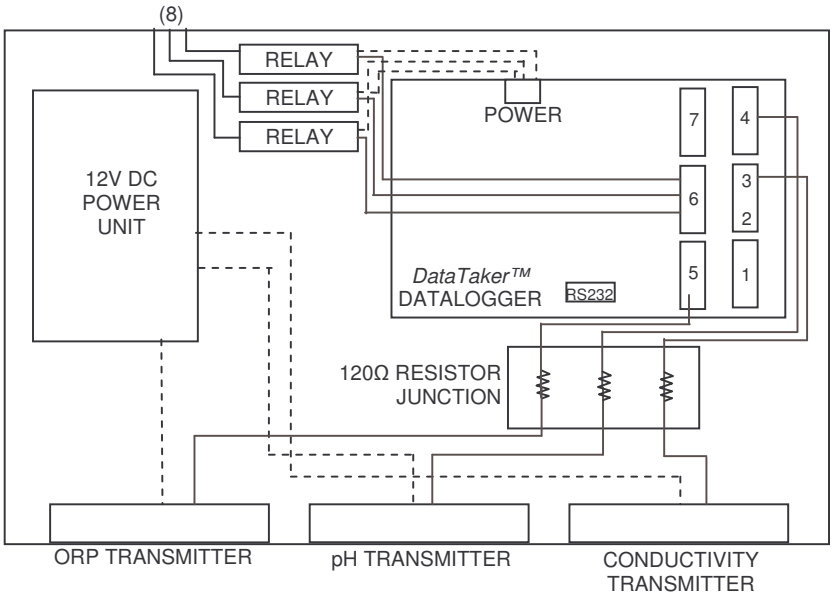


Figure 2c.1: Schematic showing the setup of the reactor system and all the components. 1 – reactor, 2 – electrode box, 3 – recycle reservoir, 4 – data logger and controller, 5 – feed reservoir, 6 – HCl reservoir, 7 – NaOH reservoir, 8 – dosing pumps, 9 – feed pump, 10 – recycle pump, 11 – bypass service line, 12 – backwash line, 13 – solid-liquid separator, 14 – waterjacket, 15 – circulating waterbath, 16 – magnetic stirrer, 17 – overflow outlet, 18 – strainer filter.

(A)



(B)

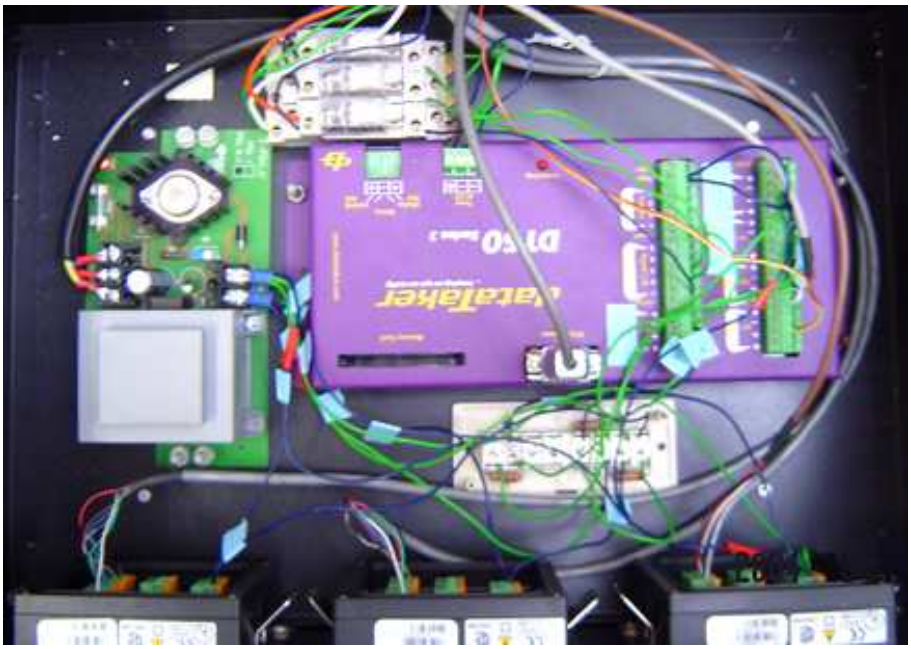


Figure 2c.2: Technical drawing of the reactor control and monitoring unit. (1) and (2) are for the environmental and reactor temperature respectively. The pH, ORP and conductivity transmitters each pass signal through a 120Ω resistor to decrease voltage going into the logger (3) was the attachment for the conductivity sensor, (4) for the ORP sensor and (5) for the pH sensor. (6) was the point connecting the relays to the digital output function of the logger, which are in turn connected to the peristaltic feed and pH dosing pumps through (8). (7) represents the ground point through which all the electrodes are placed. The logger was connected to the computer via the RS232 port on the logger.

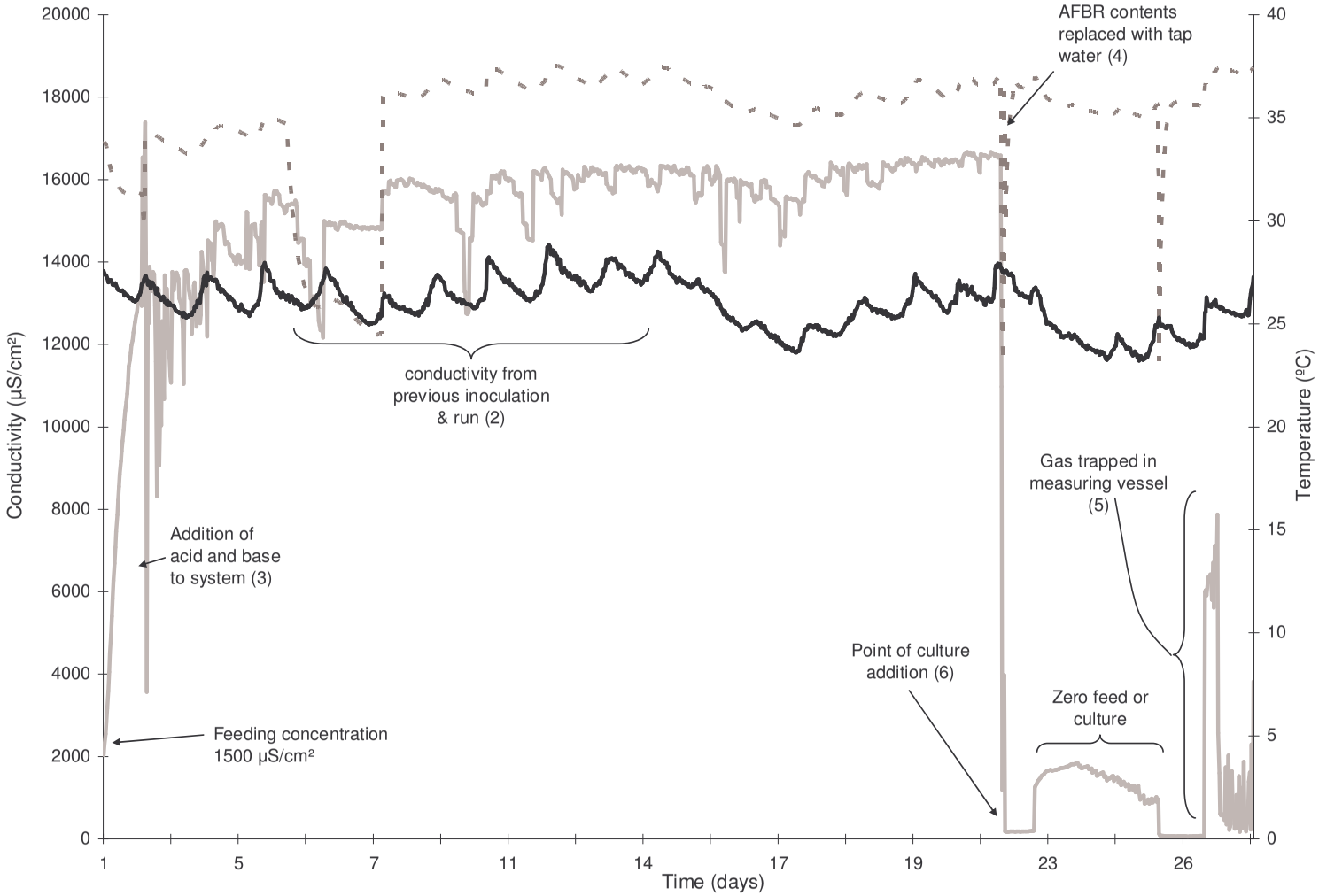


Figure 2c.3: Combined graph showing the relationship of both environmental (▬) and reactor temperature (▪▪▪▪▪) on the change of conductivity (µS.cm^{-2}) (▬) of the wastewater within the reactor. Also noted is the influence of the environmental temperature on the internal temperature of the reactor as well as the effect of the reactor temperature on the conductivity of the wastewater.

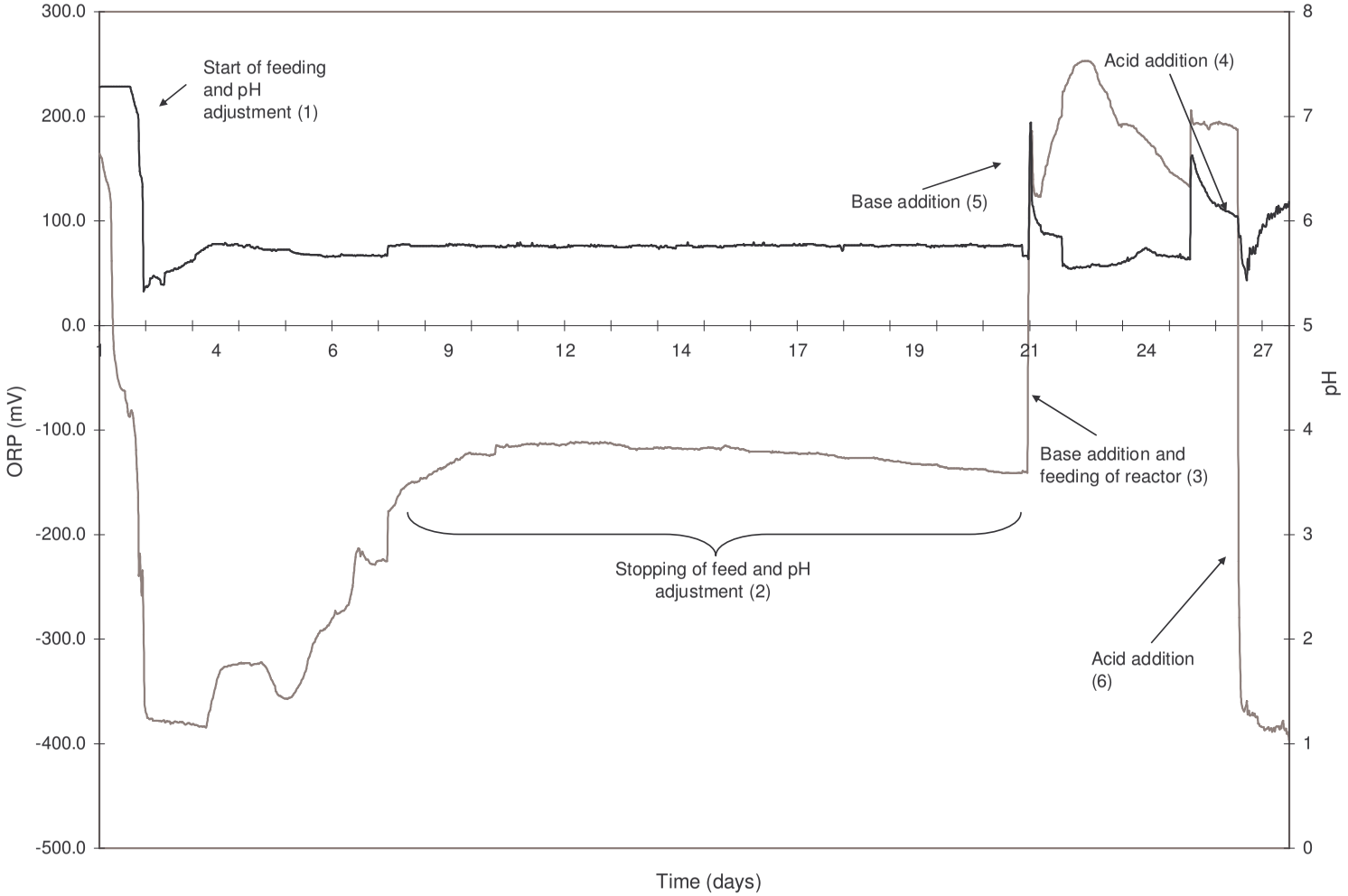


Figure 2c.4: Combined graph showing the similar trends of pH (▬) and ORP (▬) over the reactor monitoring period of 27 days.

CHAPTER 3

BIOHYDROGEN PRODUCTION USING AN ANAEROBIC FLUIDISED BED BIOREACTOR

Abstract

Alleviation of water and air pollution generated by conventional power generation facilities, as well as fresh water shortages, may be facilitated by bioenergy generation from wastewater in the form of H_2 gas. The benefits of directing bioenergy generation towards H_2 are well known, however, conversion efficiencies remain low at 15-20%. This research undertook to determine the feasibility of producing H_2 gas for fuel cell use, in a rural household, using a 13L lab scale fluidised bed bioreactor containing two facultatively anaerobic bacterial isolates, *Enterobacter cloacae* Ecl (*E. cloacae* Ecl) and *Citrobacter freundii* Cf1 (*C. freundii* Cf1). In addition, the hydraulic retention time (HRT), pH, oxidation-reduction potential (ORP), VFAs, biogas production and biofilm forming ability of the isolates in the reactor were also monitored for approximately 18 days after a steady state had been achieved. Endo formulation, using sucrose as the limiting C substrate and modified to a C:N:P ratio of 334:28:5.6, was used as the growth medium. The H_2 production rate (HPR), tested at 4.6 and 2.4 hour HRTs, showed an increase from 35 mmol H_2 / (l x h) to approximately 95 mmol H_2 / (l x h), respectively. The relative H_2 fraction of the biogas remained static around 42.3%±4.8. ORP and pH were maintained at -408±35mV and pH 5.8-6.5 respectively. Acetic, propionic and butyric volatile fatty acids remained low, with propionic and butyric acid detected at a maximum 56.8 and 135.7 ppm, respectively over the 18 days. Biofilm counts around 9.0 log cfu/g GAC were observed for both *E. cloacae* Ecl and *C. freundii* Cf1 isolates. The efficiency of converting sucrose into H_2 was calculated to be 20.5% at the 2.4 hour HRT. The HPR was comparable to other studies, however, the absence of mineral enzyme co-factors, such as Ni, Zn, Mo and Se suggested that no H_2 production occurred through the formate pathway due to the requirement of these co-factors for the formate H_2 lyase enzyme. Therefore, H_2 production occurred only through the butyric acid pathway which did not require these co-factors. In addition, the presence of propionic acid suggested that pH control and reduction of H_2 partial pressure was inadequate. At these conversion efficiencies, the use of single unit fluidised bed reactors to generate H_2 for rural household energy generation in South Africa is currently not feasible due to COD organic loads of 280kg/day required to generate sufficient H_2 to power a 5.0kW proton exchange membrane fuel cell (PEMFC).

3.1 Introduction

Wastewater treatment and subsequent renewable energy generation in the form of clean H_2 may change the dependence on climate changing fossil fuels for energy and the subsequent generation of air and water pollution (Angenent, Karim *et al.* 2004). However, the numerous connections between wastewater treatment and bioenergy generation are seldom mentioned in literature (von Uexküll 2004). Although biological methane (CH_4) production from wastewater is a well established process, carbonized fuels, such as CH_4, generate CO_2 when combusted. By contrast, the only byproduct of H_2 use is H_2O, and when used in a fuel cell, electricity plus H_2O.

The generation of biological H_2 has for a long time focused on photolysis by cyanobacteria and algae due to high theoretical conversions (Asada and Miyake 1999). However, the interest towards fermentative H_2, or dark-fermentation, has increased due to benefits, such as higher H_2 production rates and the conversion of various types of organic waste into H_2 (starch, cellobiose, sucrose, xylose etc). In addition, H_2 production via dark fermentation proceeds 24 hours a day without the need for light and can produce valuable byproducts, such as acetic, butyric and lactic acid. Importantly, fermentative H_2 production is an anaerobic process requiring no O_2.

At present, reported H_2 generation efficiencies using fermentation are low, with 15-20% efficiency under optimised conditions (Benemann 1996; Logan, Oh *et al.* 2002). To increase the efficiency of H_2 production, the use of high rate reactors, such as the upflow anaerobic sludge blanket reactor and fluidised bed, has been proposed (Chang, Lee *et al.* 2002; Wu, Lin *et al.* 2003; Chang and Lin 2004). These reactor configurations are preferred as they are more efficient in solid/liquid/gas separation and they can be operated at higher dilution rates without the detrimental washout of biomass.

There have been two previous studies using anaerobic fluidised bed bioreactors (AFBRs) for H_2 generation, both using an undefined mixed inoculum (Guwy, Hawkes *et al.* 1997; Wu, Lin *et al.* 2003).

Although there have been numerous H_2 production studies using pure cultures, the use of pure cultures in AFBRs specifically for H_2 production has not been sufficiently explored.

This study evaluated the feasibility of producing H_2 in an AFBR loaded with two bacterial species growing on granular activated carbon (GAC) at different hydraulic retention times, using sucrose as the limiting substrate. Further analysis was made to estimate scale-up sizes necessary to run various kW proton exchange membrane fuel cells (PEMFC).

3.2 Materials and Methods

Fluidised Bed Reactor Design, Setup and Operation

Fig. 3.1 provides a schematic description of the perspex lab-scale fluidised bed reactor. Wastewater was passed through the reactor (ID=7cm, Height=100cm) bed of 0.6-1.1mm granular activated carbon (GAC) (Associated Chemical Enterprises, South Africa), with volume of 1154cm^3, making up 30% of reactor volume. This volume was maintained by continually adding fresh GAC when needed. The effluent was recycled at 1.5L/min using a Boyser AMP-16 peristaltic pump (Boyser, Spain) through a 6L reservoir. The total system volume was approximately 13L. The biogas flow rate generated during the fermentation process was measured using the acidified water (Franson, Clesceri *et al.* 1998) displacement method (Lee, Huang *et al.* 1995). The gas volumes were corrected to a temperature of 35^{o}C and 760mmHg, with 1 mole gas occupying 24.8L (Levin, Pitt *et al.* 2004). The planktonic (log cfu/ml) and biofilm (log cfu/g GAC) bacterial cell counts and sucrose concentration within the reactor were also monitored at regular intervals. After startup, the reactor operated at HRTs of 4.6-2.4 hours by adjusting the volumetric flowrate of the feed. At 4.6 hours HRT, feed was introduced for 23 minutes per hour, or 140ml every 3 minutes. At 2.4 hours HRT, there were seven 4 minute feeds at 140ml/min, and two 5 minute feeds at 140ml/min, spread evenly over one hour. The operational temperature of the reactor was controlled at 35-37^{o}C using a waterjacket connected to a digital Grant GD120 waterbath (Monitoring and Control Laboratories, South Africa). The reactor pH was also controlled between pH 5.8-6.5 using 3M HCl and 6M NaOH for acid and

base adjustments respectively. Electrodes were calibrated weekly using appropriate standards for the pH and ORP meters.

Seed Culture

C. freundii Cf1 was obtained from sewage sludge samples (Olifantsvlei Municipal Sewage Treatment Plant, Johannesburg, South Africa), *E. cloacae* Ecl was obtained from garden soil samples and were identified and characterised as described previously (Chapter 2a).

Substrate

The reactor growth medium was a modification of the Endo formulation (Endo, Noike *et al.* 1982), with a C:N:P ratio modified to 334:28:5.6 (Table 2b.1) from the original 334:42:1. This was done to ensure that neither the P nor N concentration was limiting to biofilm development. Results from Chapter 2B indicated that this ratio gave the best counts for attached bacteria in binary biofilms. The following concentrations were used (g/l): Sucrose 17.65g/L (20 000 mg COD/L), NH_4HCO_3 3.464, $NaHCO_3$ 6.72, K_2HPO_4 0.692, $MgCl_2.6H_2O$ 0.1, $FeSO_4.7H_2O$ 0.025, $CuSO_4.5H_2O$ 0.005, $CoCL_2$ $1.24x10^{-4}$ (Table 2b.1). The substrate was fed into the reactor in a semi-continuous mode from concentrated feed and appropriately diluted with H_2O.

Procedure of Reactor Startup and Biofilm Generation

An initial 30 day startup procedure was performed in the reactor. This phase consisted of growing 2L of nutrient broth (Merck) for both *E. cloacae* Ecl and *C. freundii* Cf1 overnight, at 37^{o}C and 150rpm. The HRT started at approximately 9.3 hours at a feed rate of 1.4L/hour. The HRT was subsequently decreased in a stepwise manner every 3 days by increasing the feed rate an additional 140ml per hour. Two hundred and fifty millilitres of both *E. cloacae* Ecl and *C. freundii* Cf1, grown overnight in nutrient broth at 37^{o}C and 150rpm to a cell count of approximately 8.9±0.08 log cfu/ml was added to the reactor every day to keep

the number of planktonic cells in the reactor high. This was stopped after the reactor was deemed to have reached a steady state.

Analytical Methods

Biogas from the fluidised bed were analysed for H_2 and CO_2 gas using a Pye Unicam (Gomac) gas chromatograph equipped with a thermal conductivity detector and Poropak-Q column. The carrier gas was He. CH_4 was determined using a flame ionisation detector with N_2 as the carrier gas. The injection temperature for both analyses was 250^{o}C.

Detection of VFAs produced during fermentation in the fluidised bed was performed by gas chromatography (HP5890) using a flame ionisation detector. The carrier gas was He and the column was a Nukol (Supelco, South Africa).

Counts of bacterial cells attached to the GAC in the reactor were estimated after dislodging the biofilm from 1g GAC (Lindsay and von Holy 1997) using 20g sterile glass beads in 9ml sterile saline. Samples were then allowed to recover for 20 minutes before being serially diluted in saline and plated using the droplet plate technique as described previously (Lindsay and von Holy 1999). MacConkey agar modified with 1.5g/L ferric citrate and 5.0g/L sodium thiosulphate was used for plating. These additives allowed differentiation between *E. cloacae* Ecl and *C. freundii* Cf1 colonies. Planktonic populations were sampled in parallel with attached cells by preparing a dilution series in saline, of 1ml aliquots from the reactor fluid and plating on MacConkey agar modified with 1.5g/L ferric citrate and 5.0g/L sodium thiosulphate using the droplet plate technique. Both biofilm and planktonic samples were plated on non-selective nutrient agar to obtain a total count of bacteria present. All plates incubated at 37^{o}C.

Significant differences obtained between attached counts at different time points between *E. cloacae* Ecl, *C. freundii* Cf1 and the total count were calculated by multi-factorial analysis of variance (ANOVA) at the

95% confidence interval using STAGRAPHICS V. 7 (Manugistics Inc. and Statistical Graphics Corporation, 1993) program.

Microscopy

Light microscopy using a Dialux EE20 equipped with a digital camera was used to monitor the growth of biofilms on the GAC particles. Biofilm thickness was calculated using an optical micrometer. Samples of GAC for scanning electron microscopic (SEM) analysis were sampled every 7 days for the 35 days reactor biogas was measured, and at both HRTs from the top of the reactor bed and fixed in 3% glutaraldehyde. Samples were then dehydrated in an alcohol series (Lindsay and von Holy 1997), coated with gold-palladium and viewed on a JEOL JSM-840 (Japan) at 20kV and a working distance of 15mm.

In addition, the viability of *E. cloacae* Ecl and *C. freundii* Cf1 biofilms on GAC were evaluated using Confocal Scanning Laser Microscopy (CSLM). Samples of GAC were taken at 4.6 hour HRT and 2.4 hour HRT, stained using the *Bac*light™ Bacterial Viability Kit™ (Molecular Probe, Leiden, Holland) and viewed on a LSM Zeiss-410 Confocal Scanning Laser Microscope (Zeiss, Germany)

Efficiency Calculations

The efficiency of converting sucrose into H_2 was calculated to determine the percentage of sucrose in feed (17.65g/L or 93.9g/h) converted to H_2 relative to CO_2, butyric and propionic fatty acids. The average flowrate and percentage composition of the biogas with regard to CO_2 and H_2 were used in the calculation. These values were then used to calculate the amount of sucrose used in the H_2 consuming propionic acid pathway as compared to the H_2 producing butyric acid pathway (Vavilin, Rytow *et al.* 1995). The acetate pathway was used as a theoretical maximum for comparative purposes. It was assumed that carbonate dissolution did not contribute to the biogas CO_2 fraction as inorganic carbon in the effluent was not quantified.

$C_{12}H_{22}O_{11} + H_2O \rightarrow 2CH_3CH_2CH_2COOH + 4CO_2 + 4H_2$ (butyric acid pathway) (1)

$C_{12}H_{22}O_{11} + 4H_2 \rightarrow 2CH_3CH_2COOH + 2H_2O$ (propionic acid pathway) (2)

The amount of H_2 consumed by the propionic acid pathway (2) was calculated by the difference between H_2 and CO_2 molarities as they should be the same according to (2). This difference was 35.12 mmol/h. The amount of sucrose used in (2) was then determined as being one quarter the molarity of H_2 which was 8.78 mmol/h.

Similarly, the amount of sucrose used in the butyric acid pathway can be calculated from knowing the molarity of the CO_2 produced (144.67 mmol/h), as the sucrose molarity is one quarter of this (36.14 mmol/h). This brings the total amount of sucrose being used by these two pathways to 44.92 mmol/h. The efficiency of the reactor was then calculated by adding the total sucrose used in both pathways to the outlet sucrose concentration (44.92 mmol/h + 11.26 mmol/h = 19.23g/h) and dividing by the total influent feed flow rate of 90.04g/h. This gives an efficiency of 20.5% in terms of converting sucrose in H_2 gas production considering only these two pathways (Table 3.1). If the total input of sucrose (263 mmol/h) and the output of H_2 (109.5 mmol/h), is compared to the theoretical maximum of 2105 mmol/h H_2, based on the acetate pathway (1mol sucrose : 8 mol H_2), then the efficiency is 5.2%.

The concentration of sucrose within the reactor, the reactor effluent and feed was measured colorimetrically using the sucrose-resorcinol method (Kerr, Huber *et al.* 1984). Reactor effluent samples were obtained by sampling effluent that had been collected for one hour to obtain an average for one hour.

3.3 Results

Reactor Startup

The startup of the reactor took approximately 30 days, when the attached counts of both *E. cloacae* Ecl and *C. freundii* Cf1 were approximately 9.0 log cfu/g GAC. The visible change in biofilm volume took

approximately 12 days and represented only about 10% of the volume of the uninoculated bed. At the 4.6 hour HRT, the entire GAC bed of the reactor had been colonised. Visible biofilm growth caused the bed volume by to expand 100%.

Reactor Operation

The results of the reactor operation during the 17 days of gas measurements are presented by Fig 3.2. The ORP (a), pH (b) showed good stability over the two different HRTs at which H_2 production was tested. The ORP remained around -408±35mV indicating the anaerobic status of the reactor. The pH was maintained within the desired range at pH 5.8-6.5. The H_2 percentage of biogas remained stable at an average of 42.3%±4.8 over the testing period, showing no real change in percentage over the two different HRTs (Fig 3.2 c). The HPR (Fig 3.2. d) and VFA concentration (Table 3.2 e) showed an increase over the 17 days with the HPR trebling from 35 mmol H_2 / (l x h) on Day 1 to approximately 95 mmol H_2 / (l x h) on Day 17 (Fig 3.2 e). During this time the propionic acid and butyric acid concentrations trebled in concentration from 17.5 to 56.8 and 46.4 to 135.7ppm respectively. Acetic acid remained below the detection limit of 17ppm during this period.

Bacterial Biofilms

Attached counts of *E. cloacae* Ecl showed an increase over the 22 day analysis period from 7.37±0.06 log cfu/g GAC to 8.98±0.07 log cfu/g GAC as shown in Fig 3.3. Similarly *C. freundii* Cf1 showed an increase from 6.99±0.13 log cfu/g GAC to 8.99±0.09 log cfu/g GAC. The total counts performed on nutrient agar also rose from 7.3±0.0 log to 9.6±0.08 log cfu/g GAC over the same period. The total bacterial count performed on NA plates showed a statistically significant difference ($P < 0.05$) compared to both *E. cloacae* Ecl and *C. freundii* Cf1 counts which were performed on modified MacConkey agar plates. Counts of *E. cloacae* Ecl in binary biofilms were consistently statistically ($P < 0.05$) greater than counts of *C. freundii* Cf1 throughout the study.

Planktonic Growth

The planktonic population within the reactor showed increasing counts over the analysis period from 6.50±0.18 log cfu/ml to 7.17 for *E. cloacae* Ecl and 5.34±0.13 log cfu/ml to 5.75 for *C. freundii* Cf1. The total count performed on nutrient agar for the planktonic population also showed an increase from 6.60±0.08 log cfu/ml to 8.16±0.11 log cfu/ml. All counts decreased sharply when the HRT was changed from 4.6 to 2.4 hours (Fig 3.4) with *E. cloacae* Ecl showing a 1.17 log cfu/ml decrease from 7.75±0.11 to 6.58±0.06 log cfu/ml and then recovering to 7.17±0.07 log cfu/ml. *C. freundii* Cf1 showed a decrease of 1.12log from 6.77±0.02 to 5.65±0.08 log cfu/ml followed by a slight increase to 5.75±0.12 log cfu/ml. The total count also showed a sharp decrease in counts from 8.68±0.03 to 7.01±0.01 log cfu/ml before recovering back to 8.16±0.11 log cfu/ml.

Microscopy

A qualitative increase in biofilm coverage of the GAC particles was observed in scanning electron micrographs, evidenced by a decrease in the visibility of the GAC surface substructure. The scanning electron micrographs of the GAC granules, Figs 3.8 and Figs 3.9, showed a qualitative increase in biofilm coverage of the GAC particles evidenced by a decrease in the visibility of surface substructure. Day 1 (Fig 3.8 A1-A3) shows patchy biofilm coverage, however by Day 11 (Fig 3.8 B1-B3) the surface of the GAC was completely covered by biofilm. Further increases in biofilm complexity and coverage is shown on Day 25 (Fig 3.8 C1-C3), there is evidence of multiple biofilm layers. The biofilm coverage increased in maturity (Fig 3.8 D1-D3) until sloughing of biofilm became evident on Day 51 (Fig 3.8 E1-E3).

Confocal microscopy shows the presence of viable (green) (Fig 3.10), damaged (yellow/orange) (Fig 3.10 A2, B1) and dead (red) cells (Fig 3.10 B1, B3). Fig 3.9 A1-A3, taken at the 4.6 hour HRT showed that the majority of cells are viable, with a portion of the cells in the biofilm being damaged. There was a small portion of dead cells within the biofilm. The biofilm at the 2.4 hour HRT also showed that the qualitative

majority of cells are viable. There was a greater presence of dead cells at the 2.4 hour HRT (Fig 3.10 B1-B3).

Process Efficiency & Inefficiency Sources

The efficiency of the process was calculated to be 20.5% in terms of converting sucrose into through the butyrate and propionate pathways H_2. When total input and output of sucrose considered and pathways disregarded, the efficiency is 5.2%.

3.4 Discussion

Reactor Startup

The reactor startup time of 30 days proved relatively short compared to reported fluidised bed bioreactor startup times (Chapter 1a, Table 1a.4). A steady state could have been reached earlier had the HRT been reduced on a 2 day rather than 3 day schedule as sucrose is a readily degraded carbon source. Once the reactor had reached a steady state at 4.6 hour HRT, the control of biomass overgrowth proved a problem as constant biomass washout occurred. Consequently, GAC was continuously added to the reactor daily to maintain the volume of the bed. It was noted visually that the main factor affecting the biomass growth was a decrease in HRT and increase in feed rate. The concentration of feed within the reactor at the 4.6 hour HRT was low at 0.046g/L, resulting in low nutrient availability for attached and planktonic cultures for H_2 production. The concentration with the reactor was affected largely by the dilutory effect of the total system volume (≈13L). A decrease in HRT to 2.4 hours showed a reactor sucrose concentration of 0.745g/L, an approximate 16 times increase.

Reactor Operation

The redox potential of -408±35mV over the gas measurement period was similar to other studies (Zoetemeyer, Matthijsen *et al.* 1982). It was not possible to determine a trend between the H_2 production rate and redox potential as too few gas samples were taken (Fig 3.2 (a) and Fig 3.2 (d)). The HPR showed a clear correlation to the change in HRT from the 4.6 hour to 2.4 hours. The trebling of HPR from

35 to 95 mmol H_2 / (l x h) shows that the reactor was operating below its capacity at the 4.6 hour HRT. The reactor was approaching it's maximum metabolic rate maximum at the 2.4 hour HRT as the residual sucrose in the reactor showed a 16 times increase in concentration, and a drop in sucrose utilisation from 99.7% to 95.7%.

Wastewaters containing recalcitrant compounds (Wilson, Khodadoust *et al.* 1998; Koran, Suidan *et al.* 2001; Maloney, Adrian *et al.* 2002) would be more justified in using GAC or one of its variants due to its adsorptive properties (Xiaojian, Zhansheng *et al.* 1991; Zhao, Hickey *et al.* 1999). GAC was chosen in this study as a carrier substrate due to its high rugosity and irregular surface structure, and also due to its use in previous H_2 production studies (Chang, Lee *et al.* 2002). However, results from this study indicated that the GAC used was not suited to this reactor. It was noticed during the entire study that the GAC particles showed a tendency to disintegrate over time. A structurally more robust carrier, such as silica sand, would be required for future studies particularly when a carrier particle recycling system is installed.

Bacterial Biofilm Growth

The initial focus of inoculating the reactor was to achieve high levels of attachment (> 9.0 log cfu/g GAC) on the GAC carrier. However, bacterial counts from the reactor startup and counts performed prior to the gas measurement phase showed that attachment of bacteria was not a concern, as counts were regularly above 9.0 log cfu/g GAC. The problem was rather the increase in volume of the biofilm. Literature reports contain little information on the generation of biofilm volume. Logically, as the biofilm EPS matrix is comprised of 50-80% carbon (Allison 1998; Sutherland 2001; Donlan 2002), excess carbon should encourage its expansion. Therefore, supplying carbon sufficient only for metabolic purposes was unlikely to promote volumetric growth. Carbon in the form of sucrose was therefore added in excess of basal requirements by a stepwise reduction of HRT, thereby facilitating volumetric expansion of the biofilm and fluidisation conditions within the reactor. Though the change in biofilm volume was not reflected in the counts obtained from GAC samples, steady increases in biofilm coverage were shown in the scanning electron micrographs taken of GAC particles at various stages in the experiment. The statistical difference

between *E. cloacae* Ecl and *C. freundii* Cf1 attached counts suggested that *E. cloacae* Ecl was better adapted to conditions within the reactor, and therefore attached in greater numbers. This contrasted to the results in Chapter 2B, where no difference in attached counts was found between the isolates in binary biofilms. The higher total bacterial count suggested that the injured or dying bacterial cells could not grow on the modified, selective, differential MacConkey agar, but could grow on nutrient agar which presented a lower growth inhibiting pressure.

Though contamination, based on colony morphology of *E. cloacae* Ecl and *C. freundii* Cf1, in the reactor system was not evident in plate counts, it was found that low levels of suggested fungal contamination also may have been present (Fig 3.7) due to the unsealed and accessible nature of the reactor. One contaminating fungal isolate was obtained from the reactor and given the identification of *Basipetospora* gen. nov. based on morphological features in Fig 3.7 and from light microscopy (Cole and Kendrick 1968; Straker 2004). The contribution of the fungus to the volume of the biofilm on the GAC particles or to the production or sequestration of H_2 within the reactor was not established. The fungal contamination observed in (Fig 3.7 A) was eventually "lost" as the biofilm on the GAC grew to maturity. The contamination of treatment plants by fungal contamination has occurred in past studies, and has been explained due to the lack of P in the wastewater (Hendrickx, Meskus *et al.* 2002). This fungal proliferation was probably due to nutrient competition between bacteria and fungi within the wastewater.

Several previous H_2 studies have used pure isolates (De Corte, Dries *et al.* 1989; Rachman, Furutani *et al.* 1997; Rachman, Nakashimada *et al.* 1998; Kumar, Monga *et al.* 2000; Palazzi, Fabiano *et al.* 2000; Yokoi, Saitsu *et al.* 2001; Collet, Adler *et al.* 2004) and several have used undefined mixed cultures (Zoetemeyer, Arnoldy *et al.* 1982; El-Farhan and Shieh 1999; Lin and Chang 1999; Chen, Lin *et al.* 2001; Fang and Liu 2002; Yu, Zhu *et al.* 2002; Lin and Lay 2004a). There are several problems using either pure or undefined mixed cultures. Pure cultures are useful for determining baseline data on H_2 production and growth kinetics, however mono-cultures or in this study co-cultures, do not contain sufficient versatility in their metabolic capacity to accommodate as many system disturbances or nutrient conditions as a mixed culture. Undefined mixed cultures are known to be more stable to changes within the composition of

wastewater (Pynaert, Smets *et al.* 2003). The increased ability of these cultures to use alternative removal pathways is both an advantage for system stability and a disadvantage for system efficiency as the alternative pathways are a likely cause of inefficiencies and H_2 sinks (Hashsham, Fernandez *et al.* 2000). A potential solution to the selection of suitable microbial cultures for use in H_2 production could be the use of defined mixed-species. Selection of microorganisms could be aided by mining genomic databases to identify potentially useful H_2 producers (Kalia, Lal *et al.* 2003). This would be useful as the presence or absence of key H_2 producing pathways could be identified beforehand. Selection could involve using several *Clostridia* spp. for their H_2 generation capacity (De Corte, Dries *et al.* 1989; Taguchi, Mizukami *et al.* 1995; Collet, Adler *et al.* 2004) and heat tolerance, several *Bacillus* spp. for their facultatively anaerobic metabolism and heat tolerance and perhaps several species of *Enterobacteriacae*, e.g. *E. aerogenes* (Rachman, Nakashimada *et al.* 1998; Palazzi, Fabiano *et al.* 2000), *E. cloacae (Kumar and Das 2001), C.freundii,* (Kanayama, Sode *et al.* 1987), and hyperthermophilic or genetically enhanced cultures.

Bacterial Planktonic Growth

The planktonic component of the reactor was always lower than the biofilm component, with the counts (4 x 10^6 cfu/ml) equaling approximately 20% of the biofilm (2.0 x 10^7 cfu/g GAC) component just prior to gas measurements, after which the percentage of planktonic (1.62 x 10^8 cfu/ml) versus biofilm (3.85 x 10^9 cfu/g GAC) counts dropped to an average percentage ratio of 3%. This comparison provides a numerical estimate of the contribution the planktonic component of the reactor made towards the H_2 production rate. There was a momentary decrease in counts immediately following the reduction in HRT from the 4.6 to 2.4 hour HRT, probably resulting from the increased feed or dilution rate.

Reactor Culture Selection

The contamination present in this reactor (Fig 3.7) presented an interesting contradiction to several other studies which used heat or acid treated sewage sludge as a source of inoculum (van Ginkel, Sung *et al.* 2001; Chang, Lee *et al.* 2002; Oh, van Ginkel *et al.* 2003; Wu, Lin *et al.* 2003; Lin and Lay 2004b). Both heat treatments of sewage sludge at 80^{o}C and 100^{o}C for 20 minutes, as well as 24 hour pH treatments at

pH 5.0 revealed a mixture of heat and pH stable, non-obligatory anaerobic bacterial species. Many of the bacterial colony morphologies presented similarities to species of the facultatively anaerobic spore forming *Bacillus* genus i.e. irregular, undulate, umbonate, white, dry colonies (Krieg and Holt 1984). *Bacillus* spp. have however been used in H_2 production studies (Kalia, Jain *et al.* 1994). They may even be used to induce an anaerobic state in reactors with obligatory anaerobic *Clostridia* spp. as opposed to a non spore forming bacterium such as *E. aerogenes* (Yokoi, Saitsu *et al.* 2001). Inaccuracies arise when *Clostridia* spp. are claimed to predominate in a reactor based on prevalence of butyric acid or propionic acid which are known to be produced by *Clostridium butyricum* and *Clostridium propionicum* respectively (Wu and Lin 2004). The linkage of certain bacterial species to fatty acids widely produced in fermentative bacteria without microscopic or genomic confirmation lacks accuracy. Genomic analysis of H_2 production from food wastes at mesophilic and thermophilic showed a lack of *Clostridia* spp., but instead a wide variety of bacterial species including *Bacillus* spp. (Shin, Youn *et al.* 2004).

Microscopic Examination of GAC Biofilm

Scanning electron microscopy served as a useful too to observe the biofilm macrostructure on the GAC particles Figs 3.8 and 3.9. The micrographs showed an increase in biofilm complexity and volume as the HRT was reduced from the Day 1 to Day 51. There were in addition contaminating bacteria, seem in Fig 3.7.B as cocci shaped bacteria. It was likely that there were several types of contaminating microbes in the reactor despite the use of aseptic technique.

Confocal Scanning Laser Microscopy pictures of 4.6 hour HRT biofilm (Fig 3.10 A1-A3) showed that the majority of the cells in the biofilms were viable with a few isolated pockets of injured or dead cells present. The 2.4 hour HRT biofilm (Fig 3.10 B1-B3) showed a similar pattern of viability within the biofilm although there seemed at least qualitatively, to be larger numbers of dead and injured cells, possibly due to the maturity of the biofilm.

Process Efficiency & Inefficiency Sources

The H_2 production rate shown in Table 3.2, had an average HPR at 2.4 hour HRT of 95.4 mmol H_2 / (l x h). These results were similar to the anaerobic reactor studies conducted by (Chang, Lee *et al.* 2002) and (Chang and Lin 2004) where the H_2 rates were recorded as 121.0 and 113.4 mmol H_2 / (l x h), respectively. In this study, the rate of H_2 production was lower than expected when considering that only 5.2% of total sucrose feed was used for H_2 generation, or some 20.5%, if only the butyrate and propionate pathways are considered. Other studies have reported efficiencies approaching 23% using sucrose as the carbon source (Benemann 1996; Logan, Oh *et al.* 2002). The method used to collect gas was problematical as constant adjustment of the flowrate going through the bypass line (Fig 3.1) was needed for gas collection. There is a possibility that the collection method resulted in an under recovery of biogas, hence resulting in an under-estimation of the H_2 production rate. An appropriate gas disengagement system would have to be used for future studies. The presence of propionic acid and the absence of acetic acid in the volatile fatty acid profile suggested that reactor conditions were not optimal for H_2 production. While the exact activation mechanism of the propionic acid pathway has yet to be elucidated, the pathway presents a H_2 sink, reducing the overall H_2 production rate. We suggest that that reduction of propionic acid production will ensure that more carbon source goes to the production of H_2 through more favourable pathways such as the acetic or butyric acid pathways. Biochemical re-direction will ensure that the volatile fatty acids generated within the H_2 reactor can be further utilised for CH_4 production in a methanogenic reactor. The accumulation of propionic acid has often been associated with methanogenic reactor failure as it cannot be utilised directly by methanogens (Ren, Wang *et al.* 1997). It has been suggested that anaerobic digestion processes can withstand almost ten times the concentration of acetic acid and butyric acid as opposed to propionic acid (Inanc, Matsui *et al.* 1999). In addition, the oxidation of propionic acid to acetic acid is the slowest amongst all fatty acids (Dohanyos 1985) and so presents a rate limiting step in acetogenesis.

There are several mechanisms proposed to initiate the propionic acid pathway. Feed rate and feed regime, pH range and H_2 partial pressure presumably each have a role to play in lowering the efficiency of the H_2 production rate.

The propionic acid pathway is reportedly activated due to a high H_2 partial pressure (Harper and Pohland 1986). However *E. cloacae* Ecl and *C. freundii* Cf1 are both part of the *Enterobacteriacae*, which contain formate H_2-lyase enzymes (Gray and Gest 1965). These bacteria produce a portion of the total H_2 in the following manner.

$$HCOOH \rightarrow H_2 + CO_2 \ (E_o = -432mV) \qquad \text{(De Corte, Dries } et\ al. \text{ 1989)}$$

The low redox potential of the above equation allows H_2 to be released, provided the H_2 partial pressure is below 1atm. However research has shown that sparging experimental *Escherichia coli* systems with gas increased the levels of formate being produced, thus indicating a partial pressure effect on the production of H_2 (De Corte, Dries *et al.* 1989). Even so, conflicting evidence (Inanc, Matsui *et al.* 1999)showed that neither artificially increased H_2 pressure, over-pressurised H_2 gas (2atm), nor reduced H_2 partial pressure (0.13atm) affected the accumulation of propionic acid and the distribution of other fatty acids from anaerobic sludge (Inanc, Matsui *et al.* 1996; 1999).

Propionic acid is however not the only fermentation product that leads to a reduced H_2 production rate. Although not all measured in this study, the end products of glucose fermentation proceed through pyruvate (Chapter 1, Fig 1b.1). The evolution of H_2 through the NADH pathway is driven by the metabolic necessity to reoxidise residual NADH as seen in the reaction below.

$$NADH + H^+ \rightarrow NAD^+ + H_2$$

Thus the biochemical pathways of the cultures in a reactor system need to be controlled to ensure excess NADH, thereby increasing the H_2 production rate. Accordingly, products such as fumarate, succinate, lactate, butanol and ethanol have no connection with the production of H_2, but only contribute to the reoxidation of NADH, thereby reducing the pool of NADH available for H_2 production (Tanisho, Kuromoto *et al.* 1998).

Fumarate $CH_3COCOOH + \mathbf{CO_2} + \mathbf{NADH + H^+} \rightarrow (CHCOOH)_2 + H_2O + NAD^+$ (1)

Succinate $CH_3COCOOH + \mathbf{CO_2} + \mathbf{2NADH + 2H^+} \rightarrow (CH_2COOH)_2 + H_2O + 2NAD^+$ (2)

Both fumarate and succinate are synthesized secondarily using CO_2 and pyruvate through NADH. CO_2 is a by-product from another metabolic pathway, e.g. acetic acid or butyric acid pathway. Therefore if the partial pressure of CO_2 is reduced, one may curb this reaction. This action would reduce the amount of succinate and fumarate in the reactor, making more NADH available for H_2 production. It seems evident that sparging a reactor system to remove CO_2 and H_2, or employing other removal means e.g. vacuum systems, will not prevent the initiation of the propionic acid pathway but instead prevent the propionic acid pathway becoming the predominant fatty acid and preventing loss of H_2 through this sink.

The feeding regime of a reactor also purportedly has an effect on the production of certain fatty acids in a reactor. This is especially evident in mixed-culture reactors where irregular feeding can select for non-spore propionic acid formers (Cohen, Distel *et al.* 1985). Although this reactor was not inoculated with a mixed culture, there is a possibility that the semi-continuous feeding regime used caused the cultures within the reactor to proceed along a propionic acid pathway. It was also reported that glucose was the limiting substrate for butyric acid production (Vavilin, Rytow *et al.* 1995). However when the feeding rate was increased, there was not the suggested increase in butyric fatty acid production (Fig 3.2 e). Longer monitoring periods at the 2.4 hour HRT could in future provide evidence to the contrary.

Furthermore, it is unclear why propionic and butyric acids were present at such low concentrations. For fermentation reactions using hexose sugars, the concentration of butyric acid and propionic acid are generally 10-100 times greater than present in this study. Concentrations of butyric acid in a study on the anaerobic digestion of glucose showed a butyric acid concentration of approximately 1000ppm and a propionic acid concentration of 1500ppm (Khanal, Chen *et al.* 2004). This inconsistency could be that the predominant pathway leading from sucrose fermentation was neither the acetic, butyric nor propionic acid pathways. Several other pathways are known to be active during fermentation with the ethanol, lactic acid, formic acid, valeric acid, caproic acid and iso-butyrate being examples alternative pathways found

(Cohen, Zoetemeyer *et al.* 1979; Zoetemeyer, Van Den Heuvel *et al.* 1982; Fang and Liu 2002; Kim, Hwang *et al.* 2004). Assaying for a wider number of fatty acids in future would be needed to identify the predominant fatty acid species within in the reactor.

The monitoring and control of the pH in a H_2 producing reactor is important not only for the control of metabolic pathways (Lay 2000) but also because pH serves as an inhibition mechanism for methanogens (Kim, Hwang *et al.* 2004). The choice of pH is important not only for the optimal production of H_2, but also for the production of fatty acids and control of biomass growth. The inability of the isolates used in this study to grow properly below pH 5.0 and above pH 9.0 (Chapter 2a, Fig 2a.1) resulted in the range selection of pH 5.8-6.5. This range was chosen to prevent methanogens from contaminating the system, although during the 4.6 hour HRT, CH_4 was detected twice at 0.29% v/v. The source of methanogenic contamination is unclear.

The reported optimum pH for H_2 production is widely variable in the literature, from pH 9.0 for the batch fermentation of sucrose (Lee, Miyahara *et al.* 1999) to pH 4.0-4.5 and pH 4.7-5.7 for the continuous fermentation of sucrose (Ren, Wang *et al.* 1995) and starch (Lay 2000), respectively. It has been reported that pH alone is insufficient to prevent methanogenesis from occurring in a reactor and that pH control together with HRTs below 9 hours need to be employed to prevent methanogenic growth (Kim, Hwang *et al.* 2004). Recent literature suggests that the best pH to operate H_2 reactor, both for the prevention of methanogenic growth and propionic acid production is approximately pH 5.0 (Inanc, Matsui *et al.* 1999). It has been suggested that in mixed culture reactors propionic acid production is probably initiated during pH fluctuations, which cause population shifts within the reactor (Inanc, Matsui *et al.* 1996). It has been found that propionic acid producers were inhibited by low pHs. However the effect of a low pH on the production of propionic acid using the *E. cloacae* Ecl and *C. freundii* Cf1 isolates is unclear, as it is unknown what effect pH 5.0 has on the biochemical pathways of these isolates.

The nutrient formulation used for feeding the reactor was important not only for biofilm formation but also for HPR, production efficiency and biomass yield as loading rates and COD:N:P are misleading ratios

(Ammary 2004). Studies done by Lin *et al*., (2004a) suggest that the C:N ratio use in this study of 12:1 was almost 4 times more concentrated than the suggested optimum ratio. Lower ratios such as the one in this study suggest high ammonia concentration. Higher ratios suggest an inadequate nitrogen supply. This ratio was chosen primarily for the prevention of N and P limited biofilm growth, however it proved more than just beneficial for biofilm attachment, as high C:N ratios are known to produce reduced compounds (Yu and Fang 2001; Lin and Lay 2004a). Previous studies on concentrations of carbonate and phosphate such that $NaHCO_3$ and K_2HPO_4 used in this study could be replaced using Na_2HPO_4 (Lin and Lay 2004b). Studies on the concentrations of nutrient elements showed that $MgCl_2.6H_2O$, NaCl, $ZnCL_2$ and $FeSO_4.7H_2O$ were salts of elements having the largest effect, all of which were lower in this study than the recommended levels. Zn has been the most neglected nutrient trace metal in H_2 production studies (Lee, Miyahara *et al.* 2001; Lin and Lay 2005). Low levels of Fe in the nutrient medium has been know to cause end product shifts in both obligate anaerobes and facultatively anaerobic bacteria (Gray and Gest 1965). There exists the possibility that the Fe concentration within the reactor was suboptimal as the Fe^{2+} ions within the concentrated feed ($FeSO_4.7H_2O$) were naturally oxidised to Fe^{3+} and precipitated out of solution, forming a sediment layer at the bottom of the feed tank. This was partly remedied through re-suspension of the precipitate using a centrifugal pump, however the flow rate was low and could have resulted in the intended Fe concentrations not being introduced into the reactor. In addition, the formate-hydrogen lyase which comprises formate dehydrogenase H and hydrogenase 3 together lyse formate into CO_2 and H_2. The catalytic activity of formate-hydrogen lyase requires not only a Mo and Ni co-factor which was not supplied in this experiment, but also Fe which was suspected to be deficient. Formate dehydrogenase H has the presence of selenocysteine as a novel amino acid, however Se was not supplied. It is likely that the formate produced by the cultures within the reactor was simply excreted out of the cell resulting in the process deriving no further H_2 production from this end product (Lengeler, Drews *et al.* 1999).

It seems that although the feed used in this study was sufficient for biomass growth and cellular metabolism, the sup-optimal supplementation of mineral elements probably resulted in a lowered H_2 production rate.

Scale-up Feasibility

One of the uses of biologically produced H_2 include use in proton exchange fuel cell systems (PEMFCs). Fuel cell systems require a continuous supply of H_2 gas which needs to be free of CO and H_2S gases (<10ppm). These gases could be removed using biological reactors (Jung, Kim *et al.* 2002; Oh, Seol *et al.* 2003; Sipma, Lens *et al.* 2003; Levin, Pitt *et al.* 2004) and stripping respectively in parallel with the H_2 biological reactor.

Knowing the flowrates of H_2 necessary for different size fuel cells (Table 3.3), one can estimate the size of reactor which will be able to deliver the flowrate, assuming that no change in H_2 production occurs in the process (Table 3.4). The calculated sizes are only meant to serve as indicators of practicality. From the values in the tables, one can see that at the current H_2 production rate of 95.4 mmol H_2 / (l x h), one would need a reactor of approximately 1250L to allow the operation of a 5.0kW fuel cell, which is not unattainable. Values from the studies of Chang *et al.*, (2002) and Chang *et al.*, (2004) showed a similar bioreactor size to ours. The thermophilic studies are not feasible at this stage as bioreactor sizes of 14600L are not practical.

While the H_2 production rates of various dark fermentations processes are promising there are several problems that present technical problems. The presence of contaminating gases such as CH_4, H_2S or NH_4 is problematic. In addition, many fermentation gas streams are less than 50% H_2, although PEMFCs require H_2 purity in excess of 99%.

According to Table 3.5, 57% of the rural electrical power requirement could be met with solar energy and methane for cooking and heating water. Demand for electrical power for household electrical appliances would be approximately 43% of the total household energy demand. This would be equivalent to 10.5 kWh/day or 3 832 kWh/year. Power for this level of electrical demand in remote rural settings could be generated from PEMFCs. This 43% would require a 1.0 kW PEMFC per rural household.

However in the absence of solar heating or methane a rural household would require an electricity supply from a 5kW PEMFC. There are several assumptions to be considered for the successful implementation of such a scheme.

- A single rural household consumes 24.42 kWh/day of power per day or 744.81 kWh/month
- H_2 biogas production rate = 95.4 mmol H_2 /(h x L).
- PEMFC power per household = 5 kW.
- Bioreactor volume per household = 1250 L.
- COD conversion efficiency = 1.0 g H_2 / 48g COD or 11.9 L H_2/48 g COD.
- 1 g COD is equivalent to 0.9 g glucose.
- A 5 kW PEMFC requires 2968 L H_2/h.
- COD required = 280kg COD per day per household.

Considering the large COD per household necessary to run a 5.0kW fuel cell, it would be necessary to pool household COD production capacity to ensure technological feasibility and economic viability of electricity supply from a H_2 generating FBBR-PEMFC utility. Therefore electricity would be supplied from a central power utility based on AFBR and PEMFC technology. Wastewaters with a high COD would be required for sufficient H_2 generation; therefore the most plausible idea would be to convert conventional sewage works into electricity generating facilities. These types of sewage plants could convert domestic, agricultural, agro-industrial and timber processing waste from the surrounds and generate electricity for consumption by end users. Therefore while it would not be feasible to use fluidised beds in individual homes for H_2 generation at current conversion efficiencies (20-23%), the option of converting existing and future sewage plants in H_2 generating facilities provides the most likely way forward.

3.5 Conclusions

The results from the conversion of sucrose to H_2 show 4 major conclusions:

1. The low percentage of planktonic cells (~3%) and the high attached bacterial counts (≥ 9.0 log cfu/g GAC) showed that the majority of the H_2 production was likely due to biofilm activity which confirms that the reactor was working as a fluidised bed bioreactor.

2. Additional mineral elements such as Ni, Zn, Mo and Se need to be included in the Endo formulation to ensure that all the H_2 production pathways requirements for cofactors are met. In addition, the C:N:P ratio needs to be further modified as the N concentration currently used seemingly caused NH_3 toxicity in the reactor. As biomass is a critical factors in AFBRs, both the biomass and H_2 production must be optimized for the process to improve further.

3. Results from this study suggested that the collection and removal of H_2 and CO_2 from the system as the method used was too cumbersome and was a possible cause of increased H_2 partial pressures and activation of H_2 consuming pathways (propionic acid) and H_2 reducing (succinic acid) pathways.

4. The conversion efficiency of carbohydrates into H_2 in this study was comparable when considering the butyrate and propionate pathways (20-23%), however when calculating the molar quantity of H_2 that could have been generated from sucrose fed in the reactor, the efficiency was a low 5.2%. Therefore the use of fluidised bed bioreactors in individual homes, at these conversion efficiencies, would present a challenging prospect. Looking forward, greater control of system functions and careful selection of reactor cultures would ensure increases in conversion efficiency, and therefore make investigations for small scale use of these reactors feasible. Furthermore, on a larger scale, the conversion of existing and future sewage and wastewater treatment plants into H_2 generating facilities could serve pollution reduction, bioenergy generation and water reuse concerns better.

Table 3.1: Variables used for the calculation of the process efficiency of converting sucrose into H_2 gas at the 2.4 hour HRT.

Measurement Variable	**Mass flowrate (g/h)**	**Molar flowrate (mmol/h)**
Sucrose concentration of feed	93.9 g/h	274.32 mmol/h
Sucrose concentration of effluent	3.86 g/h	11.26 mmol /h
Sucrose utilised	90.04 g/h	263.03 mmol/h
% Sucrose utilisation	95.8%	
Biogas Measurement	**Flowrate/ Composition**	
Biogas flowrate (average)	6.35 L/h	
H_2	41.8%	109.55 mmol/h
CO_2	55.2%	144.67 mmol/h
Pathway efficiency*	**20.5%**	
Total Efficiency	**5.2%**	

*using butyrate and propionate pathways

Table 3.2: The H_2 synthesis rate from the present study compared to synthesis rates from other hydrogen production studies. All rates have been converted to common units and corrected to STP (30°C and 101.3kPa) (Levin, Pitt *et al.* 2004). Rate was calculated per area of uncolonised GAC bed which was 1.154dm^3.

BioHydrogen System	Reactor Type	H_2 Synthesis Rate mmol H_2 / (l x h)	Reference
Mesophilic, pure strains[a]	Fluidised	95.4	Current Study
Mesophilic, pure strain[b]	Chemostat	21.0	(Ueno, Otsuka *et al.* 1996)
Mesophilic, undefined	Photo	64.5	(Jouanneau, Lebecque *et al.* 1984)
Mesophilic, mixed undefined	Fixed Bed	121.0	(Chang, Lee *et al.* 2002)
Mesophilic, undefined,	UASB	113.4	(Chang and Lin 2004)
Thermophilic, undefined,	Photo Reactor	8.2	(Lindblad, Christensson *et al.* 2002)
Extreme Thermophilic, pure strain[c]	Photo Reactor	8.4	(Ko and Noike 2002; Kondo, Arawaka *et al.* 2002)

[a] – Current Study, *Enterobacter cloacae* Ecl, *Citrobacter freundii* Cf1
[b] - *Clostridium* species 2
[c] - *Caldicellulosiruptor saccharolyticus*.

Table 3.3 Different sizes of Proton Exchange Membrane Fuel Cells (PEMFC) and H_2 flow rate required to run them (Levin, Pitt *et al.* 2004).

Size of PEMFC (kW)	H_2 Flow Rate Required mol/h
1.0	23.9
1.5	35.9
2.5	59.9
5.0	119.7

Table 3.4: Approximate sizes of biological reactor required to run a 1.0, 1.5, 2.5 and 5.0 kW PEMFC fuel cell.

BioHydrogen System	H_2 Synthesis Rate mmol H_2 / (l x h)	Size of bioreactor required to power a[a] :				Reference
		1.0 (kW) FC (L)	1.5 (kW) FC (L)	2.5 (kW) FC (L)	5.0 (kW) FC (L)	
Mesophilic, pure strain[a]	95.4	$2.5x10^2$	$3.76x10^2$	$6.27x10^2$	$1.25x10^3$	Current Study
Mesophilic, pure strain[b]	21.0	1.14×10^3	1.71×10^3	2.85×10^3	5.70×10^3	(Ueno, Otsuka *et al.* 1996)
Mesophilic, undefined	64.5	3.71×10^2	5.57×10^2	9.29×10^2	1.86×10^3	(Jouanneau, Lebecque *et al.* 1984)
Mesophilic, mixed undefined	121.0	1.98×10^2	2.97×10^2	4.95×10^2	9.89×10^2	(Chang, Lee *et al.* 2002)
Mesophilic, undefined,	113.4	$2.11x10^2$	$3.17x10^2$	$5.28x10^2$	$1.05x10^3$	(Chang and Lin 2004)
Thermophilic, undefined,	8.2	$2.91x10^3$	4.38×10^3	7.31×10^3	1.46×10^4	(Lindblad, Christensson *et al.* 2002)
Extreme Thermophilic, pure strain[c]	8.4	2.85×10^3	4.28×10^3	7.13×10^3	1.43×10^4	(Ko and Noike 2002; Kondo, Arawaka *et al.* 2002)

[a] - Approximate volumes. Calculated volumes were rounded up to nearest whole value
[b] - *Clostridium* species 2
[c] - *Caldicellulosiruptor saccharolyticus*.
FC – Proton Exchange Membrane Fuel Cell

Table 3.5: The average rural South African household has the following electricity consumption pattern.

Application	**Energy Consumption (kWh/month)**[a]
Hot water	332
Stove	87
Heating (2 cold months)	200
Appliances	104
Lights	55
Weighted Averages	**(kWh/unit time)**[a]
Annually	8 857
Monthly	738
Daily	24
Percentage Usage per Application	**%**
kWh used for heating water	45
kWh used for cooking	12

[a] – values rounded off to nearest whole value

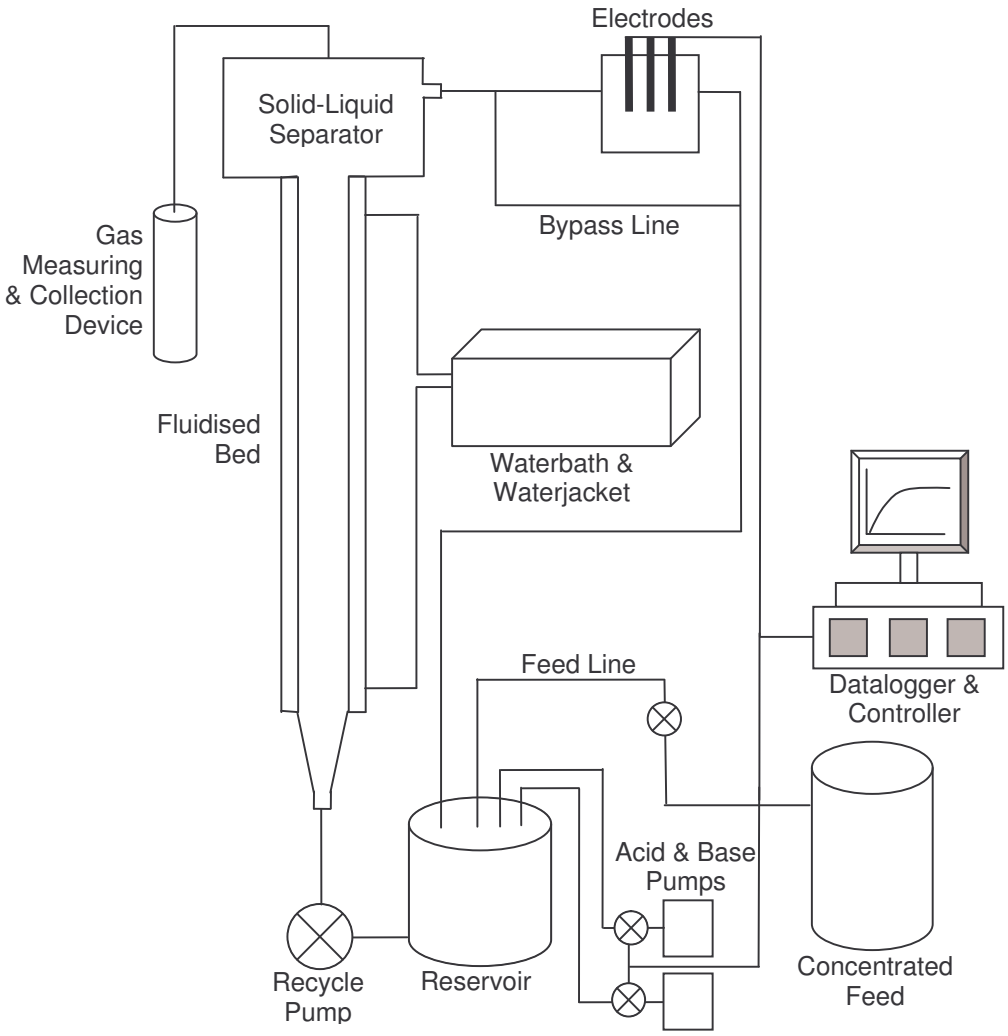


Figure 3.1: Schematic description of the fluidised bed for continuous hydrogen production.

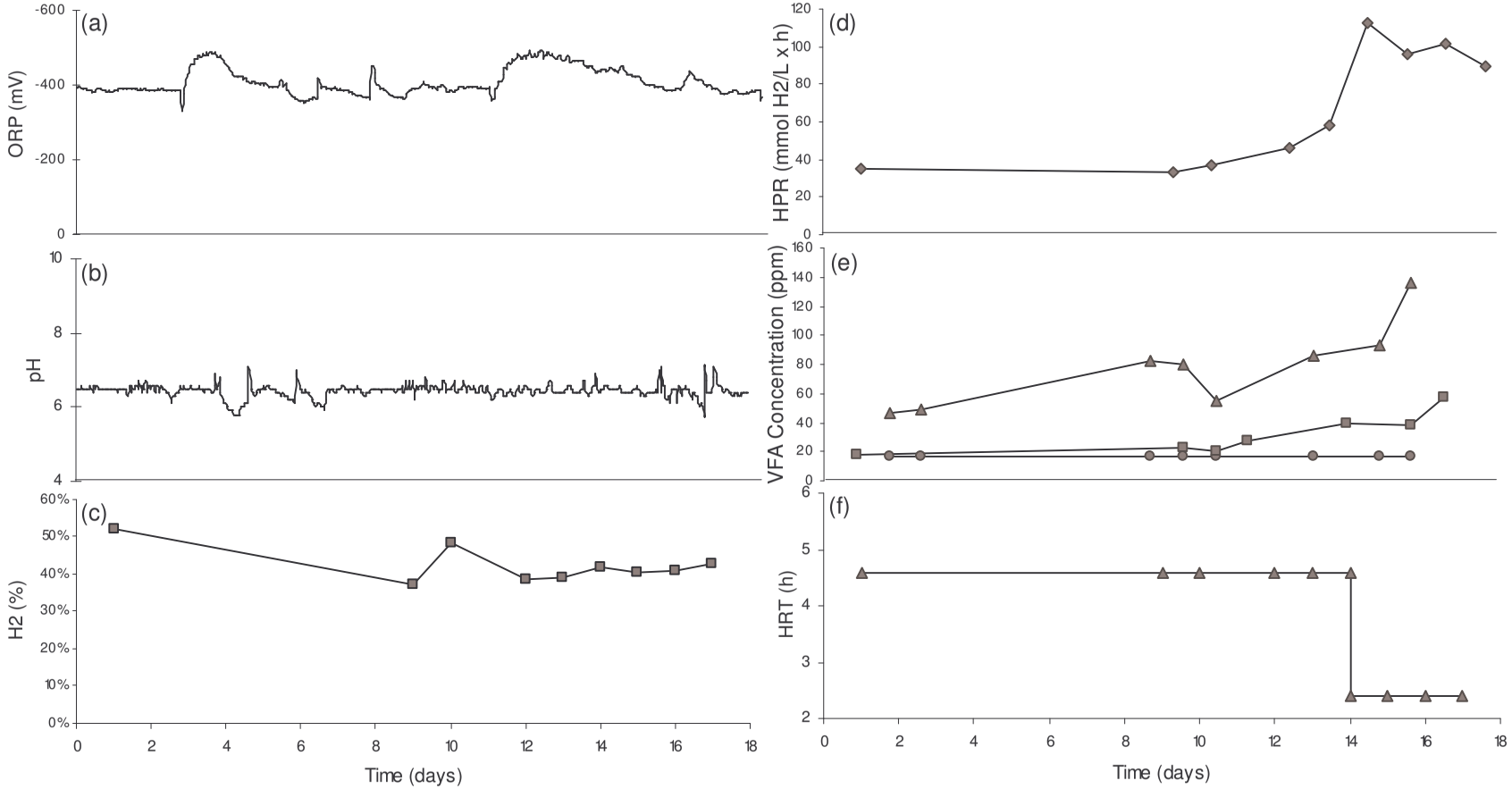


Figure 3.2: Variations in bioreactor of (a) oxidation reduction potential (ORP) (b) pH, (c) biogas hydrogen content (%) ■, (d) hydrogen production rate (mmol H_2 / l culture x h) ◆ and (e) change in VFA content: propionic acid ▲, butyric acid ■, acetic acid ●. The detection limit was 17ppm (f) HRT▲, during gas analysis over a period of 17 days.

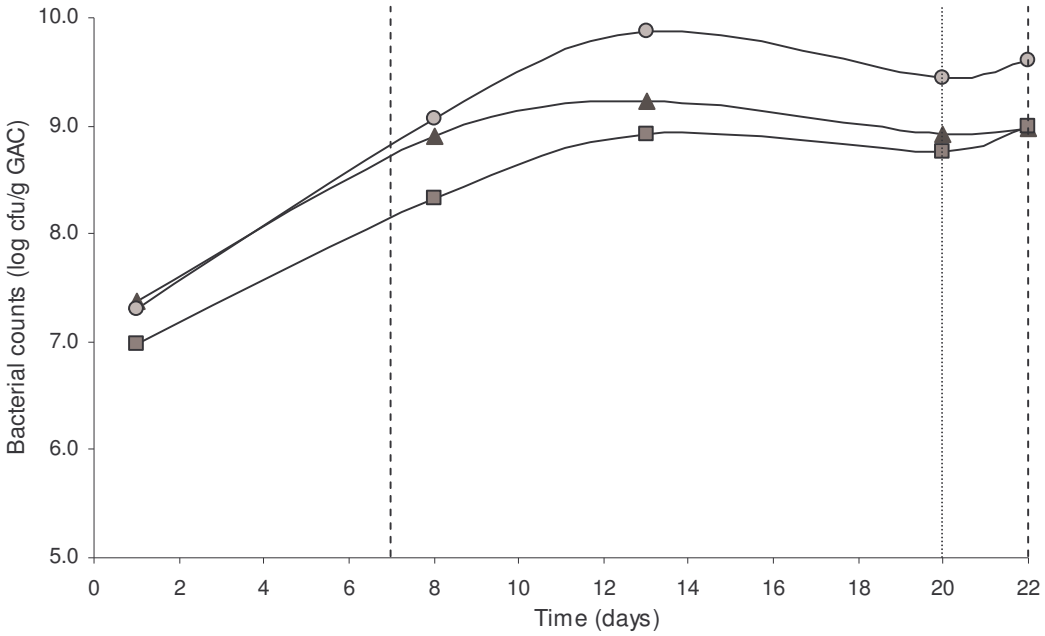


Figure 3.3: Representation of the number of cells (log cfu/g GAC) attached to the GAC through the period of bioreactor biogas measurements. *E. cloacae* Ecl ▲, *C. freundii* Cf1 ■, and the total count ● showed similar trends. The period of gas analysis is indicated by- - - - -. The point at which the HRT was changed from 4.6 to 2.4 hours is indicated by.....

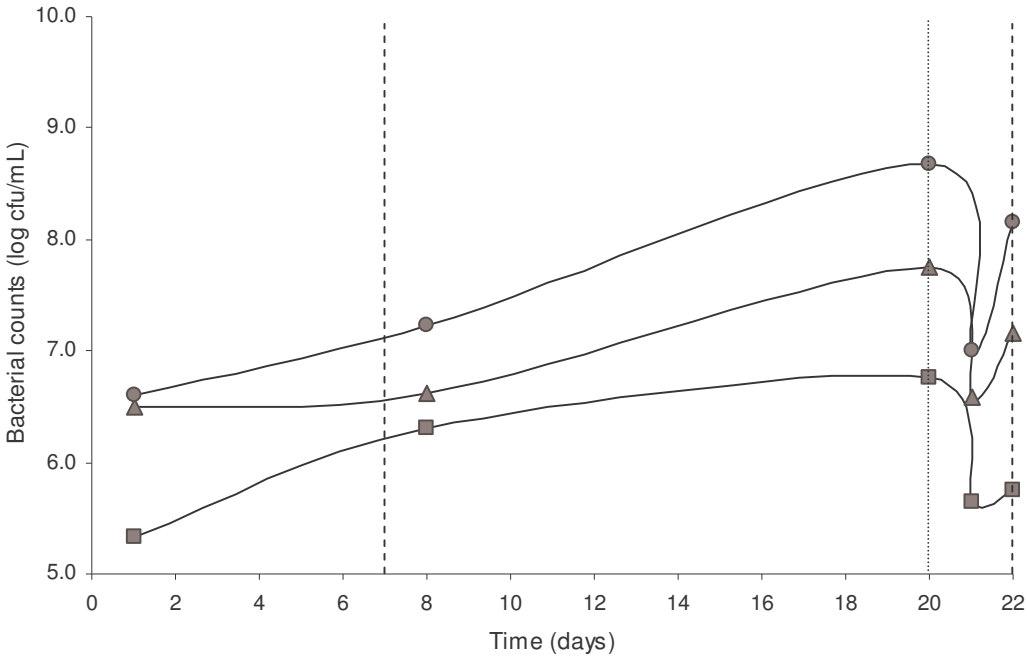


Figure 3.4: Numbers of planktonic cells present within the reactor system during the period of biogas measurement. *E. cloacae* Ecl ▲, *C. freundii* Cf1 ■, and the total count ● should similar trends. The period of gas analysis is indicated by- - - - -. The point at which the HRT was changed from 4.6 to 2.4 hours is indicated by.....

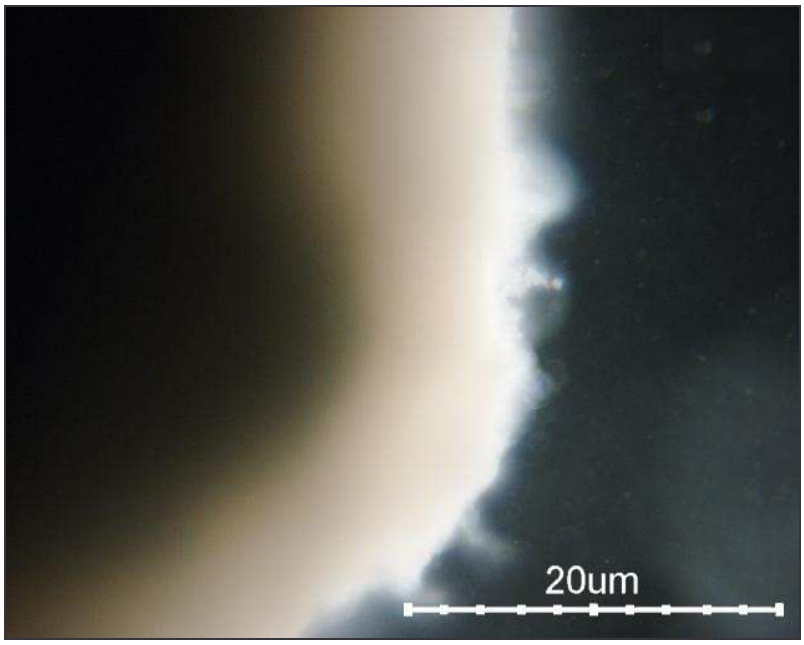


Figure 3.5: Phase contrast microscope image showing GAC particles covered in biofilm. (magnification = 160x)



Figure 3.6: Biofilm development on GAC particles in the AFBR.

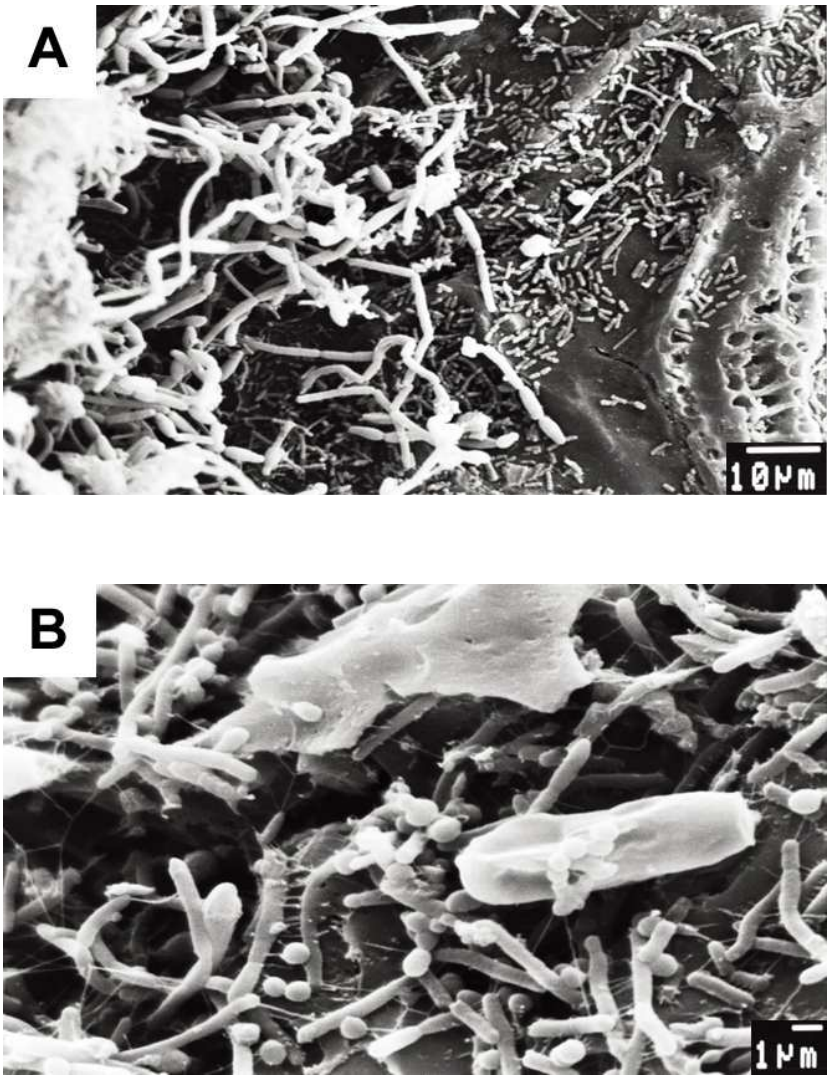


Figure 3.7: Scanning electron micrographs of suggested fungal contamination of reactor (A) observed after 10 days. (B) shows the presence of cocci shaped bacteria present in the biofilm.

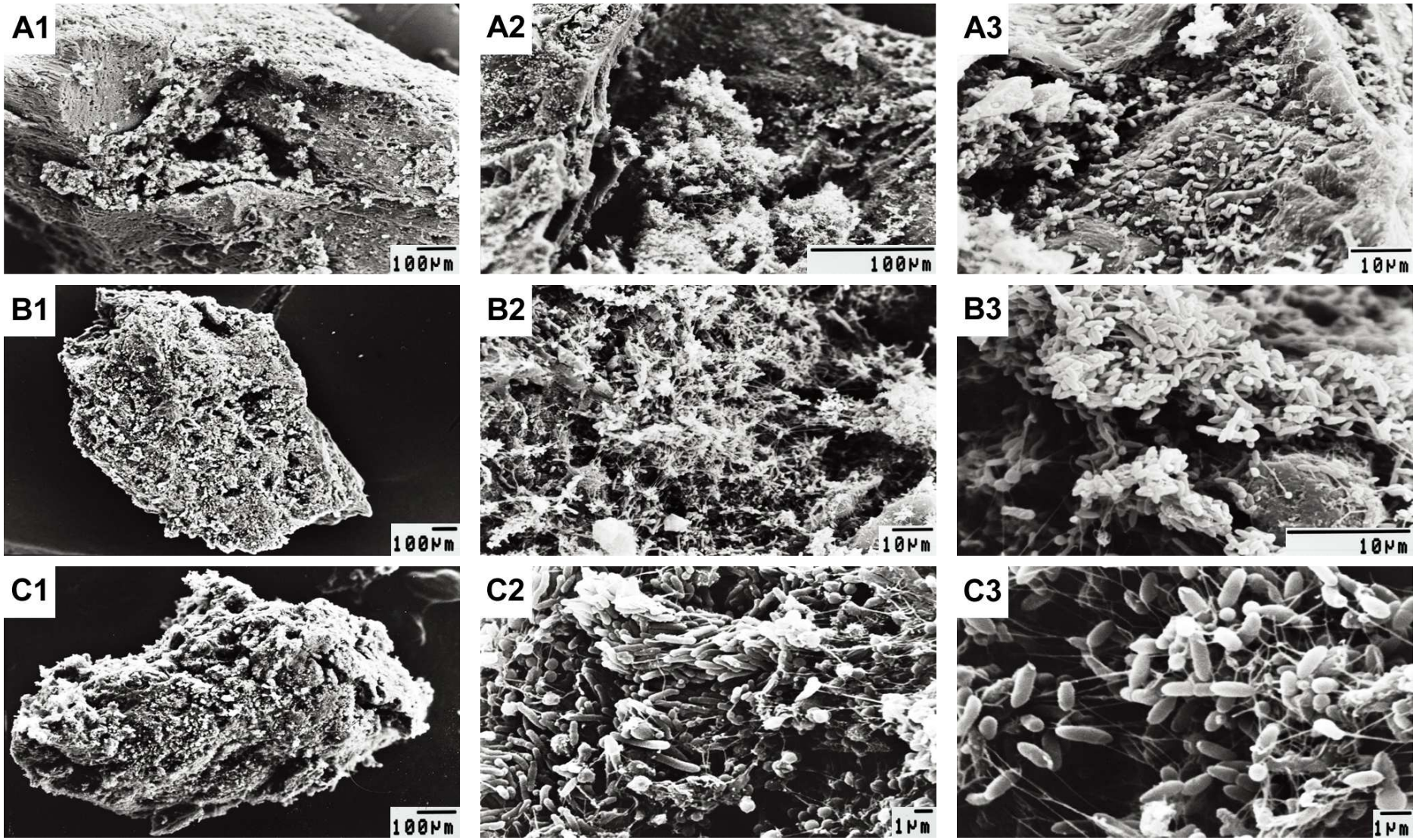


Figure 3.8: Series of scanning electron micrographs showing the development of biofilm on granular activated carbon from the fluidised bed bioreactor after 1 day, (A1-A3), 11 days, (B1-B3), and 25 days (C1-C3).

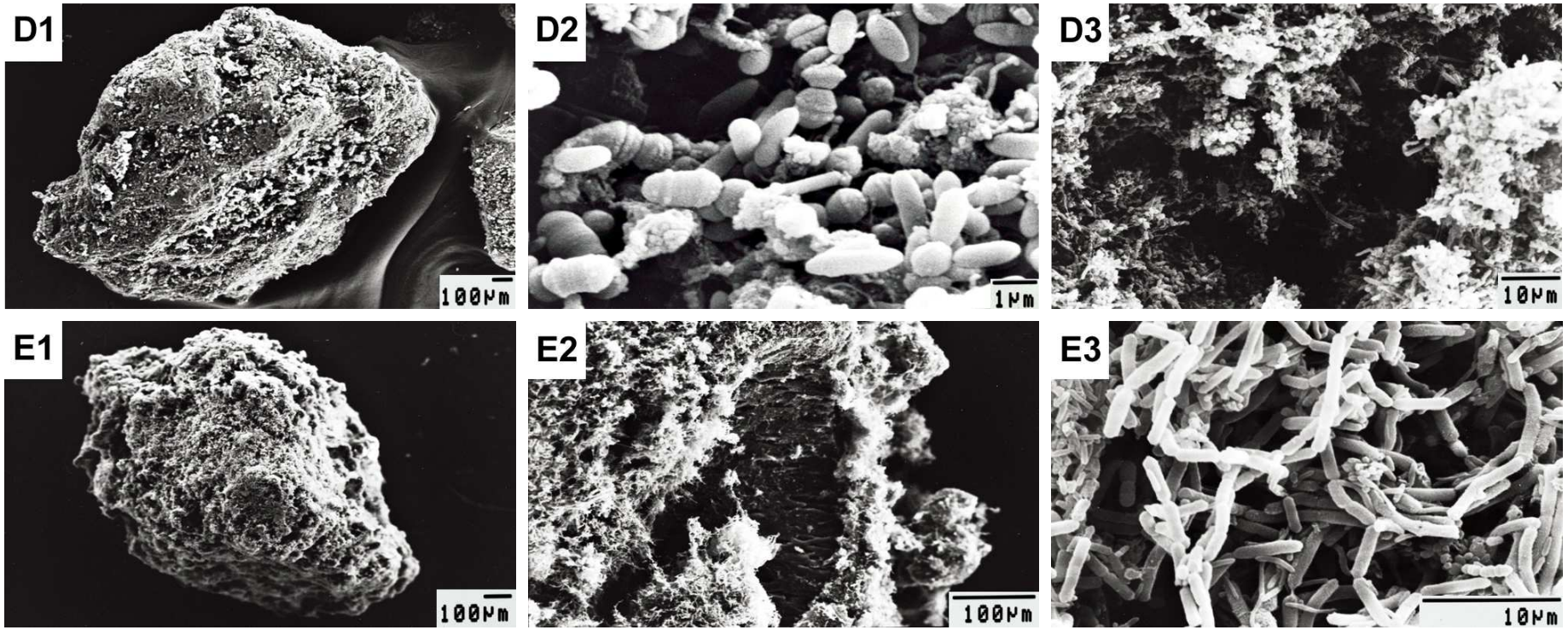


Figure 3.9: D1-D3 on Day 39 shows increasingly mature biofilm structure with Day 51 (E1-E3) showing segments of GAC exposed due to biofilm sloughing.

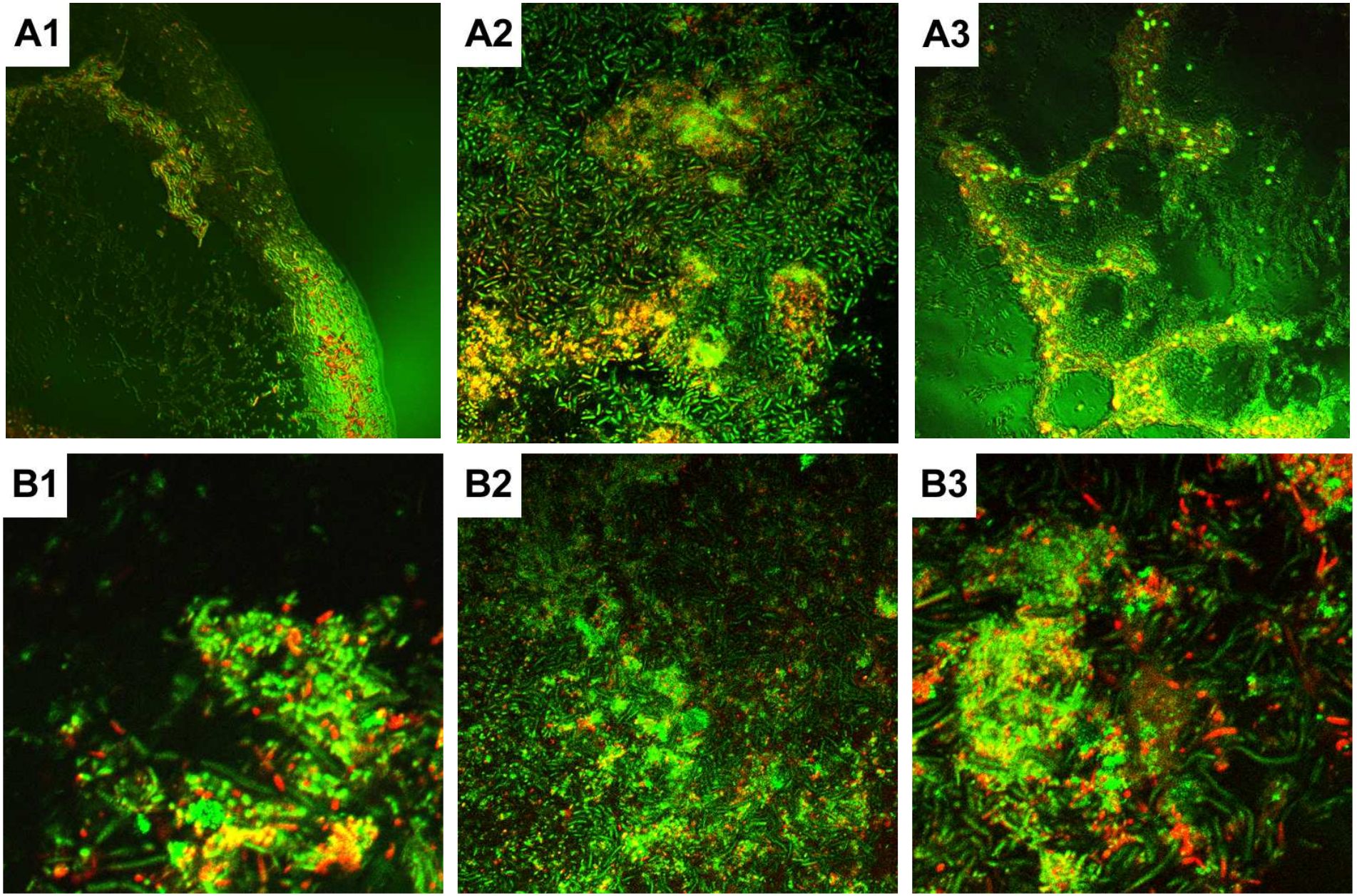


Figure 3.10: Confocal scanning laser microscope images of GAC particles taken at the 4.6 hour HRT (A1-A3) and the 2.4 hour HRT (B1-B3). Live cells are indicated with green whereas dead cells are shown in red. Injured cells are orange/yellow (Lopez, Pons *et al.* 2005).

CHAPTER 4

SUMMARISING DISCUSSION AND CONCLUSION

In Vitro Microbiology

The decision to isolate, characterise and utilise bacterial isolates from the *Enterobacter* (Rachman, Furutani *et al.* 1997; Rachman, Nakashimada *et al.* 1998; Yokoi, Tokushige *et al.* 1998; Kumar, Monga *et al.* 2000; Palazzi, Fabiano *et al.* 2000) and *Citrobacter* (Kanayama, Sode *et al.* 1987; Allan, Callow *et al.* 2002; Jung, Kim *et al.* 2002; Oh, Seol *et al.* 2003) genuses was based largely on their use in previous H_2 fermentation studies. Secondly, they are facultatively anaerobic bacteria with simple nutrient requirements and growth conditions. Further characterisation of these isolates showed that both were able to grow comfortably within the pH 5.0 – 9.0 range which proved a useful attribute for use in a laboratory scale fluidised bed bioreactor where optimal control over pH fluctuations still had to be established. The generation times of ±30 minutes for both *E. cloacae* Ecl and *C. freundii* Cf1 would help in establishing the reactor bed faster than what could be established in a conventional, methanogenic anaerobic digester. Washout of these isolates from the reactor system before steady state would also not occur unless the HRT dropped below the generation times of the isolates. The fast generation times would also help prevent microbial contamination from becoming predominant in the reactor as it could be operated at a higher flow rate, thus washing out any slower growing contaminating organisms.

The method developed to isolate *Enterobacter* spp. and *Citrobacter* spp. was useful as it helped quantify the relative proportion of *E. cloacae* Ecl to *C. freundii* Cf1 in the reactor bed biofilm and planktonic modes. As MacConkey agar only differentiates between *Enterobacter* and *Citrobacter* based on lactose fermentation, the inclusion of ferric citrate and sodium thiosulphate helped in the differentiation between the two isolates.

The C:N:P ratio of the original Endo formulation (Endo, Noike *et al.* 1982) was revisited as it was felt that generic formulations of media were not optimal for biofilm formation in all bacteria. Therefore, the N or P concentration could be too low, thus preventing biofilm growth, or the N or P concentrations could be too high, resulting in growth inhibition due to toxicity effects on the cultures. Of the three C:N ratios tested, the modified 334:84 original 334:42 ratios showed evidence of growth limitation, possibly due to NH_3 toxicity. Therefore these ratios were not used for the nutrient medium in bioreactor work.

There was little discernable difference between the N:P ratios tested on the same C:N ratios with differences between ratios showing no statistical significance ($P > 0.05$). This suggested that neither of the P concentrations used were growth limiting. The C:N ratio used in this study was higher than many other H_2 producing studies. However, a study focused on the optimal C:N ratio for fermentative H_2 production suggested that an approximate ratio of 334:7 be used based on equivalent sucrose concentrations. It is not clear whether this ratio was optimised for both H_2 and biomass production (Lin and Lay 2004a). Ratios suggested were based on COD ratios, whereas this study used atom:atom ratios.

Of the three formulations tested, the 334:28 C:N ratio was selected for use in bioreactor studies mainly because counts on dislodged binary biofilms showed the highest attachment in shake flasks using this ratio. *E. cloacae* Ecl and *C. freundii* Cf1 showed attachment counts of 8.2 log cfu/g GAC and 6.34 log cfu/g GAC respectively, however differences were not statistically significant ($P > 0.05$). Scanning electron microscopy (SEM) qualitatively confirmed that the C:N ratio of 334:28 had a more dense distribution of biofilm coverage compared to the other formulations tested. Even though there was little difference between counts of identical C:N ratios using different N:P ratios, the N:P ratio of 28:5.6 was selected to ensure that P did not become growth limiting within the reactor.

Attempts to perform *in vitro* growth curves (results not shown) in the chosen 334:28:5.6 C:N:P Endo formulation proved unsuccessful as both isolates showed no evidence of planktonic growth in the medium. Possible reasons for this included NH_3 toxicity to the cells or the lack of an attachment substrate which is known to improve attachment amongst environmental bacterial isolates (Davey and O'Toole 2000).

Fluidised Bed Reactor Pilot Study

The testing and control optimisation of the fluidised bed reactor for H_2 production was conducted to determine the response of the pH, oxidation-reduction potential, conductivity and temperature electrodes to changes within the bioreactor system. Results from the conductivity electrode showed that interference

in readings due to both biofilm growth on the electrode and gas bubble accumulation around the electrode nullified their value.

Significant hysteresis was observed when the control system attempted pH corrections resulting in the pH overshooting the intended range of pH5.8 - 6.5. The cause of hysteresis was the low recycle flow rate of the pumping system, which indicated that the acid or base dose had not corrected the pH fully before the next reading and correction was made. This was remedied by allowing the controller to perform pH correction only once per hour. Temperature fluctuations within the reactor showed that the external environmental temperature had a sizeable effect on the ability of the heat exchange to keep the reactor temperature constant.

AFBR Startup

The final reactor startup was accomplished in 30 days, which was in part due to the high growth rate of both *E. cloacae* Ecl and *C. freundii* Cf1. The startup regime was conservative and it is possible that the period could have been reduced had the HRT been reduced on a 2 day rather than 3 day schedule. Due to the lack of a biomass overgrowth control mechanism, there was significant washout of GAC particles. Despite this, frequent additions of GAC ensured that the reactor functioned adequately. The concentration of sucrose remained low throughout the experiment, and was found to be the main limiting factor in controlling biofilm growth on the GAC particles. The only time a significant increase in sucrose within the reactor was observed was when the HRT was reduced from 4.6 to 2.4 hours, resulting in a roughly 16 times increase in sucrose concentration per litre. Sucrose utilisation remained high throughout the experiment with 99.7% utilisation at HRTs above 4.6 hour, down to 95.8% at the 2.4 hour HRT. The ORP readings showed that the reactor remained anaerobic throughout the period with values of -408±35mV. pH was maintained with the pH5.5-6.5 range suggested in fermentative H_2 production studies.

AFBR Microbiology

This was the first study to successfully use *E. cloacae* Ecl and *C. freundii* Cf1 binary biofilms to generate H_2 in an AFBR. Bacterial biofilm counts were high for both *E. cloacae* Ecl and *C. freundii* Cf1 at > 9.0 log cfu/g GAC, however there no significant different between the two ($P > 0.05$). The volume of biofilm on the GAC particles showed a close relationship with the decreasing HRT, where decreasing HRTs gave increased biofilm volumes. Scanning electron micrographs showed a similar increase in complexity of biofilm attachment and growth due to decreasing HRTs. The planktonic mode of growth of the *E. cloacae* Ecl and *C. freundii* Cf1 isolates showed a smaller presence in relative to biofilm counts as counts were only around 3% at the 4.6 and 2.4 hour HRTs. This suggests that the majority of H_2 produced was likely due to the biofilm component of the reactor. Scanning electron micrographs showed the presence of contaminating cocci shaped cells which were not isolated, as well as the presence of a fungus identified as *Basipetospora* gen. nov (Straker 2004).

AFBR H_2 Production and Process Efficiency

The hydrogen production rate (HPR) showed a close correlation with the HRT, increasing from 35 to 95 mmol H_2 / (l x h) when the HRT was changed from 4.6 to 2.4 hours. The composition of the biogas remained stable at 42.3%±4.8 during the analysis period. The concentrations of butyric and propionic acids also showed a correlation with decreasing HRT, although the concentrations of the acids were uncharacteristically low. It is possible that other species of undetected volatile fatty acids such as ethanol, lactic acid, formic acid, valeric acid, caproic acid and iso-butyrate were present or predominant in the reactor, explaining the low levels of the expected butyric, acetic and propionic acids.

The process efficiency was calculated to be 5.2% in terms of converting sucrose into H_2 compared to a theoretical maximum. This was comparable to other studies (Benemann 1996; Logan, Oh *et al.* 2002) however it was felt that the reactor was operating sub-optimally due to the absence of acetic acid, which produces 8 mols H_2 per mol sucrose, and the predominance of propionic acid. Propionic acid is

considered as a H_2 sink, and therefore its presence indicates this process was not operating optimally. The exact activation mechanisms of the propionic acid pathway are not known, however there are several potential possibilities. Although high H_2 partial pressure is most often suggested cause, research has shown that this is not the case (Inanc, Matsui *et al.* 1996; 1999). Other possible mechanisms include an irregular feeding rate, and incorrect pH ranges within the system. Both of these mechanisms are likely to have played a part in this process as the pH range was not below the suggested pH6.0.

A further source of sucrose conversion inefficiency may lie in the absence of mineral nutrient co-factors such as Mo, Zn, Ni and Se all of which are known to be necessary for the formate-hydrogen lyase enzyme complex. This enzyme complex is present in the Family *Enterobacteriacae* of which both *E. cloacae* Ecl and *C. freundii* Cf1 are part (Gray and Gest 1965). This means that H_2 production was proceeding only via the butyric acid pathway. Formic acid is the most likely alternative fatty acid to have been present in the reactor, as if it is not degraded into H_2 and CO_2 with the enzyme complex it is simply excreted as waste from the cell (Lengeler, Drews *et al.* 1999).

Reactor Scale-up Considerations

The estimated size of a fluidised bed reactor with the same HPR as the current study of 95 mmol H_2 / (l x h), required to power a 5.0kW proton exchange membrane fuel cell (PEMFC) is 1250L, assuming no change in the HPR occurs during scaleup. This scaleup size is similar to studies which used fixed and upflow anaerobic sludge blanket reactors, thus indicating potential industrial application of AFBR technology in bioenergy generation. There are several technical complications with the use of biogas for PEMFC fuel as highlighted in this study. Biogas is composed of 20-60% H_2 in combination with continuously varying concentrations of CO_2, CO, H_2O and H_2S. PEMFCs require a H_2 supply that is greater than 99% purity and levels of CO and H_2S below 10ppm otherwise poisoning will occur. Therefore significant purification of H_2 from biogas is needed to achieve this purity. It is clear that the reactor used in this study cannot simply be connected to a PEMFC without these challenges being addressed.

Feasibility of H_2 Production for a Rural Household

If one assumes the absence of solar heating and the use of a scaled-up 1250L version of the reactor used in the current study, then approximately 24 kilowatt hours of energy is utilised by an average rural household in South Africa per day. The organic load required to produce the 2968 L/H_2 per hour to power a 5kW PEMFC is a COD load of approximately 280kg COD. It becomes obvious that a rural household could never generate sufficient COD necessary. It would therefore be necessary to pool household COD generation capacity to ensure that sufficient COD is generated to supply a PEMFC with sufficient H_2. The conversion of conventional sewage plants into AFBR H_2 generating facilities provides the most plausible idea for biological H_2 generation. Domestic, agricultural, agro-industrial and timber processing waste could be collected from the surrounds and converted into H_2, and thereafter electricity for consumption for end users. Certainly if conversion efficiencies improve from the current 5.2% achieved in this study, the process of converting waste into H_2 and electricity will become more economically feasible and certainly economically sustainable.

Future Research & Design Improvements

Future shake flask studies should focus on the growth rates of isolates on attachment substrates due to the difficulty in getting these environmental isolates to grow planktonically in the Endo formulation (du Plessis, Senior *et al.* 1998). These results would be more relevant to bioreactor studies. Culture selection should be widened to include multiple H_2 producing bacterial phyla.

The applicability of the conductivity electrode to this study was limited due to the interference of gas bubbles with electrode readings produced during the fermentation process. It is recommended that this electrode be used only to monitor the quality of the feed being fed to the reactor, and could be used as a measure of the organic load that is being fed into the reactor.

The vessel housing the electrodes experienced numerous seal integrity problems that allowed either air to enter the system or reactor liquid to escape out of the system. As a result, the electrode housing was completely redesigned and reconstructed to allow the electrodes to be properly fixed onto the vessel. The reconstructed electrode housing performed adequately, however additional improvements in the design of the electrode housing and the reactor plumbing system are needed to permit a greater portion of the wastewater to flow through the vessel. Modifications to the heat exchange system and insulation would be needed to reduce excessive heat loss and to reduce the variability in the temperature profile of the reactor. This could help prevent unwanted metabolic pathways from being activated in the reactor culture. A system for the recycling of carrier substrate needs to be included in future AFBR research as the biomass lost due to carrier washout was considerable during the experimental period. This would ensure that the active biological surface area remained constant within the reactor.

Additional considerations should include the prevention of biogas entry into the vessel which interfered with both pH and ORP readings and interfered with conductivity readings. A possible measure to counter this problem could be to improve the disengagement and removal of biogas from the recycle stream, thus reducing the amount of gas within the system. This would in addition help with preventing the washout of biomass caused by the fluidisation effect of the recycling biogas.

The datalogger performed satisfactorily although the accumulation of duplicated data points indicated that system variables were being over measured. Future programs should take this into account and should incorporate elements of predictive rather than reactive control algorithms.

The feeding regime was also possibly erroneous, as feed was introduced in a semi-continuous basis, with a fixed amount of feed being introduced evenly over one hour. In addition, precipitation problems occurred with the inadequately re-circulated reservoir of concentrated feed. All of these factors, including the omission of mineral nutrient co-factors such as Zn, Ni, Mo and Se needed for the formate-H_2 lyase enzyme, were likely contributors to the lower than expected conversion efficiency of sucrose to H_2.

Undoubtedly, redirecting wastewater treatment towards biohydrogen production is a step in the right direction for alleviating demands on energy infrastructure in addition to combating water and air pollution. However, the low conversion efficiencies of waste to H_2 currently observed, suggests that the implementation of this technology as a primary bioenergy source for both industry and consumer households is premature, even when considering process scale-up. The slow rate of progress in improving H_2 yields through technical interventions suggests the problem is more microbiological in nature. Therefore future efforts should focus on culture selection which may need to include genetic manipulation to induce slower growth rates and therefore smaller metabolic energy requirements and the removal of H_2 consuming pathways. However the technical obstacles still present a challenge for researchers as strict pH control, low H_2 partial pressures, the recycling of biomass, capture and purification of H_2 have still not been optimised for fermentative H_2 production.

Manipulation of culture conditions such as fine pH control and low H_2 partial pressures are unlikely to produce the substantial increases in H_2 required to improve conversion efficiencies beyond 40%. However, industrial implementation of H_2 producing AFBRs as an alternative to methanogenic reactors or sewage discharge penalties is still favourable due to greater system stability and lower capital outlay, even though larger, more expensive, complex and often unstable single-stage methanogenic digesters are currently relied upon for urban wastewater treatment. Alteration of wastewater treatment from purely treatment to energy generation and treatment will help reduce expenditure and reliance on conventional energy supplies and therefore free up more cash which could be used on process expansion and therefore job creation. The inclusion of secondary reactors able to degrade volatile fatty acids produced in a primary reactor into H_2 or CH_4 could also be considered as this would improve the overall conversion efficiency of the treatment process. Until such advances or implementations are made, indications are that fermentative H_2 production will remain a supplementary source of bioenergy, although superior to CH_4 production. This mode of H_2 production may not yet compete with more efficient and cost effective methods such as steam reformation and electrolysis or with other renewable energies such as solar and wind power. However, it should in future be considered as a source of energy for cost reduction, however minor, which would reduce fossil fuel requirements and the production of air and water pollution.